Summer 7-24-2013

Roles of Neurotransmitters in the Regulation of Neuronal Electrical Properties and Growth Cone Motility

Lei Zhong
Georgia State University

ROLES OF NEUROTRANSMITTERS IN THE REGULATION OF NEURONAL ELECTRICAL PROPERTIES AND GROWTH CONE MOTILITY

by

LEI ZHONG

Under the Direction of Dr. Vincent Rehder

ABSTRACT

In addition to acting in synaptic transmission, neurotransmitters have been shown to play roles in the development of nervous system. Developing neurons extend neurites to connect to their target cells, and growth cones at the tip of growing neurites are critical for pathfinding. Although evidence for the regulation of axonal growth and growth cone guidance by neurotransmitters and neuromodulators is emerging, less is known about the mechanisms by which neurotransmitters affect developing neurons. Here, I focus on three neurotransmitters/ neuromodulators and describe their actions (a) at the level of growth cone, especially on filopodia, which serve as sensors that allow growth cones to probe the environment they are traversing, and (b) on how neurotransmitters modulate neuronal electrical properties, which, in itself, have been shown to affect neurite extension. The goals of this dissertation are to

investigate 1) the cholinergic modulation of neuronal activity and its effects on growth cone motility; 2) the excitatory modulation of neuronal excitability by nitric oxide (NO); and 3) the inhibitory modulation of neuronal activity by dopamine (DA).

The work uses a well-established model system to investigate growth cone motility and neuronal activity: identified neurons from the pond snail *Helisoma trivolvis* studied in cell culture or in the intact ganglion *in situ*. The study of B5 neurons demonstrates that acetylcholine (ACh) induces filopodial elongation, which is mediated by opening of nicotinic ACh receptors, membrane depolarization, and elevation of intracellular Ca level in growth cones. This dissertation also shows that NO inhibits two types of Ca-activated K channels to depolarize the membrane potential of B19 neurons. Additionally, the study reveals that DA serves as an inhibitory neurotransmitter to hyperpolarize and silence the electrical activity of firing B5 neurons via a D2-like receptor/PLC/K channel pathway. Taken together, this dissertation elucidates novel cellular mechanisms through which neurotransmitters can regulate growth cone motility and neuronal electrical properties, further supporting evidence for potential roles of neurotransmitters in axon pathfinding and synaptic transmission *in vivo*.

INDEX WORDS: Acetylcholine, Calcium, Cell excitability, Dopamine, Electrical activity, Filopodia, Growth cone, *Helisoma trivolvis*, Membrane potential, Nicotinic acetylcholine receptor, Nitric oxide, Potassium channel

ROLES OF NEUROTRANSMITTERS IN THE REGULATION OF NEURONAL ELECTRICAL PROPERTIES AND GROWTH CONE MOTILITY

by

LEI ZHONG

A Dissertation Submitted in Partial Fulfillment of the Requirements for the Degree of

Doctor of Philosophy

in the College of Arts and Sciences

Georgia State University

2013

ROLES OF NEUROTRANSMITTERS IN THE REGULATION OF NEURONAL ELECTRICAL PROPERTIES AND GROWTH CONE MOTILITY

by

LEI ZHONG

Committee Chair: Dr. Vincent Rehder

Committee: Dr. Chun Jiang

Dr. William Walthall

Electronic Version Approved:

Office of Graduate Studies

College of Arts and Sciences

Georgia State University

August 2013

ACKNOWLEDGEMENTS

I will try to list all the people who have helped and supported me during my Ph.D. study in the past 6 years. Please forgive me if I missed someone to acknowledge, but I will always appreciate and cherish those moments we have spent together.

First and foremost, I would like express my deepest gratitude to my Ph.D. advisor Dr. Vincent Rehder for his tremendous help over the past six years. Dr. Rehder, seems to me, not only is a great mentor transforming me from a non-experienced student into an enthusiastic neuroscientist, but also is a godfather for me to guide me through difficulties and provide me the perspectives about all parts of my life. Without his guidance, I do not believe that I can walk this far and have enough confidence to pursue the academic life as I have set my career goal.

Secondly, I am so thankful for the support and guidance from my wonderful committee members, Dr. Chun Jiang and Dr. Bill Walthall. The opportunities Dr. Jiang offered me to learn in his lab and the passion he has about science truly inspired me to elevate my scientific thoughts into a higher level. Dr. Walthall is not only in my dissertation committee but also in my qualifying committee. He is always so supportive and helpful to improve the way I think about science.

I am so grateful to my lab colleague Dr. Liana Artinian. The enthusiasm and scientific skills she brought into the lab refreshed and benefited me to conduct better science. I also thank my lab 'buddy' Stephen Estes. We studied, worked, and grew up together over my Ph.D. period.

Additionally, I would like to thank all the current and previous lab members in Dr. Rehder's lab, especially Dr. Karine Tornieri, Julia Eidelman, Hansoo Yang.

I also thank all the faculty members, including but not limited to Dr. Sarah Pallas, Dr. Tim Bartness, Dr. Chungdar Lu, Dr. Paul Katz, Dr. Laura Carruth, Dr. Kyle Frantz, Dr. Gennady Cymbalyuk, and Dr. Anne Murphy, for generously providing their suggestions and advice to help me become a better scientist. I thank all the staff members at Biology Department, especially Ms. LaTesha Warren for her professional assistance. I also appreciate the financial support from Brain and Behavior program and Ms. Elizabeth Weaver for organizing all the interesting events for B&B fellows.

I would like to express my appreciation of the friendship my friends and I have built over the past six years. I especially appreciate my friend Charuni Gunaratne. Thank her for taking time to chat about science and life. Other important friends include but not limited to: Dr. Xiangyu Yao, Jing Wang, Jie Xu, Yang Wu, Zhenda Shi, Shuang Zhang, Dr. Ningren Cui, Dr. Xin Jin, Max Oginsky, Dr. Wulf Krenz, Dr. Akira Sakurai, Dr. Yuting Mao, Dr. Chen Li, Dr. Yang Yang. Thank all of you for giving me so many beautiful moments.

Finally, I thank my family for being the strong shield behind me. I feel guilty not to take care of my Mom Lindi Chen and my Dad Zhiren Zhong while in my graduate school. They are always there sharing all my happiness and sadness, and encouraging me to become a better person. I also thank my grandma Shuizhen Yu, uncle Gaoren Zhong, aunt Lingeng Chen, and cousin Li Zhong for caring and believing in me. Most importantly, I cannot express more

gratitude to my wife and soulmate, Yumin Liu, who is there for me every hour and every day. I ascribe every achievement I made to her. I cannot imagine how my life will become without her. Her trust, support, and smile gave me every reason to accomplish my Ph.D. degree.

TABLE OF CONTENTS

LIST OF FIGURES

LIST OF ABBREVIATIONS

ACh	acetylcholine
AHP	afterhyperpolarization
AP	action potential
A type	transient outward
BDNF	brain-derived neurotrophic factor
BK	large conductance Ca-activated K
Ca	Calcium
CaMK	Ca/calmodulin-dependent kinase
cGMP	cyclic guanosine monophosphate
CNG	cyclic nucleotide gated
DA	dopamine
DEA/NO	diethylamine NONOate
DMPP	dimethylphenylpiperazinium
EC_{50}	half maximal effective concentration
ER	endoplasmic reticulum
F-actin	filamentous actin
GABA	gamma-aminobutyric acid
IbTX	iberiotoxin
IP_3Rs	inositol triphosphate receptors
K	potassium
Kv	voltage gated K
Kir	inwardly rectifying K

LGICs	ligand-gated ion channels
mAChR	muscarinic acetylcholine receptor
MAG	myelin-associated glycoprotein
nAChR	nicotinic acetylcholine receptor
NGF	nerve growth factor
nNOS	neuronal nitric oxide synthase
NO	nitric oxide
PKG	protein kinase G
R_{in}	input resistance
RMP	resting membrane potential
RyRs	ryanodine receptors
sGC	soluble guanylyl cyclase
Sema3	semaphorin 3
SK	small conductance Ca-activated K
TASK	two-pore domain K
TC	tubocurarine
TEA	tetraethylammonium
TRP	transient receptor potential
UNC	uncoordinated
VGCCs	voltage gated Ca channels
4AP	4-aminopyridine
5HT	serotonin
$[Ca]_i$	intracellular Ca concentration

CHAPTER 1 GENERAL INTRODUCTION

1.1 Specific aims of dissertation

The goal of this dissertation is to examine the effects of three critical neurotransmitters and neuromodulators, acetylcholine (ACh), nitric oxide (NO), and dopamine (DA) in the regulation of two aspects of neuronal development, growth cone motility and neuronal excitability. Moreover, this dissertation aims to characterize the intracellular signaling pathways and the membrane channel targets that mediate the effects. The research uses cultured neurons isolated from the freshwater pond snail *Helisoma trivolvis* as a model system. A brief summary for the specific aims is listed below.

Specific Aim 1 (Chapter 2): How does ACh regulate neuronal activity and growth cone motility?

In addition to acting as a classical neurotransmitter in synaptic transmission in the nervous system, ACh has been shown to play roles in developing neurons such as axonal growth and growth cone guidance (Lauder and Schambra, 1999; Phillis, 2005). However, neither the functions of ACh at the level of the growth cone nor the underlying mechanisms by which ACh affects growth cone filopodial dynamics have yet been fully understood. Moreover, electrical activity has been shown to regulate cell growth (Neely and Nicholls, 1995; Ming et al., 2001), but a comprehensive study of how cholinergic modulation of neuronal electrical activity may be linked to growth cone motility is presently lacking. Therefore, the present study tests the hypothesis that ACh regulates growth cone motility and approaches the question at the cellular and electrophysiological level. These experiments provide insights in the role of cholinergic modulation in neuronal pathfinding and/or synaptogenesis.

Specific Aim 2 (Chapter 3): <u>How does NO modulate neuronal excitability of Helisoma B19 neurons?</u>

Previous studies in our lab identified nitric oxide (NO) as an important regulator for growth cone motility and cell excitability in *Helisoma* B5 neurons (Trimm and Rehder, 2004; Artinian et al., 2010), where NO acted on various ionic conductances to regulate membrane properties (Artinian et al., 2010; Artinian et al., 2012). What we do not know is whether NO serves as a general neuromodulator acting on many cells, or if the actions of NO are limited to smaller subsets of neurons. Considering its physical location in the vicinity of NO-releasing neurons inside the buccal ganglion and its contribution to feeding motor patterns, known to be regulated by NO (Susswein and Chiel, 2012), I tested the modulatory role of NO on the electrical activity of another buccal neuron, B19. In particular, I wanted to investigate potential membrane channel targets of NO and determine whether the effects of NO on buccal neurons B5 and B19 would be the same or different. An understanding of the effects of NO on the level of identified neurons would provide further evidence for NO being a crucial regulator with the potential to affect feeding behavior.

Specific Aim 3 (Chapter 4): <u>How does DA elicit effects on neuronal activity?</u>

The study of DA in modulating the electrical excitability of individual neurons to elicit various behaviors is of great interests in many systems. The fact that buccal neuron B5 innervates the esophagus and is surrounded by dopaminergic processes (Perry et al., 1998) raises the questions whether DA modulates the electrical activity of B5 neurons to exert functions in feeding. If so, what are the membrane targets and intracellular signaling mechanisms underlying

the effect of DA? Such a demonstration would help dissect and understand the role of DA in regulating neuronal development and controlling feeding behaviors.

Taken together, this dissertation addresses the roles of ACh, NO, and DA in regulating neuronal membrane properties and growth cone motility in two identified neurons. Moreover, it characterizes the intracellular signaling cascades activated by these neurotransmitters/neuromodulators in mediating their effects. It also identifies the membrane channel targets affected by these neuromodulators. Therefore, through the modulatory effects on the electrical activity, the release of ACh, NO, and DA *in vivo* may affect various processes of neuronal development and regulate the neuronal output of neural circuits in the nervous system.

1.2 Neuronal growth cones

Our nervous system consists of trillions of neurons interconnected into a variety of neural networks. The correct pattern of these intrinsic circuits is critical for the proper function of the nervous system and appropriate behaviors being produced. Formation of a functional neural circuit requires the precise execution of a sequence of developmental events starting from cell proliferation, neuronal differentiation, cell migration, growth cone formation, growth cone pathfinding and axon guidance, dendritic growth, synaptic target selection, to synaptogenesis (Waites et al., 2005; Colon-Ramos, 2009). With the full awareness of every step playing crucial roles during neuronal development, I will be only focusing on one step, growth cone pathfinding, in this dissertation, and try to promote our understanding of the underlying mechanisms how growth cones are regulated by the neurotransmitters/neuromodulators ACh, NO, and DA.

1.2.1 Growth cone structure and function

During the development of nervous system, axon guidance is one of the key steps to build correct connections between a neuron sending out an axon, tipped with a growth cone at the leading edge, and a target neuron (Tessier-Lavigne and Goodman, 1996). The growth cone of developing or regenerating neurons constantly samples the environment it traverses in search for extracellular cues. These extracellular cues act on membrane receptors or intracellular targets in growth cones, activate signaling cascades, and change the cytoskeleton, through which the growth cone will be guided towards its target area and/or build a synaptic connection (Salie et al., 2005; Shen and Cowan, 2010). Problems in the connectivity between neurons resulting from miswiring or even a lack of connectivity are associated with a variety of neurological disorders like epilepsy, autism, and schizophrenia (Mitchell, 2011; Mitchell, 2011).

Growth cones were first described by Spanish neuroscientist Santiago Ramon y Cajal, who won the Nobel Prize in Physiology or Medicine in 1906 for his contribution to help understand the structure of the nervous system. He described the growth cone based on fixed chick embryonic tissues as ‘a concentration of protoplasm of conical form, endowed with amoeboid movements’ (Cajal, 1890). From then on, the structure of the growth cone and its associated functions in the nervous system became major interests in the field of developmental neuroscience.

The growth cone is highly motile ‘fan-shaped’ structure at the tip of growing neurite. It consists of the following three major components [Fig. 1.1]:

Central domain, the thick region located in the center of the growth cone closest to the neurite enclosing bundled microtubules;

Lamellipodium, the thin peripheral region surrounding the outer edge of the growth cone containing mainly the actin-based cytoskeleton;

Filopodia, fine 'finger' like projections of the growth cone composed of bundles of actin filaments (Lowery and Van Vactor, 2009).

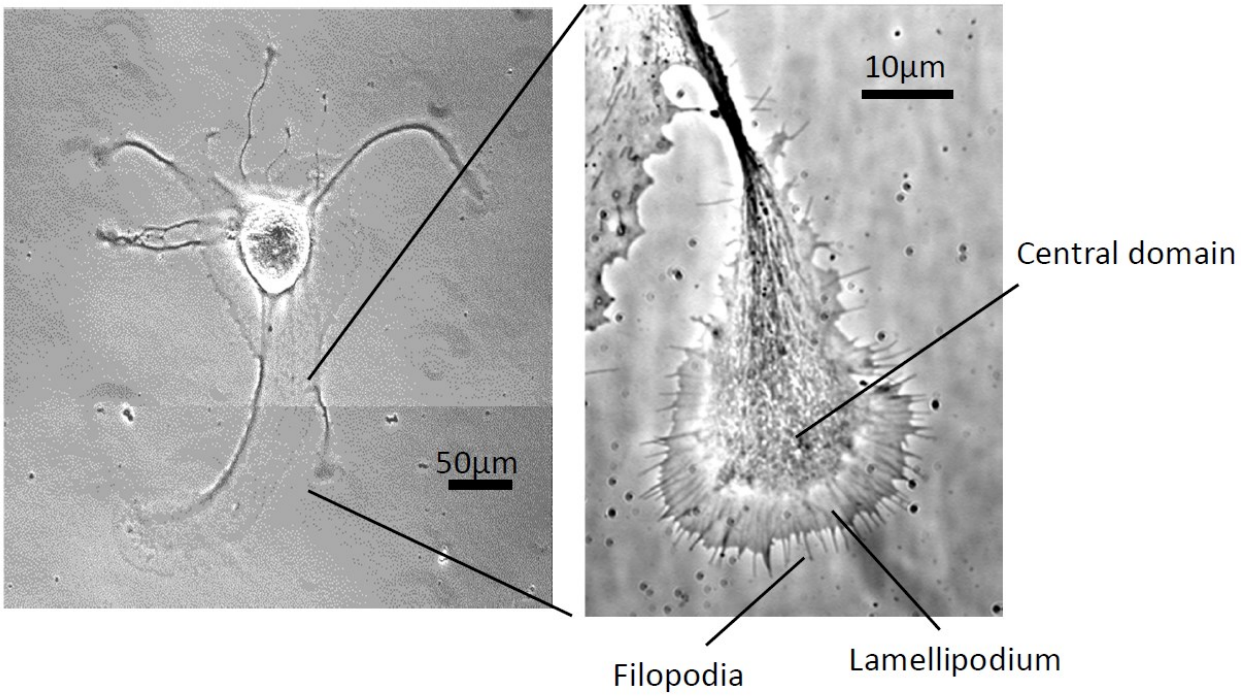

Figure 1.1 Phase contrast images of a cultured neuron with growth cones.

An entire growing *Helisoma* B5 neuron is imaged with a 20X objective (left). The enlarged growth cone shows the 3 major domains of a growth cone: the central domain, the lamellipodium, and the filopodia (right, 100X objective).

The more stable microtubule-based central domain contains vesicles and organelles and supports the rapidly growing growth cone and the extension of neurites. The actin-based filopodia act as sensors on growth cones and are important in growth cone motility and axon pathfinding (Kater and Rehder, 1995). Filopodia are extremely dynamic, and can form, elongate, and retract within minutes, or even seconds (Durkaya et al., 2009; Durkaya et al., 2009). Growth cones without filopodia lose their ability of pathfinding. A study of *Xenopus* retinal neurons showed that cytochalasin B-treated growth cones lacked filopodia but maintained active lamellipodia (Chien et al., 1993). These growth cones were found to continue to advance but made navigational errors when approaching normal turning points along their paths (Chien et al., 1993). This result emphasizes the importance of filopodia in guiding the growing neurite. Once growth cones reach the target area, filopodia again play critical roles in building the first contact with the target cell before synapse formation (Shen and Cowan, 2010). Because this dissertation focuses on the modulation of growth cone motility during neuronal pathfinding, before the event of synaptogenesis, I will next introduce how growth cone pathfinding is achieved by various guidance cues.

1.2.2 Guidance cues elicit growth cone pathfinding

Growth cones respond to a variety of guidance cues they encounter in the environment by changing growth cone motility and structure (Dent et al., 2011). Through this mechanism, a growth pathway is determined. Guidance cues are released from certain neurons or tissues and are processed by the activation of membrane receptors in growth cones, resulting in the initiation of intracellular signaling cascades to activate appropriate growth cone behaviors. Generally, these guidance cues can be divided into the following two groups based on their functions (Lowery and Van Vactor, 2009).

1) Adhesive cues. This type of cue is expressed on the cell surface of glial cells or neurons, where the growing axons encounter transmembrane cell adhesion molecules, such as cadherins (Wanner and Wood, 2002). They can also be assembled as part of the extracellular matrix, such as laminin (Evans et al., 2007; Maness and Schachner, 2007). The main function of adhesive cues is to serve as physical substrate to allow cell attachment and axon extension.

2) Chemotropic cues. They are essential for giving directional information and steering the travelling growth cone. Based on their ability to induce positive or negative turning responses, they are further grouped into chemoattractive cues and chemorepulsive cues. Chemotropic cues include a large pool of neurotrophic factors, neurotransmitters, secreted transcription factors, etc (Lowery and Van Vactor, 2009; Shen and Cowan, 2010). Here I highlight a few well-studied chemotropic cues to explain their actions in inducing growth cone turning behaviors.

The neurotrophin nerve growth factor (NGF) is long established as a chemoattractive cue, in addition to its roles in cell differentiation, maintenance, survival and morphogenesis of certain neurons (Snider, 1994), thanks to the historical study by Viktor Hamburger and Rita Levi-Montalcini (Cowan, 2001). Sensory neurons of dissociated dorsal root ganglion (DRG) from chick embryos extend their axons towards a gradient of NGF (Letourneau, 1978). *In vivo* study showed that the sympathetic target innervation is absent in neonatal NGF knockout mice (Glebova and Ginty, 2004), further supporting the importance of NGF in sympathetic axon growth and target determination. Both the low-affinity NGF receptor p75 and the high-affinity receptor TrkA are shown to be involved in the NGF-induced positive turning response in the growth cone of chick DRG neurons (Gallo et al., 1997).

Semaphorins are known as chemorepulsive cues, which repel the axons of sensory neurons by causing collapse of the growth cone (Luo et al., 1993). The main receptors for

semaphorins are plexins. Axons of DRG and hippocampal neurons from Plexin-A3 knockout mice are resistant to the repulsive response induced by Sema3 (Cheng et al., 2001). In addition, hippocampal afferent projections in Plexin-A3 knockout mice are defective, and end up in an inappropriate terminal region (Cheng et al., 2001).

Netrins are a family of proteins secreted by axonal target cells, which impact the growth cones of neurons in the developing nervous system. Interestingly, they can induce either attractive or repulsive responses depending on the receptors that netrins interact with (Moore et al., 2007). The deleted in colorectal cancer receptor in mice (UNC-40 in C. elegans) is expressed in the axons of trochlear motor neurons and mediates netrin-1-induced positive turning, thereby directing the axonal growth away from the ventral midline (Li et al., 2008). On the other hand, the interaction between UNC-6, a netrin-1 homolog in C. elegans, and its UNC-5 receptor will repel growing axons (Jarjour et al., 2003).

1.2.3 Intracellular calcium signals mediate growth cone turning

Once guidance cues bind to their membrane receptors in growth cones, a number of intracellular signaling cascades will be initiated, which translate the information of guidance cues into the meaningful changes at the level of growth cone cytoskeleton. Within the large pool of intracellular second messengers, calcium (Ca) plays a central role, because the signaling elicited by a variety of environmental cues converges on Ca signals (Henley and Poo, 2004; Zheng and Poo, 2007). The concentration of intracellular Ca ($[Ca]_i$) is important to regulate growth cone motility and neurite outgrowth. An increase in filopodial length, reduction in filopodial number, and slow down of neurite extension speed have been reported when $[Ca]_i$ is elevated globally in growth cones (Cohan and Kater, 1986; Kater et al., 1988; Rehder and Kater, 1992). More interestingly, spatially restricted $[Ca]_i$ signals mediate growth cone turning

behaviors (Gomez and Spitzer, 2000). A high $[Ca]_i$ gradient across the growth cone (200 nM) leads to attractive turning, whereas a relatively low $[Ca]_i$ gradient (100 nM) causes repulsive turning in cultured *Xenopus* spinal neurons (Henley et al., 2004). Moreover, an elevation of $[Ca]_i$ causes growth cone repulsion, normally induced by myelin-associated glycoprotein (MAG), to become attractive turning (Henley et al., 2004), further supporting the essential role of Ca signals in growth cone turning behaviors.

How is the $[Ca]_i$ regulated in growth cones? One of the major pathways is Ca influx via membrane channels and receptors permeable to Ca. Voltage gated Ca channels (VGCCs), L-type channels in particular, are obvious sources contributing to the elevation of $[Ca]_i$ in growth cones. Electrical stimulation of neurons causes Ca influx through instantly opening VGCCs to affect growth cone $[Ca]_i$ (Torreano and Cohan, 1997). Additionally, a long list of membrane channels and receptors, including transient receptor potential (TRP) channels (Wang and Poo, 2005), glutamate receptors (Zheng et al., 1996), and nicotinic acetylcholine receptors (nAChRs) (Zheng et al., 1994), allow Ca influx and have been demonstrated to regulate axon pathfinding.

Another major pathway for $[Ca]_i$ elevation is Ca release from internal stores. The endoplasmic reticulum (ER) contains inositol triphosphate receptors (IP_3Rs) and ryanodine receptors (RyRs), which control the release of Ca intracellularly (Berridge, 1998; Berridge et al., 2003; Jiang et al., 2010). Depletion of internal Ca stores by thapsigargin or the inhibition of Ca release from RyRs using a high concentration of ryanodine abolishes the MAG-induced repulsive turning (Henley et al., 2004), suggesting that Ca release from internal stores is necessary for MAG signaling.

Interestingly, some guidance cues involve both sources of Ca to elicit their effects on axon pathfinding (Henley and Poo, 2004). A Netrin-1 gradient elevates $[Ca]_i$ to result in positive

turning of the growth cones in cultured *Xenopus* neurons (Ming et al., 1997). Further study revealed that the reduction of Ca signals by either blocking Ca influx or inhibiting Ca release leads to the switch of netrin-1-induced turning from attraction to repulsion (Hong et al., 2000). Taken together, $[Ca]_i$ plays key roles in mediating growth cone responses to various environment cues. Through the fine spatiotemporal regulation of Ca signals in growth cones, guidance cues will elicit their effects on growth cone steering behaviors.

1.2.4 Cytoskeletal mechanism of growth cone filopodial dynamics

The sensory structures of the growth cone, filopodia, are essential for growth cone motility and are highly sensitive to intracellular Ca signals. Global elevation of $[Ca]_i$ leads to filopodial elongation followed by a massive loss of filopodia (Rehder and Kater, 1992). The asymmetrical elongation of filopodia in growth cones induced by localized Ca signals underlies growth cone turning (Gomez et al., 2001). The converging cytoskeletal targets of all intracellular second messengers in growth cones are actin filaments and microtubules. Whereas microtubules contribute to the neurite extension rate, filopodial dynamics are primarily determined by the changes in actin (Lowery and Van Vactor, 2009). Polymerization of filamentous actin (F-actin) will cause the initiation and elongation of filopodia (Mattila and Lappalainen, 2008).

The identification of cytoskeleton-related proteins that link intracellular second messengers to the growth cone cytoskeleton is of interest to the field. Small GTPases of the Rho superfamily are one of the key players that regulate the actin cytoskeleton. Within this family, CDC42 is particularly important in the formation of filopodia (Ridley, 2006). The Ca/CaMKII-induced activation of CDC42 stimulates neuronal Wiskott-Aldrich Syndrome protein to induce actin filament nucleation and branching in a ARP2/3 complex-dependent manner (Carlier et al., 1999; Zhou et al., 2013). RhoA, another major Rho GTPase, can also be stimulated by the

Ca/CaMKII pathway, which in turn activates downstream signaling of ROCK/LIM Kinase/cofilin, leading to actin depolymerization to inhibit growth cone motility (Yanyi et al., 2010; Chen et al., 2011; Sit and Manser, 2011; Xue et al., 2013). Moreover, actin-binding protein ENA/VASP, localized at the leading edge of the filopodia, functions to enhance filopodia formation via its anti-capping activity of actin filament barbed ends (Bear et al., 2002). The protein profilin promotes actin polymerization by forming profilin-actin complexes to be added into growing actin polymers (Li et al., 2008). In contrast, cofilin, the actin severing protein, is involved in actin depolymerization (Yang et al., 1998). Taken together, cytoskeletal changes induced by guidance cues and mediated by intracellular second messengers and cytoskeleton-binding proteins will finally lead to the changes of growth cone motility.

1.3 Electrical activity

Neurons are the most diverse cell type in the brain. They interconnect and, most importantly, communicate with each other. For example, the sensory neurons translate environmental signals, like touch on your hand, into electrical signals, which are interpreted centrally and result in the control of the movement of the hand in response to the touch. Therefore, by using electrical signals, neurons manage to rapidly and precisely conduct information over long distances, which is crucial for maintaining regular brain functions.

Electrical signals are coded by the frequency and pattern of action potentials (APs), which propagate within a neuron while transferring information from one location to another (Bean, 2007). A large number of ion channels and receptors, membrane-spanning proteins permeable to different ions depending on the channel and receptor type, are known to be important for the generation and propagation of the AP (Armstrong and Hille, 1998).

1.3.1 K channel overview

K channels are membrane proteins present in virtually all types of cells, where they are involved in a variety of physiological functions (Sandhiya and Dkhar, 2009). Generally, the opening of K channels causes hyperpolarization of the membrane potential and dampens neuronal excitability by allowing rapid and selective flow of K ions across the cell membrane, a process essential for controlling neuronal excitability (Coetzee et al., 1999). In the nervous systems, K channels are subjected to the modulation by a variety of neurotransmitters (Harris-Warrick et al., 1998; Sakurai et al., 2006).

There are four major classes of K channels: voltage gated K (Kv) channels; Ca-activated K channels; inwardly rectifying K (Kir) channels; and two-pore domain K (TASK) channels. Kv channels are purely sensitive to the transmembrane voltage. During APs, Kv channels contribute to the repolarization phase and help in returning the depolarized cells to a resting condition. Ca-activated K channels are highly sensitive to intracellular Ca. Increases in $[Ca]_i$ will lead to the opening of these channels. Kir channels pass current in the inward direction, unlike most K channels with outward currents. TASK channels are also known as leak K channels and primarily function in the maintenance of the resting membrane potential.

1.3.1.1 Kv channels

Kv channels are composed of four identical subunits, and each subunit contains six transmembrane domains. Mainly two types of purely voltage gated K channels, delayed rectifier K channels and transient outward (A-type) K channels, have been identified (Sakakibara *et al.*, 2005).

Delayed rectifier K channels mediate slowly-inactivating or non-inactivating K currents, which are slowly activated by membrane depolarization and mainly contribute to the plateau

phase of repolarization of the APs (Blaine and Ribera, 2001). They are highly sensitive to tetraethylammonium (TEA) chloride, and blockade of delayed rectifier K channels significantly broadens the AP waveform (Berdan and Easaw, 1992). In the auditory MNTB principal neurons, the Kv3 current is inhibited in postsynaptic neurons by physiological release of NO, which allows for the modulation of neuronal excitability and synaptic efficacy (Steinert et al., 2008).

A-type K channels conduct fast activating and rapidly inactivating K currents, which start to be activated at more negative membrane potentials compared to the delayed rectifier K channels. Therefore, A-type K channels not only participate in the initial repolarization of the AP (Staras et al., 2002) but also are involved in the regulation of spike frequency (Kang et al., 2000). Elimination of an A-type K current mediated by the Kv4 channel significantly shortens the latency to the first spike in response to depolarizing current injection in developing granule cells (Shibata et al., 2000). 4-aminopyridine (4AP) is a prominent blocker of A-type K channels.

1.3.1.2 Ca-activated K channels

A rise in cytosolic Ca activates a large family of K channels, namely Ca-activated K channels. They are found to regulate firing properties of neurons in a wide variety of cell types throughout the central nervous system (Faber and Sah, 2003). Two major Ca-activated K channels, large conductance (BK) and small conductance (SK) channels, have been identified at the molecular level.

BK channels, initially being cloned from Drosophila (Adelman et al., 1992), have a large unitary conductance (100 to 300 pS). They are activated by both binding of cytosolic Ca and membrane depolarization. Pharmacological blockers include TEA in the micromolar range and iberiotoxin (IbTX) from the scorpion venom (Lee and Cui, 2010). The BK channel is composed of the pore-forming α subunit with a large C terminus and the modulatory β subunit. The β

subunit has been thought to modify the voltage dependence of activation and affect the Ca sensitivity of the channel (Wallner et al., 1999). Due to their sensitivity to the membrane potential, BK channels are activated during APs and contribute to the acceleration of AP repolarization (Jaffe et al., 2011; Scott et al., 2011). In addition, BK channels are responsible for the fast afterhyperpolarization (AHP), a fast hyperpolarizing potential following an AP. Treatment with low concentrations of TEA or IbTX blocks the fast AHP in many neurons (Shao et al., 1999).

SK channels have a smaller unitary conductance (2 to 20 pS), which are solely activated by increases in intracellular Ca and are not sensitive to changes in membrane voltage (Stocker, 2004). Multiple Ca-related proteins, including calmodulin, protein kinase CK2, and protein phosphatase 2A, are involved in the regulation of the Ca sensitivity of SK channels (Adelman et al., 2012). A wide range of neurotransmitters have been found to modulate SK channels via activation of protein kinases (Torres et al., 1996). A potent pharmacological inhibitor for the channel is the bee venon, apamin, the discovery of which significantly promoted our understanding of the structure and function of SK channels (Romey et al., 1984). The slow AHP mediated by SK channels is seen after a single AP in some cell types, but it has been more commonly observed after a train of APs (Hirst et al., 1985). The slow AHP functions to progressively reduce the AP frequency, a phenomenon called spike frequency adaptation, which in turn dampens the neuronal response to long-term excitation (Yen et al., 1999; Vandael et al., 2012).

AP waveform can determine the amount of Ca influx during each AP, whereas AP frequency acts as another parameter to determine the magnitude of Ca influx. Both Kv channels and Ca-activated K channels play major roles in the modulation of the AP waveform and spike

frequency and serve as ideal targets for various neurotransmitters and neuromodulators to affect cell excitability in the nervous system.

1.3.2 Voltage gated Ca channels

One of the determinants for intracellular Ca are VGCCs. A variety of Ca channels have been identified in the plasma membrane and are grouped into two categories based on their voltage sensitivity, high-voltage activated Ca channels and low-voltage activated Ca channels (Catterall, 2000). High-voltage L-type Ca currents are distinguished by a large unitary conductance and slow voltage-dependent inactivation. Low-voltage T-type Ca currents have a small unitary conductance and rapid voltage-dependent inactivation (Catterall, 2011). Both Ca currents have been characterized in gastropods and mediate physiological functions ranging from the control of synaptic transmission to the regulation of growth cone motility (Haydon and Man-Son-Hing, 1988; Spafford et al., 2003; Spafford et al., 2006; Hui and Feng, 2008).

As the main contributor to Ca influx, VGCCs play key roles in mediating the depolarization-induced changes in neurite elongation, growth cone motility and axon pathfinding (Mattson and Kater, 1987; Cohan, 1992; Zheng and Poo, 2007).

1.3.3 Ligand gated ion channels

In addition to voltage-gated ion channels, a large Cys-loop family of ligand-gated ion channels (LGICs) are activated by the binding of neurotransmitters (Le Novere and Changeux, 1995) and function in chemical synapses to transfer information from one neuron to the other. In mammals, inhibitory glycine and $GABA_A$ receptors conduct anions that mediate membrane hyperpolarization, whereas excitatory 5-HT_3 and nicotinic ACh receptors are selective for cations, and opening of these receptors leads to depolarization of the membrane potential (Jensen et al., 2005). The LGICs are composed of two different domains, an extracellular ligand-binding

domain providing an allosteric binding site, and a transmembrane domain, which forms the ion pore for ion selectivity. Each receptor exists as a pentameric complex, assembled either by the composition of five different subunits or from five copies of a single subunit (Clementi *et al.*, 2000).

1.3.3.1 Ionotropic nicotinic ACh receptors

The nicotinic ACh receptor (nAChR) was the first characterized LGIC. It was originally discovered at the neuromuscular junction, and these receptors were subsequently found throughout the nervous system (Phillis, 2005). Mammalian nAChRs have been extensively studied (Itier and Bertrand, 2001). Depending on the composition of the receptor subunits, nAChRs are in charge of a variety of physiological functions (Clementi et al., 2000). Some heteropentameric nAChRs composed of both α and β subunits are mainly permeable to Na and K, with a minimal Ca permeability. The Na influx via nAChRs causes a strong membrane depolarization. The change in membrane voltage in turn could open VGCCs to initiate downstream signaling cascades. nAChRs of the α3β2 type located in presynaptic terminal have been found to enhance the release of ACh (Jonsson et al., 2006). Some homopentameric nAChRs formed by the subunits α7 to α9 possess a high Ca permeability (Fucile et al., 2005). ACh can induce a significant increase in $[Ca]_i$ via activation of α7 nAChR homomers, and this receptor is found to be distributed in the rat hippocampus, amygdala, cerebral cortex (Seguela et al., 1993).

ACh is known to serve as a chemoattractive cue for growing axons of *Xenopus* spinal neurons during neuronal development (Zheng et al., 1994). Moreover, nAChR α7 subunits have been found to be enriched in the growth cone of embryonic cortical neurons (Nordman and Kabbani, 2012). These results raise the possibility that ACh could be an important regulator for developing neurons. A dozen nAChR subunits have been cloned in the pond snail *Lymnaea*

stagnalis, a closely related species (van Nierop *et al.*, 2005; van Nierop *et al.*, 2006), although the functions of these receptors have yet to be characterized in the nervous system. Considering that nAChRs participate in the regulation of intracellular Ca and the exciting molecular evidence of nAChRs in gastropods, **I propose a role for nAChRs in regulating growth cone motility in this dissertation**.

1.3.4 Metabotropic dopamine receptors

Two distinct types of receptors mediate the action of various neurotransmitters. One type is the ionotropic receptor, which forms an ion channel pore, such as the LGICs mentioned above (Keramidas et al., 2004). The other type is the metabotropic receptor, a large group of G protein-coupled receptors, such as muscarinic ACh receptors (mAChRs), $GABA_B$ receptors, and dopamine (DA) receptors (Kobilka, 2007). Ligand binding to the metabotropic receptor activates G-proteins, which in turn initiate intracellular second messenger cascades and indirectly regulate membrane excitability and channel activity. Depending on the specific G-protein type that is activated by the neurotransmitter, the output of G-protein-coupled effector systems could be either excitatory or inhibitory (Marinissen and Gutkind, 2001).

DA receptors are such G-protein coupled receptors. They are grouped into 2 subtypes based on their ability to regulate adenylyl cyclase activity: D1-like receptors stimulate adenylyl cyclase via G_s, and D2-like receptors inhibit adenylyl cyclase via G_i (Sunahara et al., 1993; Beaulieu and Gainetdinov, 2011). In addition, some DA receptors have been found to activate PLC via G_q (Rashid et al., 2007). DA signaling is known to modulate a variety of ionic currents, including an A-type K current (Zhang *et al.*, 2010), an inwardly rectifying K current (Kuzhikandathil et al., 1998), and a hyperpolarization and cyclic nucleotide gated (CNG) cation current (Harris-Warrick et al., 1998; Liss and Roeper, 2008).

In gastropods, DA has been shown to be an important neurotransmitter for the initiation and regulation of respiratory and feeding circuits (Magoski and Bulloch, 1999; Kabotyanski et al., 2000). Although DA signaling is known to involve a K conductance to modulate neuronal activity (de Vlieger et al., 1986), our understanding of how DA initiates second messenger cascades and which subtypes of membrane channels are under the control of DA signaling, are incomplete. *Helisoma* B5 neurons innervate the esophagus and participate in feeding behavior (Perry et al., 1998). Inside the buccal ganglion, B5 neurons are surrounded by dopaminergic processes (Quinlan et al., 1997). Based on the information collected from other molluscan systems, **I am investigating whether DA regulates the electrical activity of B5 neurons to influence feeding behavior in *Helisoma***. Furthermore, a goal of this dissertation is to dissect the signaling pathway and membrane targets underlying the action of DA.

1.3.5 Roles of electrical activity in early neuronal development

With the knowledge that electrical activity is determined by a large number of ion channels and membrane receptors, it is not surprising to discover that electrical activity is involved in the regulation of many stages of neuronal development (Spitzer, 2006). Neural progenitor cells in the embryonic rat ventricular zone are depolarized by GABA and glutamate, which elevates intracellular Ca and, in turn, inhibits DNA synthesis to regulate neuronal proliferation (LoTurco et al., 1995). The activation of voltage gated Ca channels and NMDA receptors are required in the normal migration of postnatal mouse cerebellar granule cells (Komuro and Rakic, 1996). Neuronal differentiation is largely dependent on the correct expression of voltage gated ion channels to control the level of cell excitability (Moody, 1998). A G-protein coupled Kir channel has been implicated to be important in maintaining the membrane permeability for the normal differentiation of cerebellar granule cells (Patil et al.,

1995). Moreover, appropriate specification of neurotransmitters in embryonic neurons is regulated by the development of Ca-dependent APs (Spitzer et al., 2004). Electrical stimulation of dissociated primary sensory neurons will promote the expression of tyrosine hydroxylase, an enzyme in dopamine synthesis, in a transcription-dependent manner (Brosenitsch and Katz, 2001; Brosenitsch and Katz, 2002).

1.3.5.1 Electrical activity is important for growth cone motility and axon pathfinding

Electrical activity has also been found to regulate migrating growth cones at the tip of growing neurites. Brief electrical stimulation would not only slow the advance of neurite elongation but also reduce the filopodial number in cultured *Helisoma* neurons (Cohan and Kater, 1986). Moreover, electrical stimulation could influence growth cone steering induced by guidance cues (Ming et al., 2001). Ca signals seem to couple with electrical activity in mediating these effects, in which case extracellular Ca flows into the growth cones via ion channels, such as VGCCs (Nishiyama et al., 2011), CNG channels (Togashi et al., 2008), and TRP channels (Wang and Poo, 2005). Elevation of intracellular Ca would in turn result in changes in the cytoskeleton to affect growth cone behaviors.

The importance of the membrane potential in growth cones has been convincingly demonstrated in axon pathfinding of developing *Xenopus* spinal neurons. The attractive cues netrin-1 and brain-derived neurotrophic factor (BDNF) depolarize growth cone membrane potential, whereas repulsive cues Sema3A and Slit2 cause hyperpolarization (Nishiyama et al., 2008). During netrin-1-induced chemoattraction, L-type VGCCs are found to be directly modulated in axonal growth cones and largely contribute to the Ca elevation (Nishiyama et al., 2003). Clamping the growth cone potential at a depolarized state would convert the Sema3A-induced repulsion to attraction, further suggesting a causal relationship between membrane

potential and growth cone turning behaviors (Nishiyama et al., 2008). Interestingly, Ca signaling is involved in the Sema3A-induced hyperpolarization. CNG channels, Ca-conducting cation channels activated by cyclic nucleotides, have been found to be present in *Xenopus* spinal neurons, and Ca influx via these channels is required for the growth cone repulsion induced by Sema3A (Nishiyama et al., 2008).

In addition to those conventional ion channels involved in the regulation of growth cone behaviors, TRP channels have been suggested to play an unexpected role in axonal growth (Gomez, 2005). TRP channels are non-selectively permeable to cations including Ca (Clapham, 2003). Depending on the type of TRP channel, they can be activated by intracellular signaling via PLC, DAG, or even mechanical stretch of the membrane. TRP channels allow Ca influx near the resting membrane potential, which make them good candidates for elevating the $[Ca]_i$ inside growth cones (Talavera et al., 2008). In fact, they are found to mediate BDNF-induced positive turning in the growth cone of *Xenopus* spinal neurons (Li et al., 2005). In addition to their Ca permeability, the membrane depolarization introduced by TRP channels will be further amplified via activation of VGCCs. Both Ca channels and TRP channels have been implicated to contribute to the netrin-1-induced chemoattractive turning of *Xenopus* growth cones (Wang and Poo, 2005). Study in intact animals showed that TRP channels are required for the correct axon guidance of commissural interneurons at the midline in the developing *Xenopus* spinal cord (Shim et al., 2005). These data strengthens the notion that *the membrane potential is a critical mediator for guidance cues to elicit their effects at the growth cone level.*

1.4 *Helisoma trivolvis* as an ideal model system

Molluscan nervous systems were established as valuable model systems to study neurobiology-associated questions. They have following advantages:

1) Distinctive organization of the nervous system with a relatively small number of neurons.
2) Large identifiable neurons. Some neurons are sized 100 μm in diameter, ten times larger than average mammalian neurons.
3) Easy for neuronal isolation and culture *in vitro*, allowing to study cell growth at the single cell resolution
4) Specified circuitry responsible for behaviors such as feeding, simple forms of learning, etc.

These advantages pose opportunities for researchers to perform experiments in cellular, molecular, physiological, and behavioral neuroscience. Dr. Alan Hodgkin and Dr. Andrew Huxley won the Nobel Prize in Physiology or Medicine in 1963 for their work revealing ionic mechanism of action potentials on the squid giant axon. Dr. Eric Kandel was awarded for the Nobel Prize in 2000 for his work furthering the understanding of cellular and molecular mechanisms of memory formation using the sea slug *Aplysia californica*.

In the 1970s, Dr. Stanley B. Kater brought *Helisoma trivolvis*, a pond snail, into the laboratory, and since then, *Helisoma* has quickly become a model for studying neuronal development and neurophysiology. Dr. Don Murphy wrote an in-depth review paper discussing the neural organization underlying feeding, describing the neurons of the feeding circuitry located inside the buccal ganglion (Murphy, 2001). Among buccal neurons, neurons B5 and B19 are two of the largest neurons and they being used in the current study. The B5 neuron sends out its main axon through the ipsilateral esophageal trunk nerve, which innervates the muscle of the esophagus (Scannell et al., 2008). Excitation of the homologue neurons in *Lymnaea stagnalis*, a closely related species, leads to contraction of the foregut, whereas silencing the neuron relaxes it (Perry et al., 1998). Motoneuron B5 has been implicated to be not only cholinergic but also

nitrergic. Therefore, it could release nitric oxide to affect neuronal properties of other neurons (Haydon and Zoran, 1989; Artinian et al., 2010). Buccal neurons B19 in *Helisoma* are bilaterally symmetric motor neurons immediately downstream of the feeding central pattern generator and they innervate muscle groups in the radula, which participate in the retraction of the structure during rhythmic feeding movements (Murphy, 2001; Turner et al., 2011). The main projections of B19 neurons extend across the buccal commissure contralaterally and through the ventral buccal nerve, but they also have ipsilateral projections through both the ventral buccal nerve and lateral buccal nerve (Scannell et al., 2008).

In addition to the advantage of studying neuronal circuitry, neurons isolated from the *Helisoma* nervous system undergo regeneration processes after removal from the nervous system and being placed in culture. This setup allows for studying neuronal development and regeneration (Wong et al., 1981). Questions like what are the growth-promoting and inhibiting factors (McCobb et al., 1988; Berdan and Easaw, 1992), what are the intracellular messengers in mediating cell growth (Mattson and Kater, 1987; Mattson et al., 1988), and how do changes in cytoskeleton underlie growth cone behaviors (Welnhofer et al., 1997; Torreano et al., 2005) have been addressed using the *Helisoma* neuronal culture system. Besides, *Helisoma* neurons have particular advantages for studying growth cone motility (Kater and Rehder, 1995). The large sized growth cone (10 to 50 μm in size) enables the identification of key components including central domain, lamellipodium, and filopodia. Therefore, highly motile filopodial behavior from neurons grown on glass-coverslip can be visualized easily by phase-contrast microscopy and fluorescence microscopy at a high resolution. When B5 and B19 neurons are isolated and cultured in tissue culture dishes, they show distinct growth cone morphology and tend to keep their membrane receptor properties as they did *in vivo* (Haydon et al., 1985; Zhong et al., 2013).

In the Rehder lab, we are interested in understanding *the cellular mechanisms underlying the regulation of growth cone filopodial dynamics and neuronal excitability*. In a series of studies on NO, we provided convincing evidence that NO serves as a regulator for growth cone motility and neuronal excitability. We also characterized the signaling pathway that mediates the effects of NO on growth cone motility. NO elevation caused filopodial elongation, a significant loss of filopodia, and a slow-down of the neurite outgrowth rate in buccal neuron B5 (Van Wagenen and Rehder, 1999; Trimm and Rehder, 2004). NO activates soluble guanlylate cyclase, which initiates the production of cyclic guanosine monophosphate (cGMP) (Van Wagenen and Rehder, 2001). Downstream of cGMP is protein kinase G (PKG). The activation of PKG elevates the level of cyclic ADP ribose, which in turn releases Ca from ryanodine sensitive Ca stores in the ER along with a Ca influx component via VGCCs (Welshhans and Rehder, 2005; Welshhans and Rehder, 2007). Further studies revealed that B5 neurons not only respond to NO but also release NO (Tornieri and Rehder, 2007). NO release from B5 neurons can actually result in similar filopodial responses as seen after treatment with a NO donor, such as NOC7.

In addition to the role of NO controlling growth cone motility, we also reported that NO regulates neuronal excitability by modulating various ionic conductances. The effects of NO on ion channels are two-fold. First, extrinsic NO elevation primarily inhibited Ca-activated K channels, apamin-sensitive SK channels and IbTX-sensitive BK channels, to lead to membrane depolarization (Artinian et al., 2010). Secondly, intrinsic NO production maintained a persistent Na current, voltage-gated Ca currents and partially inhibited SK channels (Artinian et al., 2010). Interestingly, the effects of NO stimulation on growth cone motility and neuronal excitability occur with a similar time course, which raises the interesting question *whether the regulation of*

neuronal electrical activity mediates growth cone responses to external stimulation. Studies in this dissertation aim to better understand this central question.

The motoneuron B19 is located in the vicinity of NO-producing neurons in the buccal ganglion (Murphy, 2001), and it is active during the feeding motor patterns (Turner et al., 2011). NO is known to regulate the buccal feeding motor program (Susswein and Chiel, 2012). This evidence leads to the question **whether NO might affect the electrical activity of B19 neurons by volume transmission**. In this dissertation, I further characterize the ion channels affected by NO, and investigate if NO acts on similar sets of ion channels in B5 and B19 neurons. *This study will test the notion that NO serves as a general modulator of neuronal activity*.

1.5 Dissertation summary

Chapter 2 describes experiments that focus on the cholinergic modulation of growth cone motility and neuronal excitability. I report that bath application of ACh to *Helisoma* B5 neurons causes a rapid increase in filopodial length. I show that the effect of ACh requires Ca influx to elevate the $[Ca]_i$ of the growth cone. Furthermore, electrophysiological results reveal that ACh opens nAChRs to depolarize the membrane potential, which allows Ca to flow into the cell. Lastly, studies of physically isolated growth cones indicate that ACh can act locally at the growth cone to elongate filopodia, which strengthens the notion that ACh is able to act as a local signal to determine neuronal pathfinding and/or synaptogenesis.

Chapter 3 summarizes work that tests the modulatory role of NO in B19 neurons. In these experiments, I report that NO causes a sustained depolarization of membrane potential and increases neuronal excitability. I describe that K channels instead of Ca channels are the targets of NO. I further show that the depolarization induced by NO is mediated by the closure of two types of Ca-activated K channels, apamin-sensitive SK channels and IbTX-sensitive BK

channels. The depolarizing effect of NO is mainly contributed by the inhibition of the SK channels.

Chapter 4 details experiments testing the question whether DA modulates the electrical activity of B5 neurons to exert functions in support of feeding. I show that DA application causes a strong hyperpolarization in both physically isolated B5 neurons *in vitro* and B5 neurons within the buccal ganglion *in situ*. The signaling mechanism underlying the hyperpolarizing effect of DA is that activation of a D2-like receptor leads to activation of PLC signaling, which opens both TEA-sensitive and 4AP-sensitive K channels.

Taken together, these experiments reveal the crucial roles of ACh, NO, and DA in determining the electrical activity and growth cone motility of developing neurons. The dissertation also characterizes the intracellular signaling pathways and ionic conductances that mediate these effects. A discussion is presented within each chapter (Chapters 2 - 4), followed by a comprehensive overall discussion in Chapter 5, which specifically discusses the potential roles of neuromodulators in regulating neuronal development and affecting neural circuits and its associated behaviors.

CHAPTER 2 ACETYLCHOLINE ELONGATES NEURONAL GROWTH CONE FILOPODIA VIA ACTIVATION OF NICOTINIC ACETYLCHOLINE RECEPTORS

Published as **Zhong L.R.**, Estes S., Artinian L. and Rehder V. (2013) Acetylcholine elongates neuronal growth cone filopodia via activation of nicotinic acetylcholine receptors. Developmental Neurobiology. DOI: 10.1002/dneu.22071.

2.1 Acknowledgements

We would like to thank Dr. Chun Jiang for expert advice on the electrophysiological experiments and their analysis. This work was supported, in part, by NSF award # 0843173 to VR, Brains and Behavior Fellowships to LRZ and SE, Sigma Xi grants-in-aid of research grant, GSU dissertation grant to LRZ.

2.2 Abstract

In addition to acting as a classical neurotransmitter in synaptic transmission, acetylcholine (ACh) has been shown to play a role in axonal growth and growth cone guidance. What is not well understood is how ACh acts on growth cones to affect growth cone filopodia, structures known to be important for neuronal pathfinding. We addressed this question using an identified neuron (B5) from the buccal ganglion of the pond snail *Helisoma trivolvis* in cell culture. ACh treatment caused pronounced filopodial elongation within minutes, an effect that required calcium influx and resulted in the elevation of the intracellular calcium concentration ($[Ca]_i$). Whole-cell patch clamp recordings showed that ACh caused a reduction in input resistance, a depolarization of the membrane potential, and an increase in firing frequency in B5

neurons. These effects were mediated via the activation of nicotinic acetylcholine receptors (nAChRs), as the nAChR agonist dimethylphenylpiperazinium (DMPP) mimicked the effects of ACh on filopodial elongation, $[Ca]_i$ elevation, and changes in electrical activity. Moreover, the nAChR antagonist tubucurarine blocked all DMPP-induced effects. Lastly, ACh acted locally at the growth cone, because growth cones that were physically isolated from their parent neuron responded to ACh by filopodial elongation with a similar time course as growth cones that remained connected to their parent neuron. Our data revealed a critical role for ACh as a modulator of growth cone filopodial dynamics. ACh signaling was mediated via nAChRs and resulted in Ca influx, which, in turn, caused filopodial elongation.

KEYWORDS: *Helisoma trivolvis*, growth cone, filopodia, intracellular Ca, neuronal excitability.

2.3 Introduction

During early development, neurons extend neurites to connect to appropriate target cells. Growth cones at the tip of growing neurites are important for pathfinding and its filopodia serve as sensors to probe the environment for guidance cues (Rehder et al., 1996; Gomez and Zheng, 2006; Farrar and Spencer, 2008). ACh, besides serving as a classical neurotransmitter in synaptic transmission, has been shown to play an unconventional role in axonal growth (Lauder and Schambra, 1999; Phillis, 2005). ACh inhibits neurite outgrowth in several neuronal cell types (Owen and Bird, 1995; Small et al., 1995; Rudiger and Bolz, 2008), and induces positive turning responses of growth cones in *Xenopus* spinal neurons *in vitro* (Zheng *et al.*, 1994). In molluscan nervous systems, ACh is suggested to have a role in neurite extension (McCobb *et al.*, 1988). However, neither the functions of ACh at the level of the growth cone nor the underlying

mechanisms by which ACh affects growth cone filopodial dynamics have yet been fully understood.

Electrical activity has been shown to affect the neurite outgrowth rate of developing neurons (Neely and Nicholls, 1995). Evoked action potentials cease neurite outgrowth and growth cone advance in both vertebrate and invertebrate neurons (Cohan and Kater, 1986; Fields et al., 1990), and the depolarization-induced suppression of neurite elongation requires an increase in cytoplasmic Ca (Cohan, 1992). A more recent study further identified the critical role of electrical activity in growth cone turning induced by various guidance cues (Ming *et al.*, 2001). Whereas ACh is known to be involved in synaptic transmission and synapse formation in gastropods (Haydon, 1988; Elliott and Vehovszky, 2000), a comprehensive study of how cholinergic modulation of neuronal electrical activity may be linked to growth cone motility is presently lacking.

B5 neurons can be removed from the buccal ganglion of the pond snail *Helisoma trivolvis* and transferred into cell culture, where they regenerate within 1 - 3 days and develop large-sized growth cones, providing the opportunity to study filopodial dynamics at high resolution. ACh is found to be used in synaptic transmission between B5 neurons *in vitro* (Haydon and Zoran, 1989), making these identified neurons a model to study the role of ACh as a modulator of neuronal activity and filopodial motility.

The main goal of the current study was to evaluate the effect of ACh on growth cones and to identify the signaling pathway(s) activated by ACh in B5 neurons. We found that ACh decreased the input resistance (R_{in}), depolarized the membrane potential (RMP), increased the spiking frequency, elevated the intracellular Ca concentration ($[Ca]_i$) in growth cones, and elongated growth cone filopodia of B5 neurons. Extracellular Ca was required for these ACh-

induced changes at the growth cone. Activation of nAChRs was both necessary and sufficient in mediating ACh signals. We further found that the ACh-induced filopodial elongation can occur locally at growth cones. Taken together, this study demonstrates a modulatory role for ACh on B5 neurons, resulting in depolarization and filopodial elongation, and thereby suggesting a role for ACh in determining neuronal pathfinding and/or synaptogenesis.

2.4 Methods

2.4.1 Animals

Freshwater pond snails, *Helisoma trivolvis*, were kept in aerated aquaria (10 gallons) containing filtered water under a 12 h light-dark cycle at room temperature. They were fed with organic lettuce and vegetable-based algae wafers (Hikari, Doctors Forster and Smith) once a day. Animals with a shell diameter of 15 – 20 mm were used for neuronal culture.

2.4.2 Neuronal culture

Identified B5 neurons were isolated from the buccal ganglion of *Helisoma*, and plated into Falcon Petri dishes as previously described (Rehder & Kater, 1992). Briefly, neurons were plated onto poly-L-Lysine (hydrobromide, MW, 70-150 kDa, 0.25 mg/ml; Sigma, St. Louis, MO, USA)-coated glass coverslips attached to the bottom of 35-mm cell culture dishes (Falcon 1008). B5 neurons were kept in conditioned medium at room temperature and used for experiments 24 – 48 hours after plating. Conditioned medium was prepared by incubating two *Helisoma trivolvis* brains per 1 mL of Leibowitz L-15 medium (Invitrogen, Carlsbad, CA, USA) for 4 days (Wong et al., 1981). The composition of L-15 medium was as follows (mM): 44.6 NaCl, 1.7 KCl, 1.5 $MgCl_2$, 0.3 $MgSO_4$, 0.14 KH_2PO_4, 0.4 Na_2HPO_4, 1.6 Na pyruvate, 4.1 $CaCl_2$, 5 HEPES, 50 μg/ml gentamicin, and 0.15 mg/ml glutamate in distilled water, pH 7.4.

2.4.3 Growth cone image acquisition and analysis

Growth cones were viewed using a 100X oil immersion objective on a Sedival microscope (aus Jena, Germany). Phase-contrast images of growth cones were captured by a regular CCD camera (C-72, Dage-MTI, Michigan City, IN, USA) and analyzed with 'Scion Image' software (Scion Corporation, Frederick, MD, USA). Images for all experimental conditions were taken before (- 5 and 0 min) and at defined times (2, 5, 10, 15, 20, 25, 30, 40, 50, and 60 min) after drug treatment. Analysis of filopodial behavior was described previously (Trimm and Rehder, 2004). Briefly, filopodial length was analyzed by measuring the length of all individual filopodia from the tip to the edge of the central domain in one growth cone. Filopodial data were expressed as a percentage change normalized to the time point t = 0, which minimized the individual variability regarding to growth cone size and baseline filopodial length between different growth cones.

2.4.4 Calcium imaging

Growth cone calcium measurement was performed as previously described (Trimm and Rehder, 2004). Briefly, B5 neurons were injected with the cell-impermeable calcium indicator dye, Fura-2 pentapotassium salt (10 mM in H_2O; Molecular Probes, Eugene, OR, USA) and used 30 min after Fura-2 injection. Growth cone calcium imaging was achieved by employing an up-right microscope (BX51 W1F, Olympus, Japan), cooled CCD camera (Andor, TILL Photonics, Germany), and calcium imaging acquisition and analysis software (Live Acquisition, TILL Photonics, Germany). Fura-2 was excited at 340 and 380 nm, and the emission ratio (340/380) was used as an indicator of growth cone $[Ca]_i$. Growth cones were imaged for 5 min before, and up to 60 min after treatment. Image pairs were routinely obtained every 60 s and analyzed by placing a box over the central domain of the growth cone to quantify average fluorescence values.

In the experiment shown in Fig. 2.1(D) (representative example of 3 such experiments), the growth cone was imaged every 10 s and $[Ca]_i$ was measured simultaneously in filopodia, the central domain, and the neurite adjacent to the growth cone proper. The $[Ca]_i$ in filopodia was measured at filopodial half length for consistency. Growth cones with baseline fluorescence ratios above 0.5 indicated a higher resting level of $[Ca]_i$ and were excluded from the analysis.

2.4.5 Electrophysiology

Recordings from *Helisoma* B5 neurons in whole-cell current-clamp mode were obtained as described previously (Artinian et al., 2010). Patch electrodes were pulled from borosilicate glass tube (OD 1.5 mm; ID 0.86 mm; Sutter instruments) on a Sutter instruments micropipette puller (P-87) and heat polished (Micro Forge MF-830; Narishige) with resistances of about 3 - 8 MΩ. Recordings were made using an Axopatch 700B amplifier (Molecular Devices) and an analog-to-digital converter (Digidata 1440). Data acquisition and analysis were performed using pClamp software version 10.0 (Molecular Devices). Current-clamp configuration was used to record membrane potential, firing properties, and input resistance (R_{in}). Normal saline was used as extracellular recording solution, which contained (mM): 51.3 NaCl, 1.7 KCl, 4.1 $CaCl_2$, 1.5 $MgCl_2$, and 5 HEPES, pH 7.3 - 7.4 (127 mOsm). Intracellular recording solution contained (mM): 54.4 K-aspartate, 2 $MgCl_2$, 5 HEPES, 5 Dextrose, 5 ATP, and 0.1 EGTA (127 mOsm). Drug treatment and washout were achieved through a gravity-based perfusion system (Warner Instruments), switching among channels containing different reagents. Resting membrane potential (RMP) of spontaneous firing neurons was determined by measuring the value at the plateau of the depolarization phase before the membrane potential reached threshold. Continuous measurement of R_{in} was achieved by small hyperpolarizing current injection of - 50 pA for 1 s and repeated every 20 s. R_{in} was determined by dividing the peak change in membrane potential

by the magnitude of the injected current, and was then expressed as the percentage change normalized to R_{in} measured before treatment in order to remove individual variability between neurons.

2.4.6 Growth cone transection

The isolation of neuronal growth cones was achieved by severing the neurites close to the growth cone proper using a glass micropipette attached to a micromanipulator. Experiments on isolated growth cones were performed 60 min after the transection of neurites. This waiting period proved to be sufficient to restore filopodial motility to normal levels after the transient transection-induced filopodial elongation previously described in isolated growth cones (Rehder *et al.*, 1991).

2.4.7 Pharmacological agents and Ca-free conditions

All agents were purchased from Sigma. Acetylcholine (ACh), dimethylphenylpiperazinium (DMPP), and tubucurarine (TC) were dissolved in water to make 100 mM, 50 mM, and 100 mM stock solutions, respectively. For growth cone filopodia and calcium imaging experiments, stock solutions were mixed with 1 ml of conditioned medium removed from the culture dish and then gently added back around the periphery of the dish. 1 ml medium was then pulled out and released back into the dish for 3 times using a pipette to facilitate the equilibration of the drugs to their final concentrations. The Ca-free solution contained (mM): 51.3 NaCl, 5.6 $MgCl_2$, 5 HEPES and 0.3 EGTA, pH 7.3 - 7.4 (127 mOsm). Extracellular Ca-free conditions were achieved by removing 1.8 ml of medium from the culture dish, adding back Ca-free solution, and repeating these steps for a total of three rinses in Ca-free solution. For electrophysiological experiments, drugs were prepared directly in the extracellular solution, and perfused into the dish to achieve final concentrations.

2.4.8 Statistical analysis

All data were expressed as mean ± SEM. For growth cone filopodial analysis and calcium imaging results, a repeated-measures ANOVA was employed for testing overall statistical significance between conditions (SPSS statistical software, SPSS Inc., Chicago, IL, USA). The Tukey test was used for *post hoc* analysis of preplanned comparisons. An unpaired Student's *t*-test or paired *t*-test was used for testing statistical significance between individual time points depending on the experimental conditions. For electrophysiological data analysis, the significance of effects was evaluated by one-way ANOVA and Tukey's *post hoc* test using ORIGIN DATA ANALYSIS AND GRAPHING software (OriginLab, Northampton, MA, USA). Significant differences are indicated as $*P < 0.05$, $**P < 0.01$, and $***P < 0.001$.

2.5 Results

2.5.1 ACh elongates growth cone filopodia and elevates $[Ca]_i$ in growth cones

To investigate the effect of ACh on growth cone filopodial dynamics, we used identified B5 neurons extracted from buccal ganglia of the freshwater snail *Helisoma trivolvis* and investigated their morphology in response to various treatments. Experiments were performed after neurons had been cultured for 24 - 48 hours, at which time these neurons had extended well developed neurites tipped by motile growth cones (Welshhans and Rehder, 2005; Tornieri and Rehder, 2007). ACh had a significant overall effect on filopodial length ($F_{3,53} = 21.67$, $P < 0.001$; repeated-measures ANOVA) [Fig.2-1(B)]. Bath application of 0.5 μM ACh led to a transient but significant increase in filopodial length compared with the vehicle-only control condition (Tukey's *post hoc*, $P < 0.001$) [Fig. 2.1(A and B)]. The ACh-induced filopodial elongation started as early as 2 min after treatment, and reached its maximal response (an increase by 40.5 ±

2.6%, n = 15) at 5 min following ACh application. After that, filopodial length slowly decreased in the continued presence of ACh and fully returned to the baseline levels 25 min after treatment.

In previous studies, filopodial elongation had been shown to be elicited by transient increases in the intracellular calcium concentration ($[Ca]_i$) in growth cones (Rehder and Kater, 1992; Van Wagenen and Rehder, 1999; Cheng et al., 2002). Therefore, we next measured $[Ca]_i$ in growth cones using the calcium indicator Fura-2. ACh had a significant overall effect on $[Ca]_i$ ($F_{3,51} = 76.94$, $P < 0.001$; repeated-measures ANOVA). 0.5 μM ACh treatment caused an immediate and significant elevation in $[Ca]_i$ compared to the vehicle-control group (Tukey's *post hoc*, $P < 0.001$)[Fig. 2.1(C)], as indicated by the fluorescence emission ratio at excitation wavelengths of 340 and 380 nm. The Fura-2 ratio was elevated significantly from the baseline level of 0.32 ± 0.01 (n = 17) to a maximal ratio of 1.18 ± 0.05 at 8 min after ACh application ($t_{16} = - 18.03$, $P < 0.001$; paired *t*-test), indicating a strong increase in $[Ca]_i$ in growth cones. $[Ca]_i$ decreased and returned to a plateau level slightly above resting levels by 35 min. To investigate the location and time course of the ACh-induced elevation in $[Ca]_i$ with increased time resolution, we next acquired fura-2 images every 10 s, instead of every 60 s. The ACh-induced elevation in $[Ca]_i$ occurred throughout the entire growth cone and $[Ca]_i$ increased simultaneously in filopodia, the central domain, and the adjacent neurite [Fig. 2.1(D)]. Taken together, ACh induced an elevation in growth cone $[Ca]_i$ and an increase in filopodial length in B5 neurons with a similar time course.

We showed previously that Ca-dependent filopodial elongation can be triggered either by Ca influx or by release of Ca from intracellular stores (Rehder and Kater, 1992; Welshhans and Rehder, 2007). Since studies of *Xenopus* spinal neurons identified the importance of extracellular Ca in ACh-induced growth cone turning behaviors, we next investigated whether extracellular

Ca was also required for the ACh-induced filopodial elongation. The culture medium was first replaced with Ca-free solution, and B5 neurons were then stimulated with ACh. Replacement with Ca-free solution caused a slight and long-term reduction in filopodial length by 10% starting at five minutes (t_{24}= - 4.24, $P < 0.001$; two sample *t*-test; data not shown), compared to control. Interestingly, the effect of 0.5 μM ACh on filopodial elongation was fully blocked in Ca-free solution compared to ACh by itself (Tukey's *post hoc*, $P < 0.001$) [Fig. 2.1(B)]. Correspondingly, Ca imaging studies on growth cones revealed that the increase in $[Ca]_i$ by 0.5 μM ACh was eliminated in Ca-free solution as well (Tukey's *post hoc*, $P < 0.001$) [Fig. 2.1(C)]. Taken together, these data suggested that ACh caused an increase in $[Ca]_i$ via Ca influx, which, in turn, resulted in filopodial elongation.

2.5.2 ACh depolarizes membrane potential and reduces input resistance in a dose-dependent manner

ACh has been shown to modulate neuronal activity in various systems, including neurons in the pond snails *Helisoma trivolvis* and *Lymnaea stagnalis* (Bahls, 1987; Perry *et al.*, 1998). Given that we had measured a significant Ca influx in response to ACh, we next tested whether ACh treatment might have caused the increase in $[Ca]_i$ and the subsequent elongation of filopodia by regulating the electrical activity of B5 neurons. We used the patch clamp recording technique in the whole-cell current clamp configuration to investigate the role of ACh on neuronal electrical activity, and injected a small negative current (- 50 pA) for 1 s every 20 s to monitor input resistance (R_{in}) continuously. B5 neurons fire spontaneous action potentials (APs) with a resting membrane potential (RMP) close to - 40 mV [Fig. 2.2(A)] (Artinian *et al.*, 2010). To test the effects of ACh on the electrical properties of B5 neurons, we stimulated neurons with various concentrations of ACh ranging from 10 nM to 100 μM using a perfusion system. ACh

began to depolarize the RMP at a concentration of 100 nM and its effect saturated at 10 μM with a depolarizing response of + 23.0 ± 0.6 mV (n = 6). Meanwhile, R_{in} started to decrease at 30 nM ACh and this response also saturated at 10 μM ACh, at which R_{in} was reduced to 10.4 ± 1.3% (n = 6). Although we observed a gradual increase in the firing frequency at lower concentrations, ranging from 10 nM to 1 μM, higher concentrations of ACh (> 3 μM) depolarized the membrane potential to a level that resulted in neuronal silencing [Fig. 2.2(A)]. ACh caused a concentration-dependent depolarization of RMP with an estimated half maximal effective concentration (EC_{50}) of 1.7 μM [Fig. 2.2(B)] and a reduction in R_{in} with an EC_{50} of 0.4 μM [Fig. 2.2(C)], based on the Hill equation. This result suggested that B5 neurons are tuned to dynamically respond to small changes in the concentration of ACh, but that they would become less responsive to synaptic inputs in the continued presence of relatively higher concentrations of ACh. Because the firing frequency could not be studied at higher concentrations of ACh, we instead quantified RMP and R_{in} in all following electrophysiology experiments.

2.5.3 nAChR agonist DMPP elongates filopodia and elevates growth cone $[Ca]_i$

To further investigate the mechanism by which ACh induced filopodial elongation, we considered the possibility that ACh may signal through nAChRs, which are widely expressed in molluscan nervous systems and whose activation mediates a significant portion of ACh-associated effects (Bahls, 1987; Perry et al., 1998; Elliott and Vehovszky, 2000). DMPP is a prominent agonist of nAChRs with little selectivity between neuronal nAChR subtypes. Bath application of 5 μM DMPP caused a significant increase in filopodial length when compared with the vehicle control ($F_{1,25} = 33.17$, $P < 0.001$; repeated-measures ANOVA) [Fig. 3(A)]. The maximal response of DMPP on filopodial length occurred 10 min after drug treatment (an increase by 33.8 ± 3.5%, n = 13). Interestingly, the peak response was not significantly different

between the groups treated with ACh (0.5 μM) and DMPP (5 μM) (t_{26} = - 1.59, P = 0.12; unpaired *t*-test), suggesting that the effect of ACh on filopodial elongation was indeed mediated through activation of nAChRs.

In addition to its effect on filopodial elongation, DMPP also affected $[Ca]_i$. Bath application of 5 μM DMPP induced a quick and significant increase in the Fura-2 ratio ($F_{1,21}$ = 73.61, P < 0.001; repeated-measures ANOVA) as compared to vehicle control, where no changes in the ratio were observed (n = 12) [Fig. 2.3(B)]. The peak ratio induced by 5 μM DMPP appeared 7 min after treatment (1.10 ± 0.10, n = 11). Taken together, both direct ACh application and treatment with the nAChR agonist DMPP produced similar effects on filopodia and $[Ca]_i$, supporting the hypothesis that ACh acted on nAChRs to regulate growth cone filopodial dynamics.

2.5.4 DMPP mimics the effect of ACh on electrical activity

We next tested whether the activation of nAChRs was sufficient to explain the effects of ACh on the electrical activity seen above. 5 μM DMPP caused a depolarization of RMP by + 4.7 ± 0.4 mV (n = 11) and a reduction in R_{in} to 46.4 ± 3.8% (n = 12) [Fig. 2.4(A)]. To study the concentration dependency of DMPP on electrical properties, we next tested one lower (1 μM) and two higher concentrations (10 μM and 50 μM), respectively. 1 μM DMPP induced a much smaller depolarization (+ 1.5 ± 0.2 mV, n = 10) and a reduction in R_{in} (74.6 ± 5.1% , n = 9) compared to the 5 μM DMPP group, whereas 10 μM and 50 μM DMPP had stronger effects on both RMP (10 μM: a depolarization by + 6.5 ± 0.7 mV, n = 10; 50 μM: + 13.2 ± 1.6 mV, n = 9) and R_{in} (10 μM: a reduction to 37.0 ± 5.4%, n = 9; 50 μM: 24.9 ± 2.4%, n = 6) [Fig. 2.4(B and C)]. In 3 out of 9 cases, 50 μM DMPP caused silencing of B5 neurons [data not shown], a phenomenon that was similar to what we observed with higher concentrations of ACh (> 3 μM).

Taken together, activation of nAChRs by DMPP mimicked the effects of ACh on electrical activity of B5 neurons, namely depolarization of RMP and reduction of R_{in} in a dose-dependent manner.

2.5.5 Inhibition of nAChRs by TC blocks DMPP-induced filopodial elongation and increase in $[Ca]_i$

If ACh indeed activated nAChRs to regulate growth cone motility, the blockade of nAChRs should inhibit the ACh-induced filopodial elongation. We tested this hypothesis by using the classical nAChR antagonist, tubocurarine (TC). TC is known to antagonize functional responses mediated by nAChRs in various organisms (Haydon and Zoran, 1989; Zheng et al., 1994). In order to activate nAChRs selectively and to avoid the potential activation of other types of AChRs, the specific nAChR agonist DMPP was used in this set of experiments. Following a 10-min pretreatment with 100 μM TC, 5 μM DMPP was bath applied into the dish. Whereas TC on its own did not affect filopodial dynamics ($F_{1,25}$ = 2.83, P = 0.107; repeated-measured ANOVA; as compared to vehicle control, data not shown), pretreatment with TC eliminated the DMPP-induced increase in filopodial length (Tukey's *post hoc*, $P < 0.001$, 100 μM TC + 5 μM DMPP compared to 5 μM DMPP alone; overall effect: $F_{2,37}$ = 33.85, $P < 0.001$; repeated-measures ANOVA) [Fig. 2.5(A and B)]. The maximal filopodial elongation normally observed at 10 min following 5 μM DMPP treatment was fully blocked in the group pretreated with 100 μM TC (100 μM TC + 5 μM DMPP: increase by 0.4 ± 1.3%, n = 14 vs. 5 μM DMPP: 33.8 ± 3.5%, n = 13; t_{25} = - 0.28, $P < 0.001$; unpaired *t*-test) [Fig. 2.5(B)]. Instead, the TC + DMPP group maintained filopodial length close to baseline levels throughout the post-treatment period. Furthermore, preincubation with 100 μM TC also fully inhibited the DMPP-induced elevation of $[Ca]_i$ (Tukey's *post hoc*, $P < 0.001$, 100 μM TC + 5 μM DMPP compared to 5 μM DMPP alone;

$F_{2,33}$ = 81.80, P < 0.001; repeated-measures ANOVA), whereas TC by itself did not have an effect on $[Ca]_i$ at growth cones ($F_{1,24}$ = 0.08, P = 0.779; repeated-measured ANOVA; as compared to vehicle control, data not shown) [Fig. 2.5(C)]. These data strongly suggested that the activation of nAChRs was necessary for ACh to elicit its effect on growth cone filopodia, and that the increase in $[Ca]_i$ played a key role in filopodial elongation induced by nAChR activation.

2.5.6 TC blocks DMPP-induced depolarization and decreases in R_{in}

We next investigated whether the electrical responses induced by DMPP could also be blocked by pretreatment with TC. 100 μM TC on its own did not have an effect on either membrane potential (a depolarization by + 0.2 ± 0.4 mV, n = 9) or R_{in} (a reduction to 107.0 ± 4.0%, n = 9) [Fig. 2.6(A)]. After perfusion with 100 μM TC, B5 neurons were treated with a solution containing 100 μM TC and 5 μM DMPP. As shown in Fig. 2.6(B), 5 μM DMPP failed to depolarize the RMP of B5 neurons in the presence of 100 μM TC (100 μM TC + 5 μM DMPP: + 0.4 ± 0.2 mV, n = 15 vs. 5 μM DMPP, + 4.7 ± 0.4 mV, n = 11; P < 0.001; Tukey's *post hoc*). Moreover, the DMPP-induced decrease in R_{in} was completely blocked in the presence of 100 μM TC (100 μM TC + 5 μM DMPP: 108.6 ± 3.8%, n = 15 vs. 5 μM DMPP, 46.4 ± 3.8%, n = 12; P < 0.001; Tukey's *post hoc*) [Fig. 2.6(C)]. Hence, the effects of DMPP further indicated that the modulation of the electrical activity of B5 neurons was mediated via activation of nAChRs.

2.5.7 ACh acts locally at the growth cone to elongate filopodia

Growth cones have been demonstrated to possess some degree of autonomous function, and contain most of the machinery required for proper responses to extrinsic stimulation (Kater et al., 1994; Gomez and Zheng, 2006). Therefore, we next tested whether ACh acted at the growth cone proper, or, alternatively, whether the ACh-induced changes in filopodial dynamics were the result of ACh acting on another region of the neuron, such as the cell body. To explore

this possibility, we physically isolated growth cones from the remaining neuron by transection of the adjacent neurites using a microknife [Fig. 2.7(A)]. Such isolated growth cones have been shown to survive for up to 24 hours and maintain many features seen in growth cones that are connected to their parent neuron (Rehder *et al.*, 1991). In this series of experiments, 0.5 µM ACh was bath applied to dishes containing isolated growth cones. Filopodia responded to the ACh treatment with filopodial elongation within 2 mins, and reached their maximal length (an increase by 34.9 ± 3.5%, n = 14) 5 min after drug treatment, followed by a gradual decrease in filopodial length towards baseline [Fig. 2.7(A and B)]. The effect of ACh on filopodial length was significant when compared to the control group, in which only solvent was applied ($F_{1,25}$ = 45.57, $P < 0.001$; repeated-measures ANOVA) [Fig. 2.7(B)]. This result supported the hypothesis that ACh acted locally at the growth cone to regulate filopodial dynamics.

2.6 Discussion

ACh has been shown to affect numerous functions in developing neurons *in vitro*, including neurite outgrowth, growth cone guidance, synapse formation and synaptic transmission (Zheng et al., 1994; Lauder and Schambra, 1999; Woodin et al., 2002; Rudiger and Bolz, 2008). Here, we describe a role for cholinergic modulation at the growth cone, where ACh affects an important component of growth cone motility, namely filopodial dynamics. We report that ACh induced a transient but significant filopodial elongation in B5 neurons of the buccal ganglion of *Helisoma trivolvis*. The signaling cascade resulting in filopodial elongation is via opening of nAChRs, a depolarization of the membrane potential, and a subsequent elevation of $[Ca]_i$ in growth cones. Moreover, by performing experiments on physically isolated growth cones, we demonstrated that ACh can act as a local signal at the growth cone to elongate filopodia.

2.6.1 ACh and nAChRs

nAChRs appeared to be both necessary and sufficient for ACh to elicit its effects on growth cone filopodial dynamics, intracellular calcium, and neuronal electrical properties. Treatment with DMPP, a non-selective nAChR agonist, fully mimicked the effects of ACh on membrane depolarization, reduction in R_{in}, elevation of $[Ca]_i$, and filopodial elongation,. Meanwhile, TC, a well-known antagonist of nAChRs, completely inhibited all DMPP-induced responses. These results not only supported the specificity of our pharmacological approach, but also provided convincing evidence that ACh acted through activation of nAChRs to produce these effects. Taken together, our results add a novel role to the critical functions of nAChRs in cholinergic modulation of cellular properties in both vertebrates and invertebrates (Fu et al., 1998; Clementi et al., 2000; Woodin et al., 2002; Cobb and Davies, 2005).

nAChRs belong to a large Cys-loop family of ligand-gated ion channels including the 5-HT_3, glycine, and $GABA_A$ receptors (Le Novere and Changeux, 1995). nAChRs exist as pentameric complexes assembled either from five copies of a single subunit or by a composition of five different subunits (Clementi *et al.*, 2000). Although the molecular identities of nAChRs are well studied in mammalian systems, much less information is available in gastropods. Van Nierop and Smit identified nAChR subunits in the pond snail *Lymnaea stagnalis*, a closely related species (van Nierop *et al.*, 2005; van Nierop *et al.*, 2006), and cloned a total of twelve subunits of nAChR. Considering that ACh treatment in this study caused the depolarization of RMP and an elevation in $[Ca]_i$ in *Helisoma* B5 neurons, it is likely that the effect of ACh was contributed by the classic, cation-selective nAChRs. A characterization of *Helisoma* nAChRs at the molecular level is beyond the scope of this study but will extend our understanding of cholinergic modulation in the *Helisoma* nervous system in the future. Because the effects of ACh

on growth cones and electrophysiological properties could be fully mimicked by the nAChR agonist, DMPP, we did not pursue any potential involvement of muscarinic ACh receptors in regulating growth cone filopodial length and $[Ca]_i$.

2.6.2 ACh and cell excitability

Cholinergic modulation of cell excitability has been studied in some detail in gastropods. Salivary gland cells in *Helisoma* respond to ACh by a long-lasting depolarization followed by hyperpolarization (Bahls, 1987). Moreover, ACh is thought to be the core neurotransmitter to control neuronal activity in the feeding central pattern generator in *Lymnaea*, such as protraction phase premotor interneurons N1L and N1M (Elliott and Vehovszky, 2000). Cholinergic projections to the *Lymnaea* proesophagus modulate foregut contractile activity (Perry *et al.*, 1998). Furthermore, ACh acts on an ionotropic receptor sensitive to nicotinic antagonists to evoke an afterdischarge in *Aplysia* bag cell neurons (White and Magoski, 2012).

We demonstrated that ACh induced rapid and significant changes in electrical activity in B5 neurons. Both treatment with ACh and the nAChR agonist, DMPP, caused a reduction in R_{in} in a dose-dependent manner, suggesting the opening of nAChRs. The activation of nAChRs, in turn, induced the depolarization of the membrane potential. Relatively lower doses of ACh or DMPP resulted in an increase in spiking frequency, whereas higher concentrations caused cell silencing at a depolarized membrane potential.

2.6.3 ACh, Ca, and growth cone motility

We report that both stimulation with ACh and activation of nAChRs by DMPP resulted in a quick and pronounced increase in $[Ca]_i$ in growth cones. Interestingly, the elevation of $[Ca]_i$ and the increase in filopodial length occurred with a very similar time course. Considering the critical role of spiking activity in regulating $[Ca]_i$ within neurons (Spitzer, 2006), and that

causality has been demonstrated between an elevation in $[Ca]_i$ and filopodial elongation in B5 neurons (Rehder and Kater, 1992), the present study is consistent with the hypothesis that ACh functions through an increase in $[Ca]_i$ to elongate growth cone filopodia. After the replacement of culture medium with a Ca free solution, both the filopodial elongation and the elevation of $[Ca]_i$ induced by ACh were blocked, suggesting that Ca influx plays a critical role in ACh-signaling at the growth cone. In fact, other neurotransmitters and neuromodulators have been demonstrated to signal through $[Ca]_i$ to regulate growth cone functions (Henley and Poo, 2004; Gomez and Zheng, 2006). For example, the gaseous messenger nitric oxide affects growth cone filopodial dynamics in *Helisoma* B5 neurons via a Ca-dependent mechanism (Van Wagenen and Rehder, 2001; Trimm and Rehder, 2004; Welshhans and Rehder, 2005; Welshhans and Rehder, 2007). An increase in $[Ca]_i$ is able to reduce neurite outgrowth rate in *Helisoma* neurons (Cohan, 1992). In addition, $[Ca]_i$ is required for glutamate, netrin-1, and myelin-associated glycoprotein to guide growth cone turning in cultured *Xenopus* spinal neurons (Zheng *et al.*, 1996; Ming *et al.*, 2001). Upon the elevation of $[Ca]_i$ at the growth cone, multiple Ca-mediated signaling pathways could be activated to translate external signals into cytoskeletal changes. Our lab previously showed that calmodulin and the Ca-dependent phosphatase calcineurin are acting downstream of Ca to elongate filopodia (Cheng *et al.*, 2002). Moreover, calmodulin-dependent protein kinase II is found to mediate ACh-induced chemoattraction in growth cone guidance (Zheng *et al.*, 1994).

ACh has been shown to regulate cell movements, cell proliferation, and neuronal differentiation in various developing central nervous systems (Lauder and Schambra, 1999). Although the roles played by ACh in neuronal development *in vivo* are yet unclear, evidence for a functional role of ACh in developing neurons came from the studies of cultured embryonic *Xenopus* spinal neurons (Zheng *et al.*, 1994). ACh was found to act as a chemoattractive

guidance cue that elicited growth cone turning behavior towards the source of ACh release. Here, we extended this research by studying the effect of ACh on growth cone filopodia. Filopodia on growth cones are essential for growth cone guidance, and filopodial elongation increases the area that a growth cone can sample during pathfinding (Kater and Rehder, 1995; Rehder et al., 1996). A transient elongation of filopodia, as seen in this study in response to stimulation with ACh, could play a critical role in decision-making at the growth cone. Longer filopodia would encounter cues located 10-20 μm ahead of the advancing growth cone proper, could result in a change in the direction of growth towards or away from the cue depending on the signal content, and ultimately, upon contact of an appropriate cellular target, could transform a growth cone into a presynaptic structure. In our experiments, ACh was bath-applied, mimicking a general, extrasynaptic stimulation of B5 neurons. To determine the location at which ACh acted to elicit filopodial elongation, we physically isolated growth cones and demonstrated that they responded to ACh treatment in a similar fashion as intact growth cones did, suggesting that ACh can regulate growth cone motility at the growth cone proper. We did not attempt to produce gradients of ACh across growth cones to determine if this would result in asymmetrical filopodial elongation, as might be expected to precede growth cone turning. In fact, filopodial asymmetry on growth cones of *Xenopus* neurons was found to precede growth cone turning in responses to glutamate gradients (Zheng *et al.*, 1996). Additionally, our lab reported that both transient changes of growth cone filopodial dynamics (Van Wagenen and Rehder, 1999) and decreases in nerve growth speed (Trimm and Rehder, 2004) can be triggered by nitric oxide, a phenomenon we described as ‘slow-down and search’ behavior. Here, the ACh-induced change in filopodial dynamics may serve as a first response of an extending neurite to ACh encountered during pathfinding.

Although the sources of ACh release and physiological concentrations reached in the *Helisoma* buccal ganglia are unknown, several studies in which ACh release was measured suggest that the concentrations used in our *in vitro* study are comparable to *in vivo* conditions. The ACh concentration detected in the vicinity of magnocellular basal forebrain neurons using the nAChR-rich patches prepared from rat myotubes as focal ACh sensors was between 480 nM to > 50 μM (Allen and Brown, 1996). This concentration range of ACh matched the concentrations used in the current study and resulted in significant electrophysiological and morphological responses in B5 neurons. B5 neurons are responsive to ACh and are themselves cholinergic (Haydon and Zoran, 1989). *In vitro*, the site of ACh release in *Helisoma* neuron B5 is thought to be mainly confined to the distal neurites, but rarely detected from the soma. ACh release from neurites and growth cones has been reported in different neurons (Hume et al., 1983; Allen and Brown, 1996; Zakharenko et al., 1999; Yao et al., 2000), suggesting that growing cholinergic axons might influence other extending axons expressing nAChRs in order to regulate their developmental status. Moreover, ACh has been reported to act in an autocrine fashion on presynaptic terminal of *Xenopus* motoneurons (Fu *et al.*, 1998), suggesting the possibility that ACh release from axonal terminals might directly affect growing axons via an autoreceptive feedback mechanism.

2.7 Conclusion

In conclusion, our results provide novel insights into the effects of ACh on developing neurons. ACh affected growth cone filopodial dynamics through the activation of TC-sensitive nAChRs by depolarizing membrane potential and increasing $[Ca]_i$. While such effect could be caused by presynaptic stimulation, supporting the well-known literature of effects of electrical activity on neurite outgrowth and growth cone motility, the finding that ACh can act locally at a

growth cone suggested that ACh might also act at extrasynaptic receptors to modulate growth cone motility, neuronal pathfinding, and possibly synaptogenesis directly at the level of the growth cone.

2.8 Figures

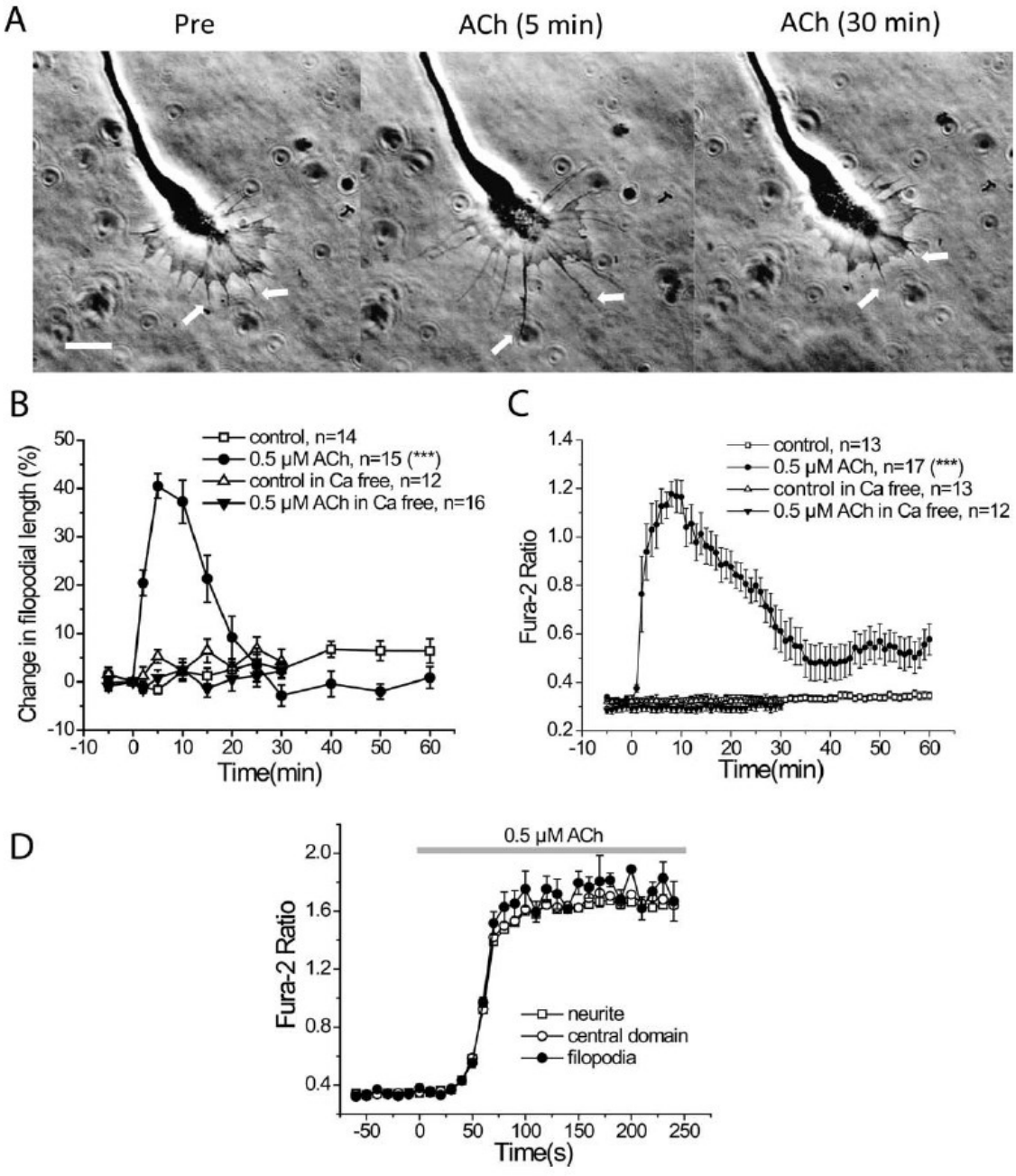

Figure 2.1 ACh induces a transient increase in filopodial length and $[Ca]_i$.

A: Phase-contrast images of a growth cone immediately before (left), 5 min after (center), and 30 min after (right) treatment with 0.5 μM ACh. *Helisoma* B5 neurons were cultured for 24 - 48 hours *in vitro*. Note the two white arrows pointing at the tips of two representative filopodia, highlighting their transient elongation and subsequent shortening. Scale bar, 10 μm. B: Bath application of 0.5 μM ACh resulted in a transient increase in filopodial length with the maximal response (an increase by 40.5 ± 2.6%, $P < 0.001$) occurring 5 min after ACh treatment, whereas growth cones receiving vehicle control did not show changes in filopodial length. Replacement of the culture medium with Ca-free solution prevented the ACh-induced filopodial elongation. C: Bath application of 0.5 μM ACh caused a transient and significant increase in the Fura-2 fluorescence emission ratio in growth cones compared to the vehicle control group ($P < 0.001$). The elevation of Fura-2 ratio suggested that the $[Ca]_i$ in growth cones was elevated after ACh treatment. Replacement of the culture medium with Ca-free solution prevented the ACh-induced increase in $[Ca]_i$. D: $[Ca]_i$ in filopodia (n=4), growth cone proper, and adjacent neurite from a representative growth cone imaged in 10 s intervals in response to 0.5 μM ACh.

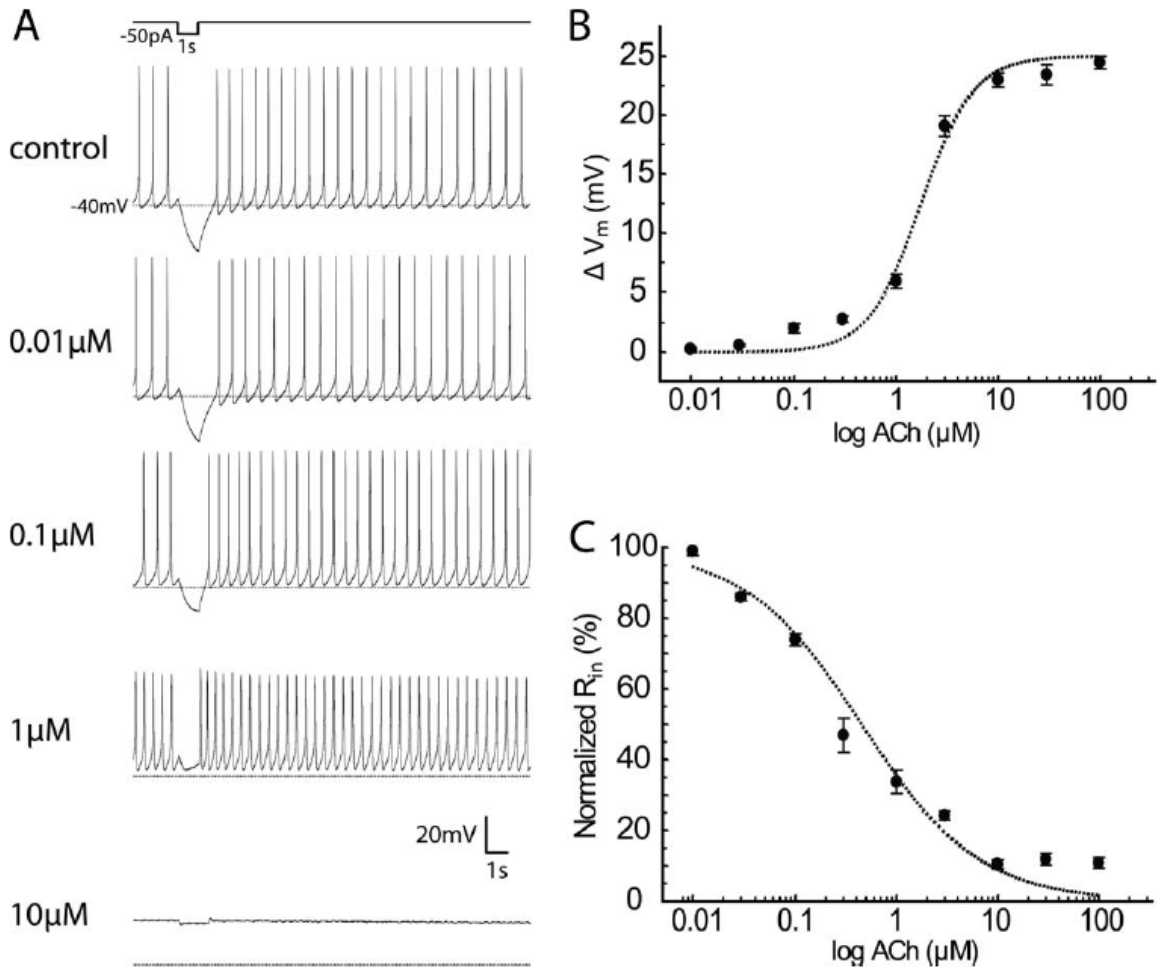

Figure 2.2 ACh depolarizes the membrane potential and reduces R_{in} in a dose-dependent manner.

A: Representative recordings of changes of the membrane potential and R_{in} in response to various concentration of ACh treatment (10 nM to 10 μM). Negative current injection (- 50 pA) was applied for 1 s of each 20 s recording trial. Note: Whereas lower concentrations of ACh (< 1 μM) resulted in a progressive increase in spiking frequency, higher concentration (10 μM) caused neuronal silencing at a depolarized RMP. B: Dose-dependent curve showing that ACh caused a depolarization of RMP with an estimated EC_{50} of 1.7 μM. C: Dose-dependent curve suggesting that ACh progressively reduced R_{in} (changes of the membrane potential in response to the negative current injection; - 50 pA, 1 s) with an estimated EC_{50} of 0.4 μM.

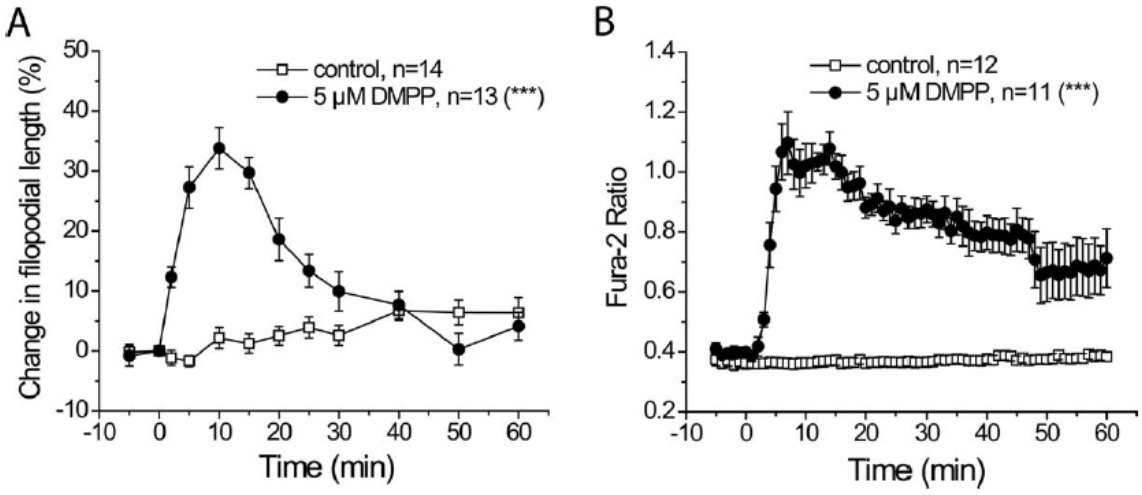

Figure 2.3 nAChR agonist DMPP elongates filopodia and elevates $[Ca]_i$.

A: Bath application of 5 μM DMPP led to a significant increase in filopodial length followed by a gradual reduction towards baseline ($P < 0.001$ as compared to vehicle control), and the maximal response (an increase by 33.8 ± 3.5%) occurred 10 min after DMPP treatment. B: Bath application of 5 μM DMPP resulted in a significant increase in Fura-2 ratio ($P < 0.001$ as compared to vehicle control), indicating a pronounced increase in $[Ca]_i$, which also peaked at around 10 min.

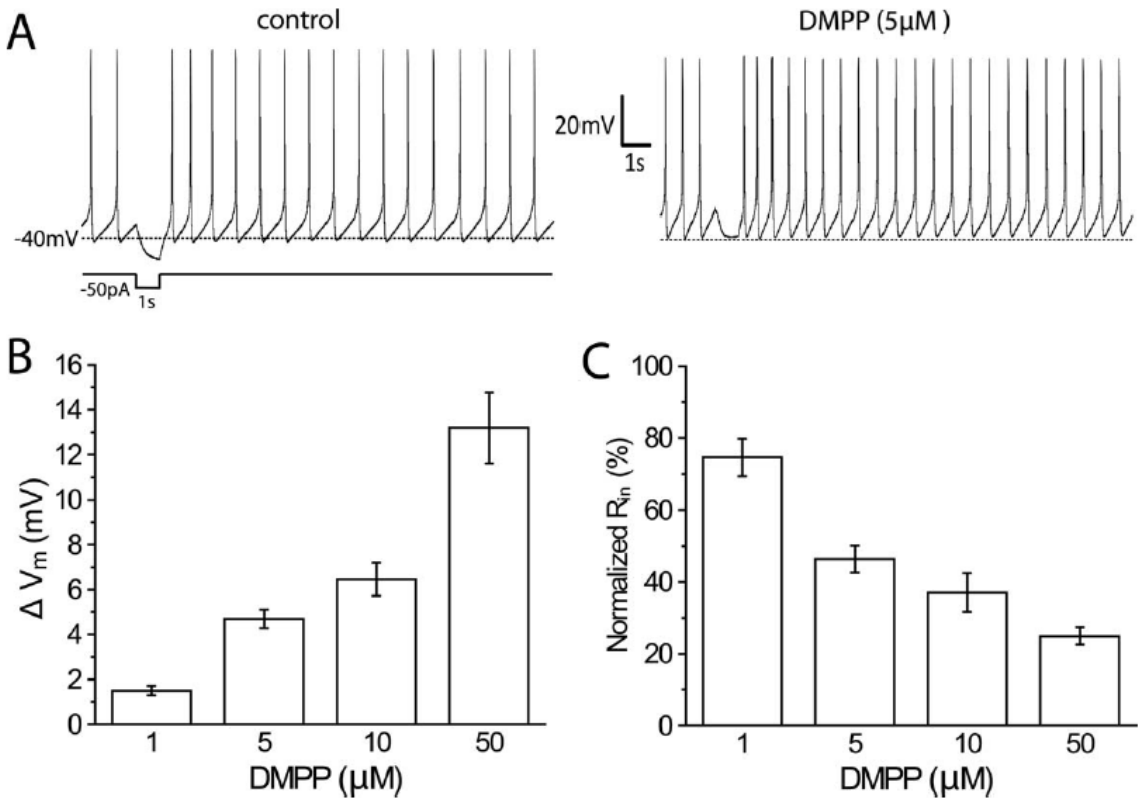

Figure 2.4 DMPP treatment results in a depolarization of RMP and a reduction in R_{in} in a dose-dependent manner.

A: Examples of a firing B5 neuron before and after treatment with 5 μM DMPP. Note that 5 μM DMPP induced a small depolarization of RMP and a decrease in $R_{in.}$ B: DMPP induced a depolarization of RMP in a dose-dependent manner. C: DMPP caused a dose-dependent reduction in R_{in}.

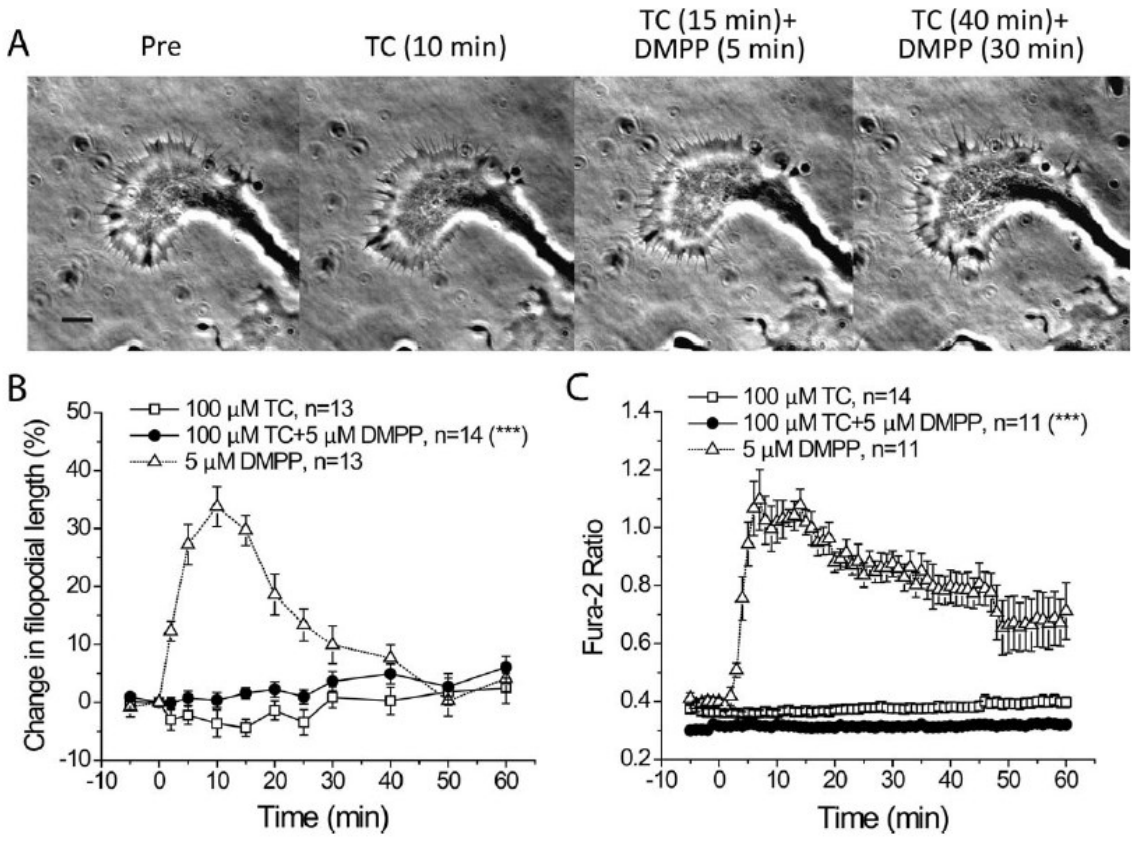

Figure 2.5 Inhibition of nAChRs by TC blocks the DMPP-induced filopodial elongation and increase in $[Ca]_i$.

A: Phase-contrast images of a growth cone immediately before (left), 10 min after 100 μM TC (center left), 5 min after addition of 5 μM DMPP in the presence of TC (center right), and 30 min after addition of 5 μM DMPP in the presence of TC (right). Note that these treatments did not result in obvious changes of filopodial length. Scale bar, 10 μm. B: The DMPP-induced filopodial elongation was significantly blocked by the treatment with 100 μM TC ($P < 0.001$ as compared to 5 μM DMPP alone). C: Treatment with 100 μM TC significantly inhibited the DMPP-induced increase in $[Ca]_i$ in growth cones ($P < 0.001$ as compared to 5 μM DMPP alone).

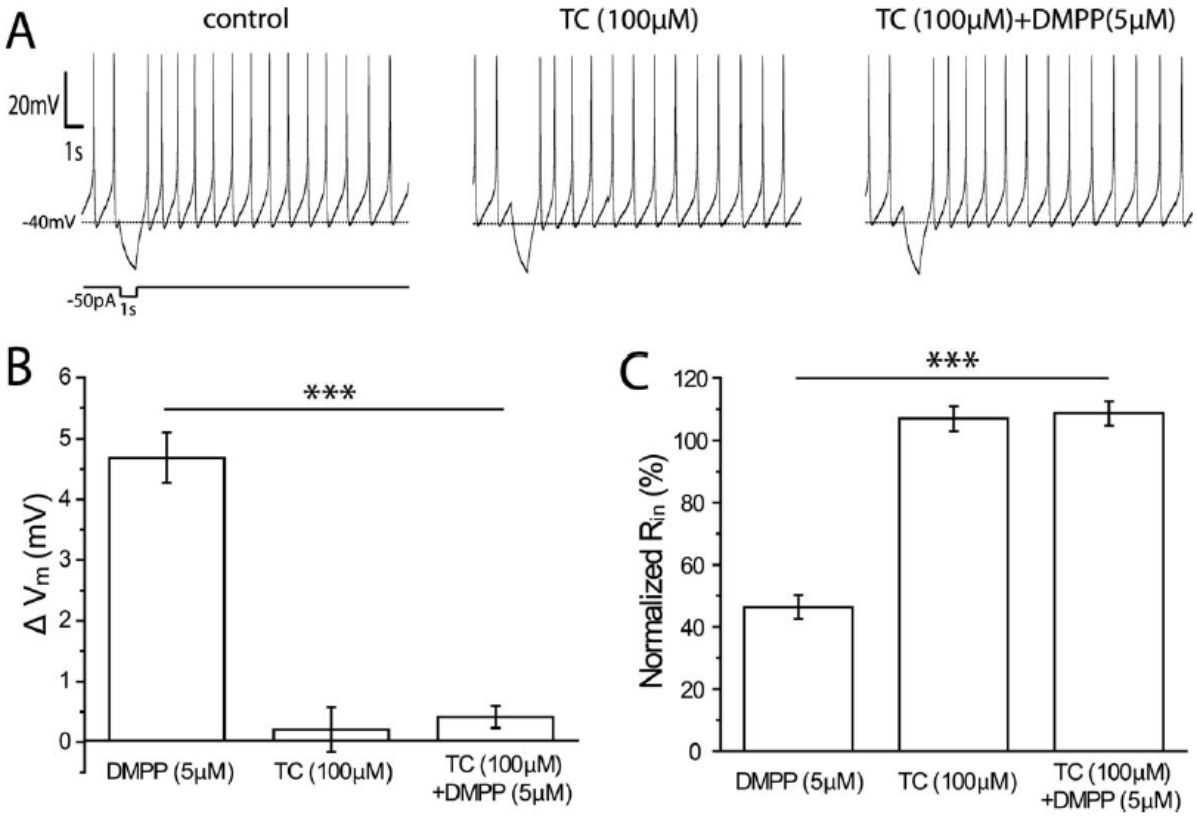

Figure 2.6 nAChR antagonist TC blocks the DMPP-induced depolarization and decrease in R_{in}.

A: Example of a firing B5 neuron before (control, left), after pretreatment with TC (100 μM, center), after subsequent addition of DMPP (5 μM, right). Note that no obvious changes in membrane potential and hyperpolarizing responses to negative current injection (- 50 pA, 1 s) were seen. B: Quantification of changes in the membrane potential from experiments such as shown in A. The depolarizing response induced by 5 μM DMPP was significantly inhibited when B5 neurons were pretreated with 100 μM TC ($P < 0.001$ as compared to 5 μM DMPP), whereas 100 μM TC on its own had no effect on RMP. C: Quantification of normalized R_{in} from experiments such as shown in A. The effect of DMPP (5 μM) on R_{in} was fully blocked when B5 neurons were pretreated with 100 μM TC ($P < 0.001$ as compared to 5 μM DMPP), whereas TC by itself had no effect on R_{in}.

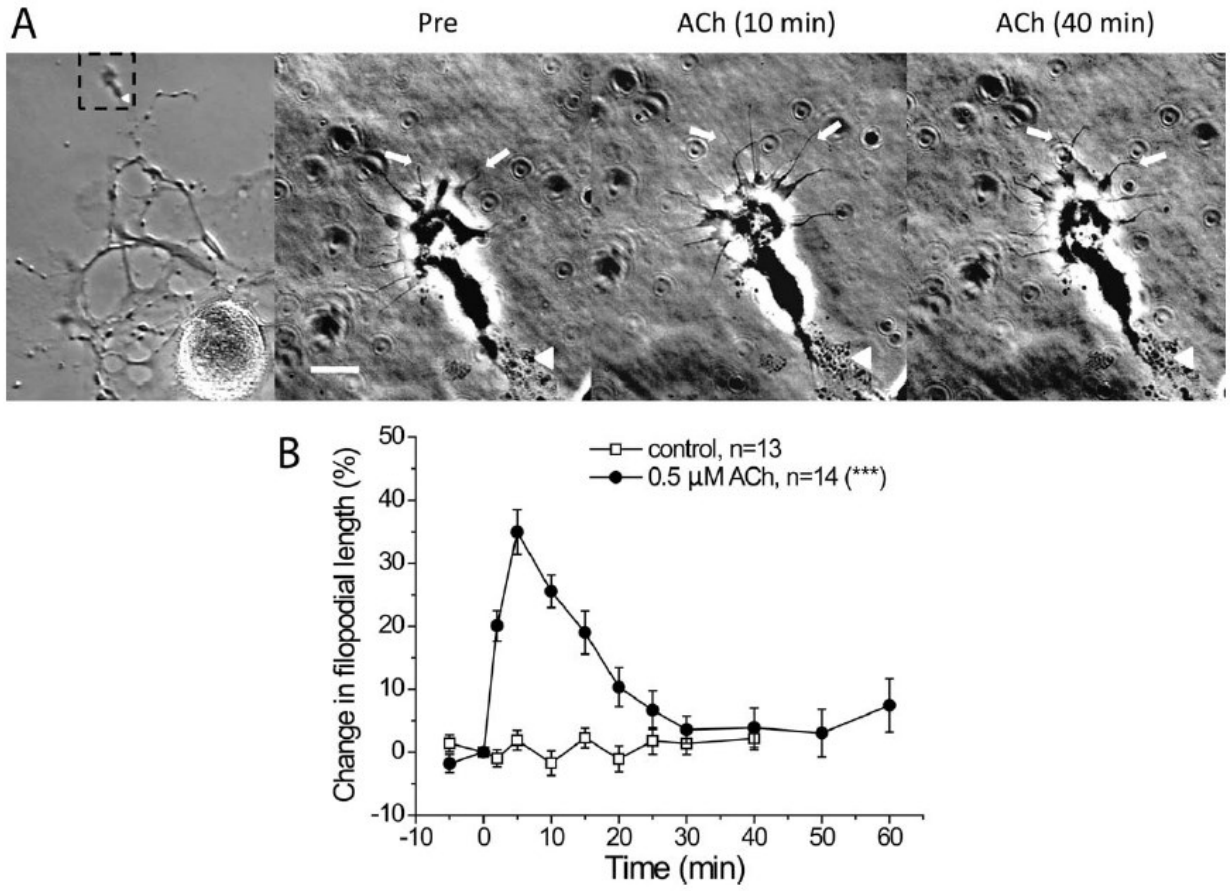

Figure 2.7 ACh causes a transient increase in filopodial length on physically isolated growth cones.

A: Phase-contrast images showing a cultured B5 neuron and a physically isolated growth cone generated by neurite transection (left, the isolated growth cone highlighted in dashed box and the transection site marked by a white arrowhead), and the same growth cone magnified immediately before (Pre), 10 min after (center), 40 min after treatment with 0.5 µM ACh (right). Note that filopodial elongation was clearly visible at 10 min after drug treatment, as indicated by the white arrows. Scale bar, 10 µm. B: Bath application of 0.5 µM ACh induced a transient and significant increase in filopodial length on isolated growth cones ($P < 0.001$ as compared to vehicle control), and the maximal response (length increase by 34.9 ± 3.5%) occurred 5 min after the treatment with ACh.

CHAPTER 3 NITRIC OXIDE REGULATES NEURONAL ACTIVITY VIA CALCIUM-ACTIVATED POTASSIUM CHANNELS

Submitted as **Zhong L.R.**, Estes S., Artinian L. and Rehder V. Nitric Oxide Regulates Neuronal Activity via Calcium-Activated Potassium Channels

3.1 Acknowledgements

This material is based upon work supported by the National Science Foundation under Grant No.(0843173) to VR. Additional support was provided by Brains and Behavior Fellowships to LRZ and SE, Sigma Xi grants-in-aid of research grant, and a GSU dissertation grant to LRZ.

3.2 Abstract

Nitric oxide (NO) is an unconventional membrane-permeable messenger molecule that has been shown to play various roles in the nervous system. How NO modulates ion channels to affect neuronal functions during neuronal development is not well understood. In gastropods, NO has been implicated in regulating the feeding motor program. The buccal motoneuron, B19, of the freshwater pond snail *Helisoma trivolvis* is active during the hyper-retraction phase of the feeding motor program and is located in the vicinity of NO-producing neurons in the buccal ganglion. Here, we asked whether B19 neurons might serve as direct targets of NO signaling. Previous work established NO as a key regulator of growth cone motility and neuronal excitability in another buccal neuron involved in feeding, the B5 neuron. This raised the question whether NO might modulate the electrical activity and neuronal excitability of B19 neurons as well, and if so whether NO acted on the same or a different set of ion channels in both neurons. To study specific responses of NO on B19 neurons and to eliminate indirect effects contributed

by other cells, experiments were performed on single cultured B19 neurons. Addition of NO donors caused a prolonged depolarization of the membrane potential and an increase in neuronal excitability. The effects of NO were mainly due to the inhibition of two types of Ca-activated K channels, apamin-sensitive and iberiotoxin-sensitive K channels. The results suggest that NO acts as a critical modulator of neuronal excitability in B19 neurons, and that Ca-activated K channels may serve as a common target of NO in neurons.

KEYWORDS: nitric oxide; electrical activity; action potential; Ca-activated K channels; BK channels; SK channels; Ca channels; *Helisoma trivolvis*; B19 neuron; depolarization; patch-clamp; iberiotoxin; apamin

3.3 Introduction

Nitric oxide (NO) serves as an unconventional membrane-permeable messenger molecule in the nervous systems of vertebrates and invertebrates, where it has been implicated in various cellular processes, including neuronal migration (Bicker, 2007), synaptogenesis (Nikonenko et al., 2008), and long-term potentiation (Kemenes et al., 2002; Hopper and Garthwaite, 2006). One mode of action by which NO has been shown to elicit its effects in neurons is by modulating ionic conductances (Garthwaite, 2008). Among ion channels, Ca channels (Tozer et al., 2012), K channels (Steinert et al., 2008), and HCN channels (Wilson and Garthwaite, 2010) have been shown to be targets of NO signaling. How NO modulates membrane channels to affect aspects of neuronal development and the functional output of neuronal circuits is of central interest in many systems.

Progress has been made towards understanding the role of NO signaling in gastropods (Moroz and Kohn, 2011). Using isolated neurons from the buccal ganglion of *Helisoma trivolvis*, NO has been characterized as a regulator of neurite outgrowth and growth cone motility (Van Wagenen and Rehder, 1999; Van Wagenen and Rehder, 2001). Application of NO-donors to the buccal neuron B5 slowed the advance of growing neurites (Trimm and Rehder, 2004), whereas growth cone filopodia underwent transient elongation (Van Wagenen and Rehder, 1999), suggesting a role for NO in neuronal pathfinding during development and regeneration. NO has also been shown to modulate neuronal excitability in B5 neurons by selectively affecting ion channels, such as K and Ca channels (Artinian et al., 2010; Artinian et al., 2012). On the level of neuronal circuitry and animal behavior, NO has been shown to be important in aerial respiration and long-term associative memory in *Lymnaea* (Kemenes et al., 2006; Lukowiak et al., 2006) and in feeding behaviors in *Aplysia* (Miller et al., 2011; Susswein and Chiel, 2012) and *Lymnaea* (Moroz et al., 1993; Kobayashi et al., 2000).

Gastropod feeding is driven by central pattern generators (Quinlan et al., 1997; Murphy, 2001), and NO has been implicated in regulating the buccal feeding motor program (Moroz et al., 1993; Kobayashi et al., 2000). Buccal neuron B19 in *Helisoma* is a bilaterally symmetric motor neuron that innervates muscle groups in the radula (Murphy, 2001; Turner et al., 2011). The somata of B19 neurons are located in the vicinity of NO-producing neurons (Sadamoto et al., 1998), suggesting that NO might affect B19 neurons by volume transmission. The goal of the current study was to investigate potential modulatory effects of NO on the electrical activity of B19 neurons, to identify the ion channels affected by NO, and to determine if NO acted on the same or a different set of ion channels than in the previously characterized buccal neuron (B5) involved in snail feeding. To eliminate possible indirect effects contributed by other cells, and to

allow cell type specific responses to NO to be investigated in isolation, we performed experiments at the single cell level in cultured neurons, where the source of NO is well controlled and the potential intracellular targets affected by NO can be investigated directly.

We found that NO caused a prolonged depolarization of the membrane potential and an increase in neuronal excitability in cultured B19 neurons. This effect of NO was achieved in large part by the inhibition of Ca-activated K channels, with apamin-sensitive K (SK) channels serving as the main target, and their inhibition by NO fully accounting for the sustained depolarization. Inhibition by NO of iberiotoxin (IbTX)-sensitive K (BK) channels contributed an early and transient effect to the overall depolarization. Our data support the notion that NO can serve as a key modulator of neuronal activity, and that Ca-activated K channels may be a common target of NO signaling via volume transmission.

3.4 Methods

3.4.1 Animals

Freshwater pond snails (*Helisoma trivolvis)* were kept in aerated aquaria (10 gallons) containing filtered water at room temperature on a 12 h light-dark cycle. Vegetable-based algae wafers (Hikari, Doctors Forster and Smith) and organic lettuce were used to feed snails once every day. Middle-sized animals with a shell diameter of 15 – 20 mm were chosen for the experiments.

3.4.2 Neuronal culture

Identified B19 neurons were isolated from the buccal ganglion of *Helisoma* and plated into Falcon Petri dishes as previously described (Zhong et al., 2013). Briefly, neurons were plated onto poly-L-Lysine (hydrobromide, MW, 70-150 kDa, 0.25 mg/ml; Sigma, St. Louis, MO,

USA)-coated glass coverslips attached to the bottom of 35-mm cell culture dishes (Falcon 1008). B19 neurons were kept in conditioned medium at room temperature. Conditioned medium was prepared by incubating two *Helisoma trivolvis* brains per 1 mL of Leibowitz L-15 medium (Invitrogen, Carlsbad, CA, USA) for 4 days. B19 neurons were used for experiments 24 – 48 hours after plating. The composition of L-15 medium was as follows (mM): 44.6 NaCl, 1.7 KCl, 1.5 $MgCl_2$, 0.3 $MgSO_4$, 0.14 KH_2PO_4, 0.4 Na_2HPO_4, 1.6 Na pyruvate, 4.1 $CaCl_2$, 5 HEPES, 50 μg/ml gentamicin, and 0.15 mg/ml glutamate in distilled water, pH 7.4.

3.4.3 Electrophysiology

Recordings from *Helisoma* B19 neurons in whole-cell current-clamp mode were obtained as described previously (Zhong et al., 2013). The patch electrodes were pulled from borosilicate glass tubes (OD 1.5mm; ID 0.86mm; Sutter instruments) on a Sutter instruments micropipette puller (P-87) and heat polished (Micro Forge MF-830; Narishige) with a resistance of about 3 - 8 MΩ. Neurons were recorded using 700B amplifiers (Molecular Devices, Union City, CA) and an analog-to-digital converter (Digidata 1440). Data acquisition and analysis were performed using pClamp software version 10 (Molecular Devices). Current-clamp configuration was used to record membrane potential, firing properties, and evoked action potentials (APs). Leibowitz L-15 medium was normally used as extracellular recording solution. In some experiments, L-15 medium was replaced with normal saline containing in (mM): 51.3 NaCl, 1.7 $CaCl_2$, 1.5 $MgCl_2$, and 5 HEPES, pH 7.3 - 7.4 (127 mOsm). Intracellular recording solution contained (mM): 54.4 K-aspartate, 2 $MgCl_2$, 5 HEPES, 5 Dextrose, 5 ATP 0.1 EGTA (127 mOsm). Mixed tetraethylammonium (TEA) chloride and 4-aminopyridine (4AP) solution was made by replacing 20 mM NaCl with 20 mM TEA(Cl) and adding 5 mM 4AP right before the experiment. Solution replacement was achieved through a gravity-based perfusion system (Warner Instruments). The

resting membrane potential of a spontaneously firing neuron was determined by measuring the value at the plateau of the depolarization phase before the membrane potential reached threshold. Measurement of the effect of NO on membrane potential was made at two separate time points in order to account for what appeared to be an initial, slightly larger increase, followed by a sustained depolarization. The initial phase was measured at approximately 30 s after NOC7 stimulation, whereas the plateau phase was measured at 3 min after NOC7 application. Neuronal excitability was tested by injecting depolarizing current with amplitudes of + 20 and + 100 pA for 1 s. Analysis of the properties of evoked APs was achieved by using the 'threshold search' function of Clampfit (pClamp 10, Molecular Devices).

Recordings of voltage-gated Ca currents were achieved in the whole-cell voltage-clamp configuration, as described previously (Hui and Feng, 2008). To characterize total Ca currents, the membrane potential was held at - 60 mV and stepped from - 60 mV to + 60 mV for 500 ms and 10 mV increments. Extracellular solution contained (in mM): 10 $CaCl_2$, 45.7 TEA(Cl), 1 $MgCl_2$, 2 4AP, 10 HEPES, pH 7.4 (TEA-OH); internal solution (in mM): 29 CsCl, 2.3 $CaCl_2$, 2 MgATP, 0.1 GTP-Tris, 11 EGTA, 10 HEPES. The internal solution was adjusted to pH 7.4 with CsOH. Recordings were filtered at 5 kHz (- 3 dB, 4 pole Bessel filters). Currents were analyzed by normalizing the peak inward current for each cell to the cell capacitance (pA/pF).

3.4.4 Pharmacological agents

NOC7 (Calbiochem) was dissolved in 100 mM NaOH to make a 100 mM stock solution. Diethylamine NONOate (DEA/NO, Calbiochem), cadmium chloride ($CdCl_2$, Sigma), iberiotoxin (IbTX, Sigma), apamin (Alomone labs) were dissolved in distilled H_2O to make 100 mM, 1 M, 200 μM, 1 mM stock solutions, respectively. For patch clamp experiments, stock solutions were mixed with 200 μl extracellular solution removed from the recording dish, gently added back

around the periphery of the dish, and aspirated for 5 times using a 200 µl pipette to equilibrate the drugs to their final concentrations. The K channel blockers, TEA and 4AP, were prepared directly in the extracellular solution. The choice of pharmacological blockers was based on their successful prior usage in *Helisoma* (Artinian et al., 2010; Zhong et al., 2013).

3.4.5 Statistical analysis

All data were expressed as mean ± SEM. Comparisons between two individual groups were made with either the Mann-Whitney U-test or the two-sample t-test, and comparisons between two paired groups were achieved by the paired-sample Wilcoxon signed-rank test using Origin Data Analysis and Graphing software (OriginLab Corporation, Northampton, MA). Significant differences are indicated as *$P < 0.05$, **$P < 0.01$, and ***$P < 0.001$.

3.5 Results

3.5.1 Nitric oxide depolarizes the membrane potential of B19 neurons

Isolated B19 neurons from the buccal ganglion of *Helisoma trivolvis* were used for whole-cell patch-clamp experiments 24 – 48 hour after plating, at which time all neurons had well-developed neurites with growth cones at their tips. 74.6 percent of B19 neurons recorded (44 out of 59) were silent with a resting membrane potential at - 41.2 ± 0.7 mV, whereas the rest of B19 neurons (25.4%, 15 out of 59) fired spontaneous action potentials (APs) and had a slightly more depolarized membrane potential of – 38.3 ± 0.7 mV ($P < 0.05$; Two-sample t-test). We first asked how nitric oxide (NO) might affect the electrical activity of B19 neurons. The NO donor, NOC7 (half life: 10 min at 22 ˚C, pH 7.4, Calbiochem), was used to activate NO signaling. Despite their initial differences in membrane potential, all B19 neurons responded to 100 µM NOC7 with depolarization. In spiking neurons, as well as in neurons in which the depolarization

was large enough to bring neurons to the spiking threshold, neurons responded with a phasic increase in firing frequency, followed by sustained firing [Fig. 3.1(A)]. To include all neurons in the analysis, we decided to quantify the amount of depolarization resulting from the stimulation with NOC7. To account for what appeared to be an initial, slightly larger increase, followed by a sustained depolarization, we measured these effects of NO on membrane potential separately. The initial phase, measured approximately 30 s after NOC7 stimulation, showed a slightly stronger depolarization compared to the plateau phase, measured at 3 min after NOC7 application (initial phase: + 3.8 ± 0.5 mV, n = 8; plateau phase: + 2.5 ± 0.4 mV, n = 8, $P < 0.01$; Paired-sample Wilcoxon signed-rank test) [Fig. 3.1(A, C and D)]. Both phases of the effect of NOC7 were significantly different from the solvent control, which had no effect (initial phase: + 0.2 ± 0.2 mV, n = 6, $P < 0.01$, compared to NOC7; plateau phase: + 0.2 ± 0.1 mV, n = 6, $P < 0.01$, compared to NOC7; Mann-Whitney U-test) [Fig. 3.1(C and D)].

We next wanted to independently confirm the effect of NO on membrane potential by using another NO donor, DEA/NO, which has been used successfully on B5 neurons in our system (Artinian et al., 2012). DEA/NO releases NO with a half-life of 16 min at 22 ˚C and pH 7.4 (Calbiochem). Similar to the effects seen with NOC7, bath application of 100 μM DEA/NO caused an initial depolarization (+ 4.1 ± 0.2 mV, n = 6) and a plateau response (+ 3.6 ± 0.4 mV, n = 6) [Fig. 3.1(B to D)]. Both phases of the DEA/NO effect were significant compared to the solvent control (initial phase: + 0.4 ± 0.1 mV, n = 6, $P < 0.01$, compared to DEA/NO; plateau phase: + 0.1 ± 0.2 mV, n = 6, $P < 0.01$, compared to DEA/NO; Mann-Whitney U-test) [Fig. 3.1(C and D)].

Taken together, stimulation with NO by the application of NOC7 or DEA/NO caused a depolarization of the membrane potential in B19 neurons, with a relatively stronger initial phase

and a sustained plateau phase. We next wanted to determine the source of the depolarization in response to NO and considered the opening of Ca channels and the closure of K channels as likely causes.

3.5.2 The NO donor NOC7 does not affect voltage-gated Ca channels (VGCCs)

To test possible effects of NOC7 on VGCCs, we recorded Ca currents in B19 neurons directly in the whole-cell voltage-clamp configuration, as previously described (Artinian et al., 2012). We used a Na-free extracellular medium combined with a K-free intracellular solution to isolate Ca currents and applied voltage steps from – 60 to + 60 mV for 500 ms and 10 mV increments to evoke Ca currents. The maximal Ca current was not affected by treatment with 100 μM NOC7 [Fig. 3.2(A and B)]. The normalized peak Ca currents during both the initial and the plateau phases of depolarization induced by NOC7 were not significantly different from the solvent control (initial phase: NOC7: 88.9 ± 3.6 %, n = 5 vs control: 91.4 ± 1.9 %, n = 4, P = 0.71; plateau phase: NOC7: 86.0 ± 8.1 %, n = 5 vs control: 85.1 ± 3.3 %, n = 4, P = 1; Mann-Whitney U-test) [Fig. 3.2(C)]. Subsequent treatment with 100 μM $CdCl_2$, a prominent inhibitor of VGCCs, fully blocked the current (2.1 ± 3.1 %, n = 5) [Fig. 3.2(C)], suggesting that the current recorded was indeed a Ca current. Therefore, an opening of VGCCs in response to extrinsic NO stimulation could be ruled out as the source of depolarization.

3.5.3 Inhibition of K channels fully blocks the depolarizing effects of NOC7

In order to investigate the contribution of K channels in the NO-induced depolarization, we first used a cocktail of 20 mM TEA and 5 mM 4AP to block the majority of K channels. While this treatment depolarized the membrane potential instantly as expected (+ 4.7 ± 1.6 mV, n = 4) [data not shown], it also completely blocked any additional effect of a subsequent treatment with NOC7 (100 μM) (initial phase: NOC7 after TEA&4AP: + 0.2 ± 0.4 mV, n = 5, P

< 0.01, compared to NOC7; plateau phase: NOC7 after TEA&4AP: - 0.6 ± 0.2 mV, n = 5, P < 0.01, compared to NOC7; Mann-Whitney U-test) [Fig. 3.3(A, C and D)]. Interestingly, the degree of depolarization obtained by inhibition of a majority of K channels (plateau phase: TEA&4AP: + 4.7 ± 1.6 mV, n = 4) was not significantly different from that seen after treatment with NOC7 (P = 0.27; Mann-Whitney U-test), suggesting that the effect of NO on membrane potential could likely be explained by an inhibitory effect of NOC7 on K channels. We next wanted to determine the class of K channels that mediated the NOC7-induced depolarization.

3.5.4 NO depolarizes the membrane potential in a Ca-dependent manner

To test for the involvement of Ca-activated K channels in the depolarizing response to NOC7, we first used $CdCl_2$ to block VGCCs and then applied NOC7. 500 μM $CdCl_2$ resulted in a depolarization of the membrane potential ($CdCl_2$: + 2.9 ± 0.3 mV, n = 4 vs control: + 0.1 ± 0.2 mV, n = 6, P < 0.05; Mann-Whitney U-test) [data not shown], suggesting a contribution of Ca influx to the resting membrane potential, likely mediated via Ca-activated K channels. Interestingly, the plateau effect of $CdCl_2$ was not significantly different from that seen after treatment with NOC7 (P = 0.44; Mann-Whitney U-test), suggesting that the effect of NO on membrane potential might be largely explained by an inhibitory effect of NOC7 on Ca-activated K channels. Indeed, subsequent application of 100 μM NOC7 caused only a small depolarization during the initial phase (NOC7 after $CdCl_2$: + 1.2 ± 0.1 mV, n = 4, P < 0.01, compared to NOC7; Mann-Whitney U-test) [Fig. 3.3(B and C)], whereas the plateau phase of the NO effect was completely blocked in the presence of 500 μM $CdCl_2$ (NOC7 after $CdCl_2$: + 0.1 ± 0.1 mV, n = 4, P < 0.01, compared to NOC7; Mann-Whitney U-test) [Fig. 3.3(B and D)].

Therefore, Ca-activated K channels were the main cellular target of NO stimulation. We next investigated which classes of Ca-activated K channels might be targeted by NOC7 using pharmacological tools.

3.5.5 IbTX-sensitive K channels contribute to the initial phase of the NO effect

Two subtypes of Ca-activated K channels have been reported in *Helisoma* to date: a large conductance (BK) channel and a small conductance (SK) channel, each with a distinct pharmacological profile and contribution to neuronal activity (Artinian et al., 2010). We first investigated the potential effect of NO on BK channels. BK channels can be inhibited pharmacologically by iberiotoxin (IbTX), a scorpion toxin that acts on the outer face of the channel (Candia et al., 1992). IbTX has been used successfully in blocking BK channels in *Helisoma* B5 neurons (Artinian et al., 2010). 300 nM IbTX caused a slow depolarization, which reached a plateau at around 10 min (IbTX: + 2.7 ± 0.7 mV, n = 4 vs control: + 0.1 ± 0.2 mV, n = 6, $P < 0.05$; Mann-Whitney U-test) [data not shown], suggesting that BK channels in B19 neurons are partially open at rest and help maintain the membrane potential at a hyperpolarized level. Subsequent application of 100 μM NOC7 in the presence of IbTX still caused additional depolarization, which was maintained throughout the recording, suggesting that NOC7 was acting on yet another conductance, in addition to BK channels [Fig. 3.4(A)]. During the early phase, in the presence of IbTX, NOC7 treatment was able to add an additional depolarization that was significantly smaller than the one produced by NOC7 itself (NOC7 after IbTX: + 1.8 ± 0.3 mV, n = 4, $P < 0.05$, compared to NOC7; Mann-Whitney U-test) [Fig. 3.4(A and B)], indicating that the initial depolarization by NO was mediated by at least two channels: an IbTX-sensitive K channel and a yet unknown channel. During the plateau phase, the depolarization in response to NOC7 in IbTX-pretreated neurons was not significantly different from NOC7 on its

own (NOC7 after IbTX: + 2.0 ± 0.1 mV, n = 4, P = 0.73; Mann-Whitney U-test) [Fig. 3.4(A and C)], suggesting IbTX-sensitive BK channels did not significantly contribute to the sustained plateau effect of NO.

3.5.6 Apamin-sensitive K channels are the main target of NO in depolarizing the membrane potential

SK channels are known to be the target of NO in *Helisoma* B5 neurons (Artinian et al., 2010), which raised the possibility that SK channels might be affected by NO in B19 neurons as well. Treatment with 5 μM apamin, a specific blocker of SK channels, instantly led to a sustained depolarization in B19 neurons [Fig. 3.5(A)]. Whereas the initial depolarization by apamin was slightly smaller than that by NOC7 treatment (Apamin: + 2.0 ± 0.2 mV, n = 5, $P < 0.05$, compared to NOC7; Mann-Whitney U-test) [Fig. 3.5(C)], the sustained depolarization achieved by apamin was similar to that of NOC7 group (Apamin: + 2.3 ± 0.4 mV, n = 5, P = 0.71, compared to NOC7; Mann-Whitney U-test) [Fig. 3.5(A and D)]. The subsequent addition of NOC7 (100 μM) to apamin-treated neurons resulted in an additional, albeit transient depolarization (initial phase: NOC7 after apamin: + 2.2 ± 0.3 mV, n = 5, $P < 0.05$; compared to NOC7; Mann-Whitney U-test) [Fig. 3.5(B and C)], suggesting that the initial depolarization partially resulted from another channel in addition to SK channels, probably IbTX-sensitive BK channels as demonstrated earlier. Interestingly, no additional depolarization could be achieved by NOC7 in the presence of apamin during the plateau phase (NOC7 after apamin: + 0.3 ± 0.2 mV, n = 5, $P < 0.01$; compared to NOC7; Mann-Whitney U-test) [Fig. 3.5(B and D)]. These results suggested that SK channels served as the main target of NO in B19 neurons, and that the sustained, plateau effect elicited by NOC7 could be fully explained by the blockade of SK channels.

3.5.7 NO increases neuronal excitability

Given its depolarizing effect on membrane potential, we next wanted to further investigate the effect of NO on neuronal excitability. Injections of depolarizing current steps for 1 s evoked APs in B19 neurons in a dose-dependent manner. In the example shown in Fig. 3.6(A), 100 μM NOC7 shortened the inter-spike interval, which allowed one more evoked AP to occur over the period of + 20 pA current injection. Statistical analysis of the firing frequency of the evoked APs showed that B19 neurons significantly increased their firing frequency elicited by + 20 pA current injections compared to the vehicle control (NOC7: 123.2 ± 8.7 %, n = 4 vs control: 100.7 ± 0.8 %, n = 4, $P < 0.05$; Mann-Whitney U-test) [Fig. 3.6(C)]. The increased firing frequency induced by NO was maintained when a larger depolarizing current was applied (+ 100 pA: NOC7: 108.6 ± 2.7 %, n = 4 vs control: 98.3 ± 0.4 %, n = 4, $P < 0.05$; Mann-Whitney U-test) [Fig. 3.6(B and C)]. Therefore, NO not only caused a depolarization of the membrane potential and increased firing frequency, but also led to a general increase in neuronal excitability of B19 neurons.

3.6 Discussion

The goal of current study was to understand the role of NO in modulating neuronal activity in B19 neurons from *Helisoma trivolvis*. We achieved this aim by investigating membrane channel targets that mediate the effects of NO at the electrophysiological level. The proposed model by which NO is thought to affect electrical activity in B19 neurons is schematically shown in Fig. 3.7. According to the model, NO depolarizes the membrane potential by inhibiting two types of Ca-activated K channels: apamin-sensitive K channels and IbTX-sensitive K channels, with the main effect of NO being contributed by the inhibition of

apamin-sensitive K channels. NO application on the other hand had no significant effect on VGCCs.

3.6.1 Effects of NO on membrane potential and cell excitability

Elevation of the NO concentration by treatment with the NO-donors NOC7 and DEA/NO led to a long-lasting depolarization of the membrane potential in B19 neurons. We divided this response into an initial phasic depolarization, followed by a tonic plateau response. The majority of B19 neurons were electrically silent before the stimulation with NO, and in most of these neurons, the NO-induced depolarization elicited transient or sustained spiking activity. Such a transition from a silent to a firing state constitutes a profound change in the physiological state of a neuron, regardless of whether a neuron is undergoing neurite outgrowth during development or regeneration, or serving as a member of a neuronal circuit in the mature nervous system. For example, neuronal spiking will increase the intracellular Ca concentration ($[Ca]_i$), which has been shown to have a wide range of effects in both developing and mature nervous systems (Rehder and Kater, 1992; Torreano and Cohan, 1997; Berridge et al., 2003; Spitzer, 2006). Increases in $[Ca]_i$ in growth cones from several neuron types have been shown to result in a decrease in neurite outgrowth (Mattson and Kater, 1987), filopodial elongation (Rehder and Kater, 1992), and growth cone turning (Henley and Poo, 2004). In the intact nervous system, an increase in intrinsic spiking activity would result in altered postsynaptic excitation, and, depending on the degree of depolarization resulting from NO, it could lead to an increase or decrease in neuronal excitability (Prast and Philippu, 2001; Steinert et al., 2008). Even neurons that were originally silent, and in response to NO treatment became depolarized without reaching the spike threshold, would likely exhibit altered responses to presynaptic inputs.

In B5 neurons, we previously showed that NO had a biphasic effect, causing transient excitation, followed by silencing at a depolarized membrane potential (Artinian et al., 2010). In this case, NO caused an initial increase in firing frequency followed by a sustained depolarization, similar to that seen in B19 neurons. The difference between B5 and B19 neurons was that B5 neurons did not show a sustained increase in excitability in response to NO, whereas B19 neurons did show such an increase in excitability (Artinian et al., 2010). Therefore, the release of NO *in vivo* is expected to have complex effects on target neurons that may differ between cell types, depending on the mode of NO's action on individual neurons.

3.6.2 Ion channels affected by NO

After ruling out the possibility that extrinsic NO might have opened VGCCs to cause depolarization, we found that the effect of NO on membrane potential was completely eliminated when K channels were inhibited with a cocktail of TEA and 4AP, supporting the hypothesis that K channels were primary targets of NO signaling. We next investigated any involvement of Ca-activated K channels by using $CdCl_2$ to block VGCCs, with the rationale that Ca-activated K channels would be largely inhibited without Ca influx (Herrera and Nelson, 2002). Interestingly, we found that VGCCs, at resting conditions, contributed to the membrane potential, perhaps by activating Ca-activated K channels that help maintain a hyperpolarizing drive on the membrane potential. After the blockage of Ca influx, Ca-activated K channels closed and resulted in depolarization. The finding that NOC7, in the presence of $CdCl_2$, was unable to elicit additional depolarization during the later phase indicated that Ca influx and NOC7 signaling might be converging on a common target, such as Ca-activated K channels. In fact, NO signaling has been shown to inhibit Ca-activated K channels in various cells including *Helisoma* B5 neurons (Cetiner and Bennett, 1993; Artinian et al., 2010).

Further investigation of specific K channel subtypes identified Ca-activated K channels, SK channels and BK channels, as the main ion channel targets of NO. This finding is consistent with what we reported in *Helisoma* B5 neurons (Artinian et al., 2010), where NO regulates the electrical activity of tonically firing neurons through inhibition of SK channels and BK channels. Here, we further dissected the contributions of different channel inhibitors on the NO-induced membrane depolarization. The inhibition of SK channels with apamin resulted in an instant depolarization of the membrane potential, and this effect was sustained throughout the recording. The apamin-induced plateau depolarization was similar to that seen after NO treatment, and subsequent application of NOC7 did not show any additional effect on the plateau phase, suggesting that the plateau depolarization was most likely mediated by the closure of SK channels. However, NO still had a small depolarizing effect on membrane potential during the initial phase in the presence of apamin, although the level of depolarization was significantly smaller than that seen with NOC7 on its own. Interestingly, the initial effect of NO was also reduced when BK channels were blocked by IbTX. Taken together, these two findings suggested that the initial NO-induced depolarization could be explained by a combined effect of inhibition of both SK and BK channels by NO. Modulatory effects of NO on Ca-activated K channels were also reported in other cell types, including mammalian vascular smooth muscle (Bolotina et al., 1994), avian ciliary ganglia neurons (Cetiner and Bennett, 1993), and other snail neurons (Schrofner et al., 2004), suggesting a conserved signaling role for NO on Ca-activated K channels.

Although the main targets of NO were found to be Ca-activated K channels, NO might also inhibit other K channels. In fact, a residual small depolarization by NO was still seen in the initial phase after inhibition of Ca channels with $CdCl_2$, which is thought to remove all

contributions of Ca-activated K channels. NO has been shown to regulate various K channels (Tricoire and Vitalis, 2012). For example, the delayed rectifier channel, Kv3, which regulates synaptic strength and intrinsic excitability, is inhibited by NO via volume transmission in the auditory brainstem and the hippocampus (Steinert et al., 2008; Steinert et al., 2011). Considering the important roles of K channels in determining action potential waveform (Bean, 2007), the modulatory effects of NO on K channels might not only have a strong impact on membrane potential but also tune the spike timing of these neurons.

3.6.3 NO and gastropod feeding

NO is free to pass the plasma membrane and capable of acting on cellular targets in the vicinity of NO-releasing neurons, making it a good candidate for the modulation of neuronal circuits (Artinian et al., 2010). How NO signaling would affect overall snail feeding is presently unclear. NO has been described as a regulator for the feeding motor patterns in Lymnaea. An early study showed that the treatment with a NO donor activates feeding movements of the buccal mass (Moroz et al., 1993), whereas a more recent study reported that NO release in situ functions to suppress rhythmic activity in buccal motor neurons, resulting in a reduced feeding rate (Kobayashi et al., 2000). These seemingly opposing effects of NO on snail feeding warrant future investigations on the effects of NO on multiple levels, including studies on isolated neurons, the neuronal circuitry generating the feeding motor program, and animal behavior.

3.7 Figures

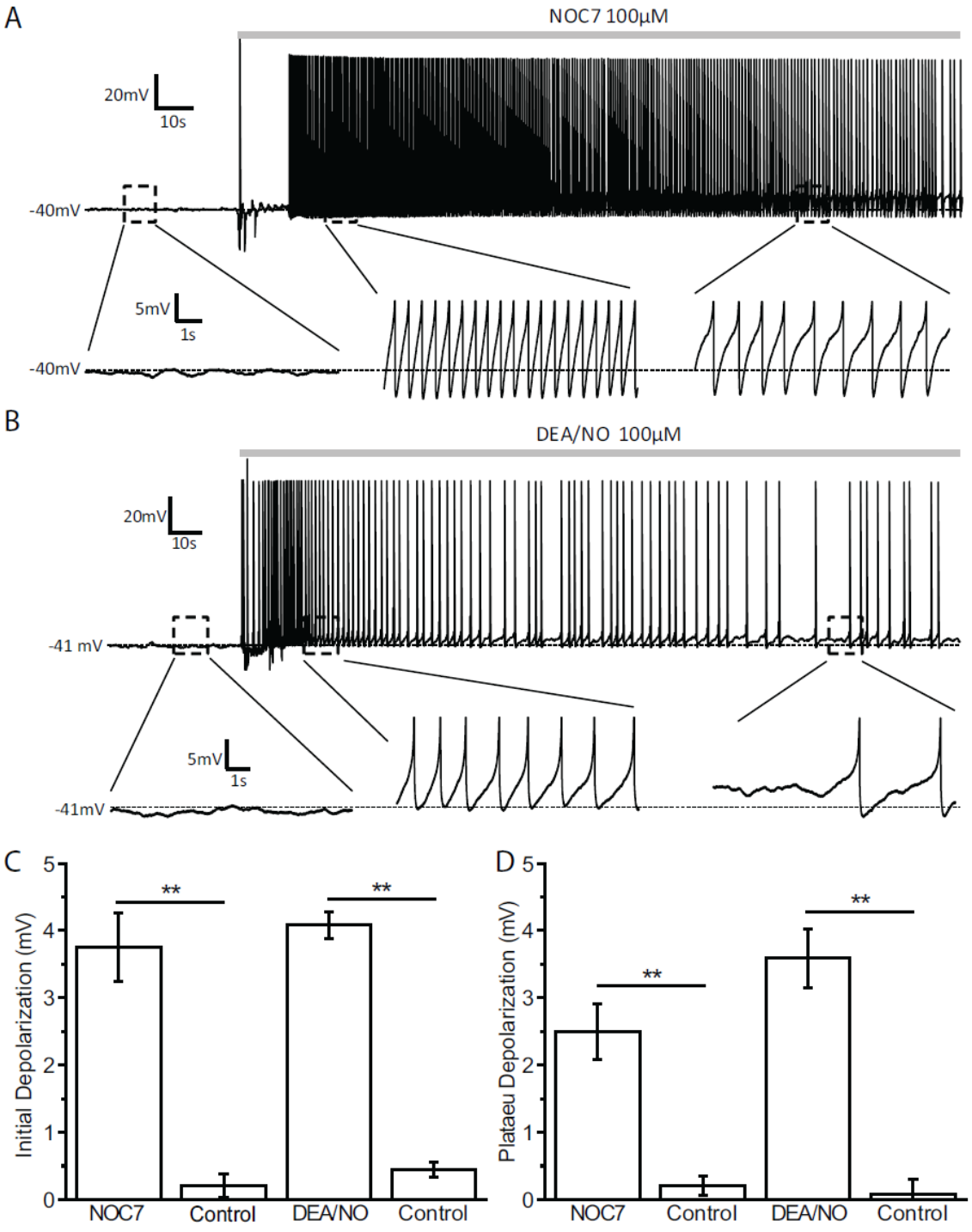

Figure 3.1 NO causes membrane potential depolarization in B19 neurons.

A: A silent B19 neuron was depolarized and started firing after treatment with NOC7 (100 μM, bath application; gray bar). Note electrical recording artifact upon drug addition. Enlarged areas of interest below the main recording trace (marked by black dashed boxed) show details of the recording (note that APs are clipped to emphasize membrane depolarization). The initial depolarization to NOC7 at 30 s was stronger than that during the plateau phase at 3 min. B: Representative data showing membrane potential depolarization of B19 neurons by another NO donor, DEA/NO (100 μM). C: Quantification of the changes in membrane potential during the initial phase such as shown in A and B. Both NOC7 and DEA/NO caused a significant depolarization compared to that of their vehicle control groups. D. Quantification of the plateau depolarization showing that both NOC7 and DEA/NO caused significant depolarization during the plateau phase.

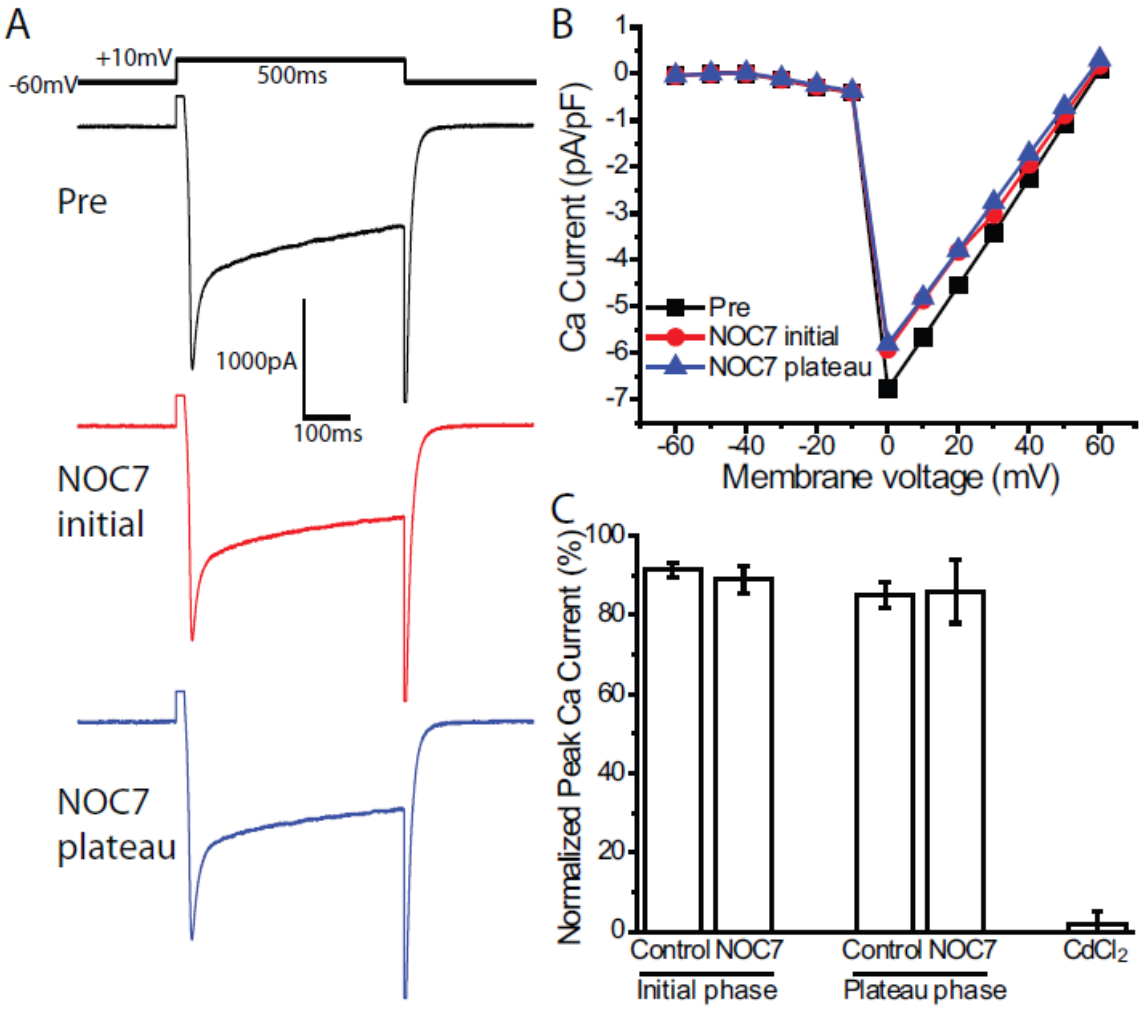

Figure 3.2 Voltage-gated Ca channels are not affected by NOC7.

Ca currents were recorded in whole-cell voltage-clamp mode. Voltage steps from a holding potential of – 60 mV to + 60 mV were applied in 10 mV increments. A: Representative traces of Ca currents evoked by a voltage step from – 60 mV to + 10 mV before (upper), during the initial phase (middle), and during the plateau phase of treatment with NOC7 (100 μM, lower). B: Representative I-V plot of Ca current measured at the peak amplitude and expressed as normalized Ca current (pA/pF) before and after NOC7 application. Note that NOC7 did not have an obvious effect on Ca currents. C: Quantification of the effect of NO on Ca currents showing

that treatment with NOC7 did not have a significant effect on normalized peak currents compared to control groups during both initial and plateau phases. Subsequent application of the Ca channel blocker $CdCl_2$ (100 μM) fully eliminated Ca currents.

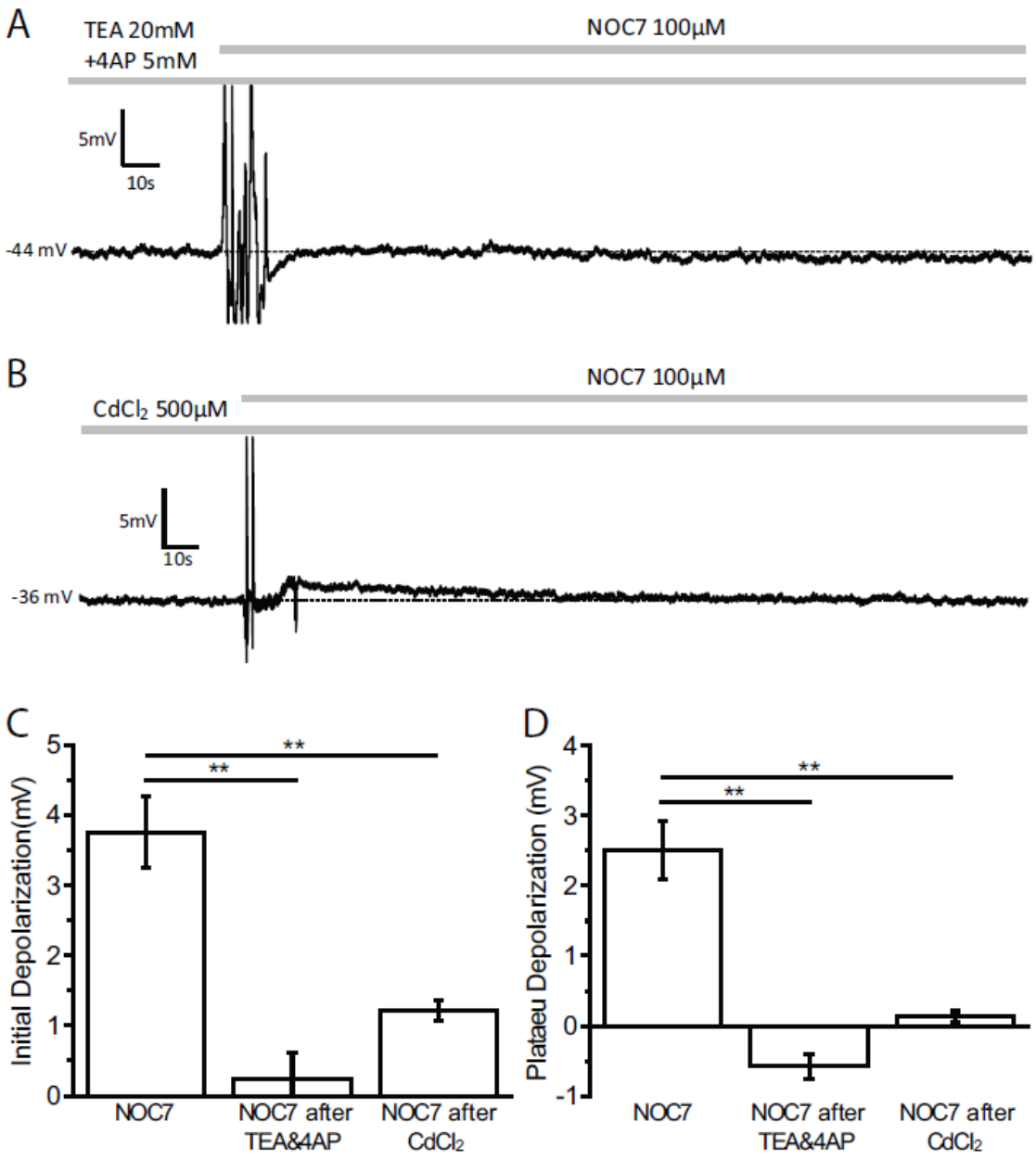

Figure 3.3 Ca-activated K channels mediate NO-induced depolarization.

A: Representative recording of a B19 neuron pretreated with a cocktail of the K channel blockers TEA (20 mM) and 4AP (5 mM), and subsequently treated with NOC7 (100 µM). Inhibition of K channels completely blocked the depolarizing effect of NOC7. B: Example of a B19 neuron pretreated with $CdCl_2$ (500 µM) before and after treatment with NOC7 (100 µM). $CdCl_2$ was

used to block Ca influx, and indirectly inhibited the activation of Ca-activated K channels. Note that NOC7 had only a small depolarizing effect on membrane potential during the initial phase, whereas any depolarization during the plateau phase was fully inhibited in the presence of $CdCl_2$. C: Quantification of the initial depolarization showing that pretreatment with TEA (20 mM) and 4AP (5 mM) fully blocked the depolarizing effect of NOC7, whereas $CdCl_2$ (500 μM) significantly inhibited the effect of NOC7 during the initial phase. D: Pretreatment with TEA and 4AP and with $CdCl_2$ prevented the NOC7-induced depolarization during the plateau phase.

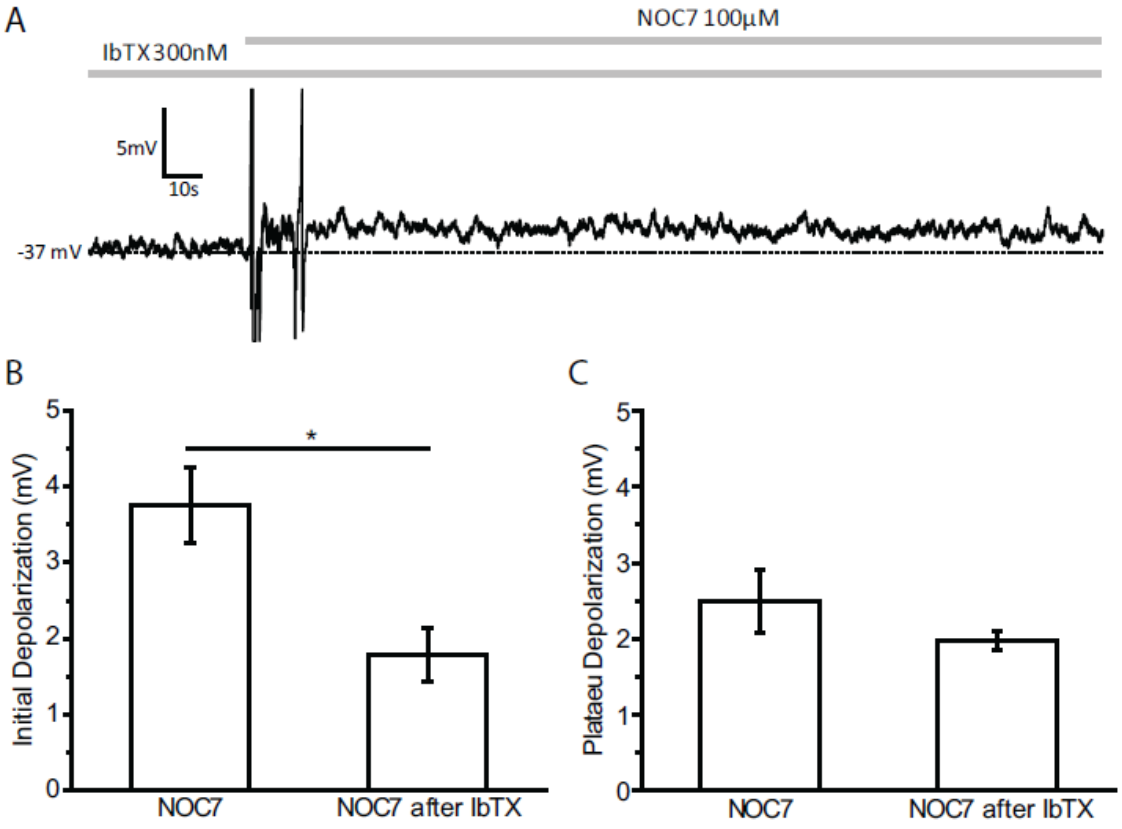

Figure 3.4 IbTX-sensitive BK channels partially contribute to the initial depolarization induced by NOC7.

A: Representative recording of a B19 neuron pretreated with IbTX (300 nM) and after addition of NOC7 (100 µM). Note that NOC7 after IbTX caused a sustained depolarization with similar initial and plateau amplitudes. B: Quantification of the initial depolarization showing that the amplitude of membrane depolarization was significantly reduced in the NOC7 after IbTX group compared to NOC7 by itself. C: Quantification of the plateau depolarization in response to treatment shown in A. IbTX pretreatment did not affect the depolarizing effect of NO during the plateau phase.

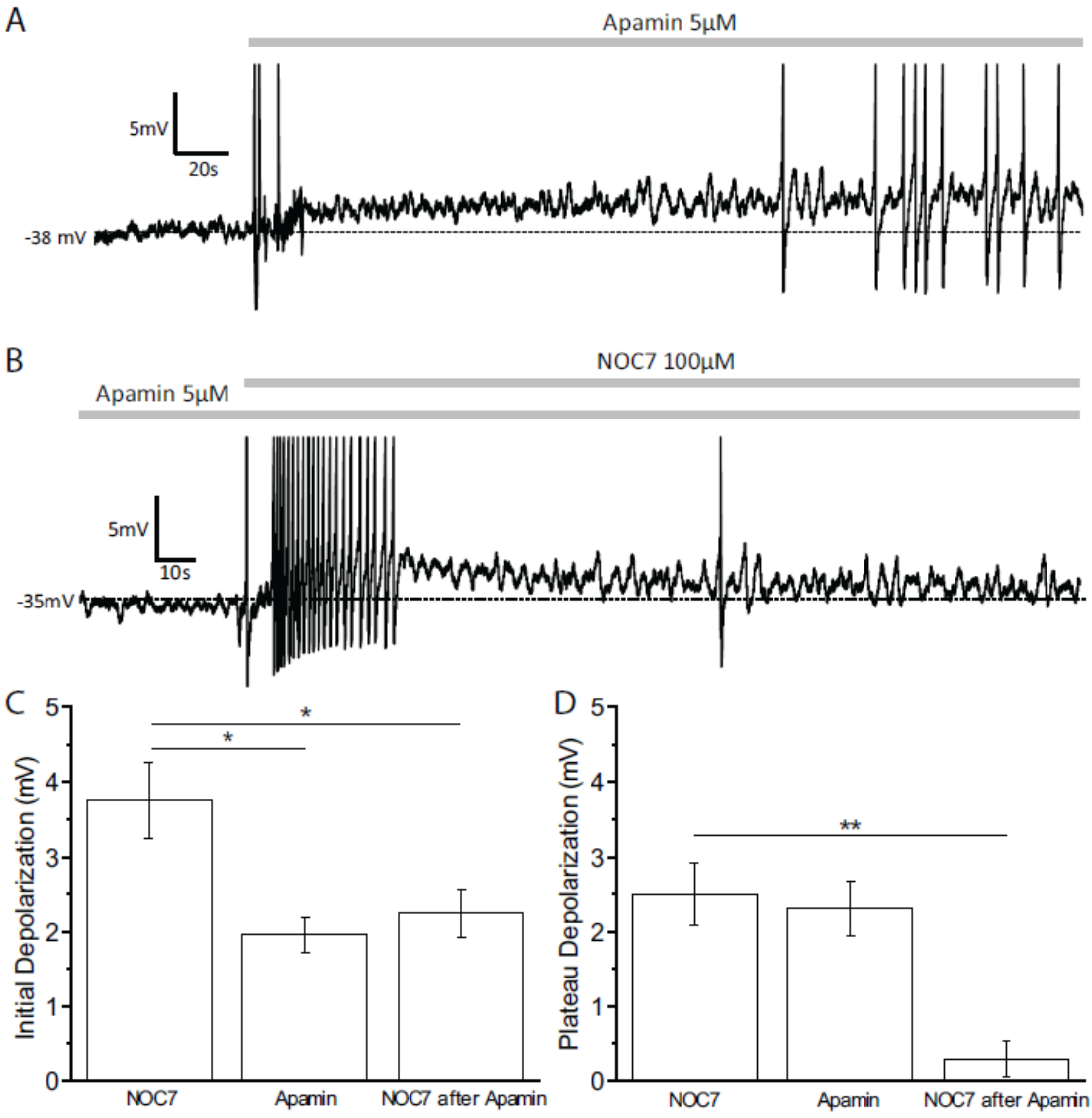

Figure 3.5 Apamin-sensitive SK channels are responsible for the main effect of NO on membrane potential.

A: Representative recording of a B19 neuron before and after treatment with apamin (5 µM). Note that apamin application led to a sustained depolarization. B: Pre-incubation with apamin (5 µM) fully blocked the plateau depolarization normally seen by treatment with NOC7 (100 µM), but a small initial depolarization was still observed. C: Quantification of the initial depolarization

such as shown in A and B. Apamin caused a depolarization, but the amplitude was significantly smaller than that of NOC7 group. NOC7 after pretreatment with apamin induced a significantly smaller depolarization than NOC7 by itself. D: Quantification of the plateau depolarization showing that treatment with NOC7 or apamin resulted in a similar depolarization. Subsequent application of NOC7 in the presence of apamin did not cause any additional depolarization during the plateau phase.

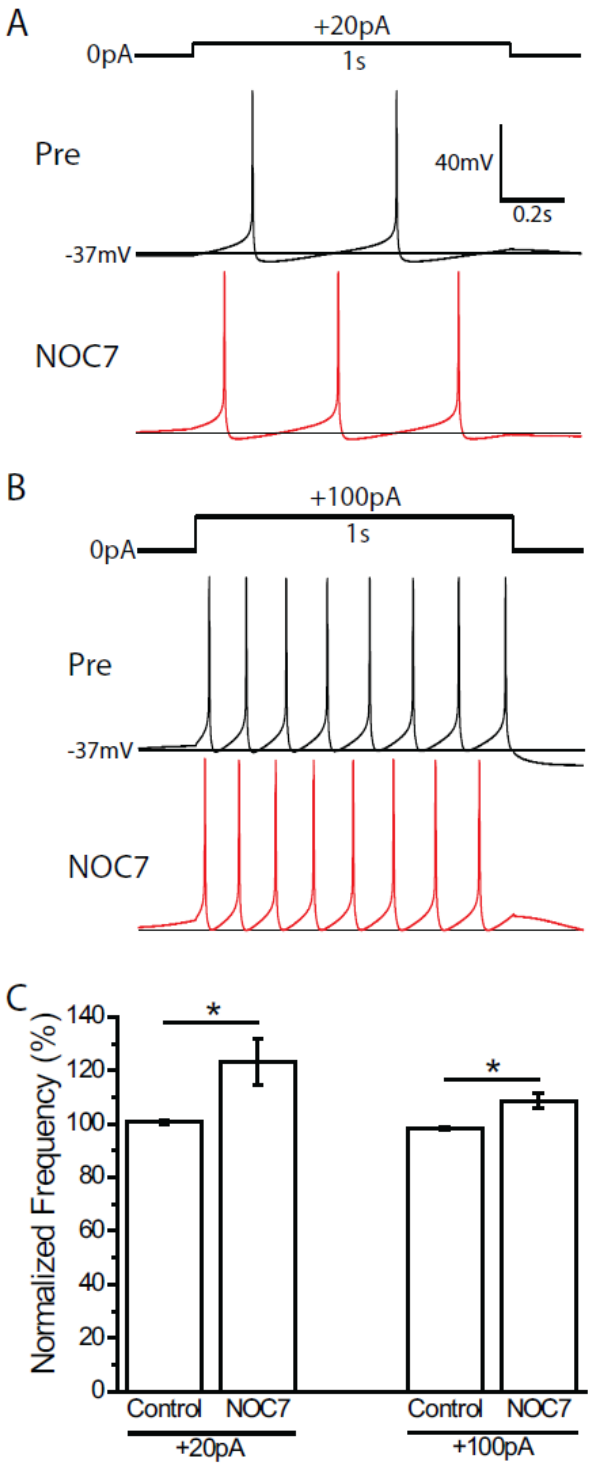

Figure 3.6 NOC7 increases the excitability of B19 neurons.

A: Comparison of action potentials evoked by injecting depolarizing current (+ 20 pA, 1s) before and after treatment with NOC7 (100 μM). Note that one more AP was induced after NOC7 application. B: Evoked APs in response to + 100 pA current injection for 1 s before and after treatment with NOC7 (100 μM). Note that NOC7 application resulted in shortened inter-spike intervals. C: Quantification of normalized spike frequency for vehicle controls and NOC7 groups. The frequency of evoked APs after treatment was normalized to that before treatment. In both + 20 pA and + 100 pA current injection conditions, NOC7 caused a significant increase in the frequency of evoked APs.

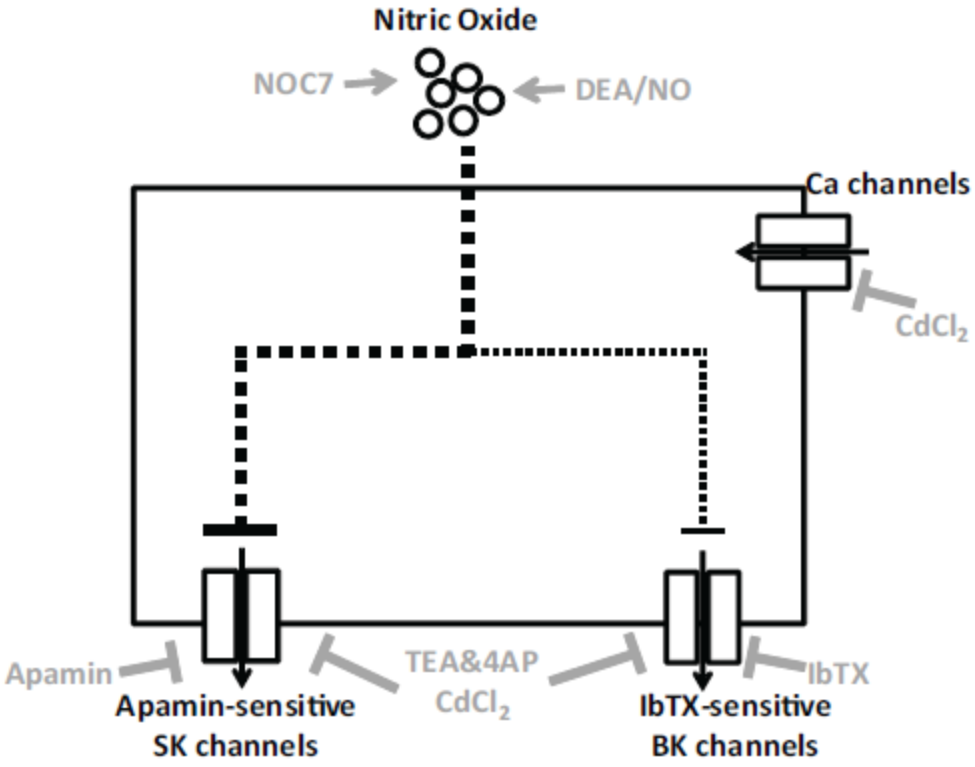

Figure 3.7 Proposed model of ion channel targets through which NO results in a prolonged depolarization.

Elevation of NO by NO donors, such as NOC7 or DEA/NO, inhibits two types of Ca-activated K channels in *Helisoma* B19 neurons. Apamin-sensitive SK channels contribute to part of the initial effect of NO and are fully responsible for its long-lasting effect on membrane depolarization, whereas IbTX-sensitive BK channels only partially contribute to the initial depolarization. Voltage-gated Ca channels do not participate in the depolarizing effect of extrinsically applied NO. The mechanism(s) by which NO inhibits these ion channels is presently unknown (indicated by dotted lines). Inhibitors used are indicated in gray.

CHAPTER 4 DOPAMINE SUPPRESSES NEURONAL ACTIVITY OF *HELISOMA* B5 NEURONS VIA A D2-LIKE RECEPTOR, ACTIVATING PLC AND K CHANNELS

Published as **Zhong L.R.**, Artinian L., and Rehder V. (2013) Dopamine suppresses neuronal activity of Helisoma B5 neurons via a D2-like receptor, activating PLC and K channels. Neuroscience. 228:109-119.

4.1 Acknowledgements

We thank Dr. Paul Katz and Dr. Akira Sakurai for assistance with the intracellular recordings from buccal ganglia, Dr. Chun Jiang for advice on experiments, and Dr. Wulf Krenz for critical reading of the manuscript. This work was supported by NSF award # 0843173 to VR and a Brains and Behavior Fellowship to LRZ.

4.2 Abstract

Dopamine (DA) plays fundamental roles as a neurotransmitter and neuromodulator in the central nervous system. How DA modulates the electrical excitability of individual neurons to elicit various behaviors is of great interest in many systems. The buccal ganglion of the freshwater pond snail *Helisoma trivolvis* contains the neuronal circuitry for feeding and DA is known to modulate the feeding motor program in *Helisoma*. The buccal neuron B5 participates in the control of gut contractile activity and is surrounded by dopaminergic processes, which are expected to release DA. In order to study whether DA modulates the electrical activity of individual B5 neurons, we performed experiments on physically isolated B5 neurons in culture and on B5 neurons within the buccal ganglion *in situ.* We report that DA application elicited a strong hyperpolarization in both conditions and turned the electrical activity from a

spontaneously firing state to an electrically silent state. Using the cell culture system, we demonstrated that the strong hyperpolarization was inhibited by the D2 receptor antagonist sulpiride and the phospholipase C (PLC) inhibitor U73122, indicating that DA affected the membrane potential of B5 neurons through activation of a D2-like receptor and PLC. Further studies revealed that the DA-induced hyperpolarization was inhibited by the K channel blockers 4-aminopyridine and tetraethylammonium, suggesting that K channels might serve as the ultimate target of DA signaling. Through its modulatory effect on the electrical activity of B5 neurons, the release of DA *in vivo* may contribute to a neuronal output that results in a variable feeding motor program.

KEYWORDS: dopamine, D2-like receptor, *Helisoma trivolvis*, PLC, K channels, excitability.

4.3 Introduction

Dopamine (DA) acts as a neurotransmitter and neuromodulator in the central nervous system, where it regulates a wide range of neuronal circuits in both vertebrate and invertebrate species (Harris-Warrick et al., 1998; Murphy, 2001; Bevan et al., 2006). How DA modulates the electrical excitability of individual neurons, alters the output of neuronal circuits, and finally affects an animal's behavior are central questions that are being addressed in many systems.

Gastropods have a relatively simple nervous system with identifiable neurons in different ganglia, providing a convenient model to study the role of DA in neuronal function. Previous studies have demonstrated that DA regulates various cellular and physiological functions in gastropods. DA plays critical roles in initiation and regulation of respiratory and feeding central pattern generator activities in *Helisoma trivolvis* and *Lymnaea stagnalis* (Quinlan et al., 1997; Magoski and Bulloch, 1999). The DA-releasing RPeD1 neuron in *Lymnaea* promotes neurite

extension in its *in vivo* target neuron, but collapses growth cones of non-target neurons (Spencer et al., 1996; Spencer et al., 2000). Electrophysiological results have revealed that DA exposure alters neuronal electrical properties (Dobson *et al.*, 2006). DA induces a sustained depolarization of the membrane potential in the *Helisoma* B19 neuron (McCobb et al., 1988). On the other hand, a hyperpolarizing response induced by DA is shown in multiple *Lymnaea* neurons (de Vlieger et al., 1986; Audesirk, 1989; Magoski et al., 1995; Dobson et al., 2006). Considering the diverse roles that DA plays in gastropod nervous systems, it is important to develop a detailed understanding of which signaling pathways are activated by DA in particular neurons.

DA receptors are grouped into 2 subtypes: D1-like and D2-like receptors (Missale et al., 1998; Beaulieu and Gainetdinov, 2011). They are G-protein coupled receptors, and separated based on their ability to modulate adenylate cyclase activity. D1-like receptors stimulate adenylate cyclase via G_s, whereas D2-like receptors inhibit it via G_i. In addition to the regulation of cAMP signaling, DA receptors can also activate PLC via $G_{q/11}$ (Lee *et al.*, 2004). These DA-activated intracellular signals have been reported to result in the modulation of a variety of ionic currents (Harris-Warrick et al., 1998). For example, an A-type K current has been shown to be regulated differentially by different DA receptors in the crustacean pyloric PD and LP neurons (Zhang *et al.*, 2010). Therefore, a study of signaling pathways activated by DA in individual neurons is necessary to explain DA-associated effects on neuronal excitability.

B5 neurons in *Helisoma*, like their homologs in the closely-related species *Lymnaea* and *Clione*, innervate the esophagus and are involved in feeding behavior (Perry et al., 1998; Malyshev and Balaban, 2009). Excitation of the neurons in *Lymnaea* leads to contraction of the foregut, while their silencing results in relaxation (Perry *et al.*, 1998). Immunohistochemistry shows the presence of dopaminergic neurons in the buccal ganglion, and DA is found to

modulate the neural circuitry of feeding (Quinlan et al., 1997; Murphy, 2001). Here, we tested the effect of DA on the electrical activity of B5 neurons and investigated the signaling pathway activated by DA.

We report that DA hyperpolarized the membrane potential and switched B5 neuron from a state of spontaneous firing to being silent in both *in vitro* and *in situ* recording conditions. To assure that DA release from sources within the ganglion could not complicate the interpretation of the data, we performed all following experiments on B5 neurons that had been physically isolated from buccal ganglia and maintained in cell culture. Investigation of the signaling mechanism underlying the DA–induced hyperpolarization revealed that DA acts on a D2-like receptor, signals via PLC, and subsequently opens two types of K channels, a 4AP-sensitive K channel and a TEA-sensitive K channel. The modulatory effect of DA on the electrical activity of B5 neurons may contribute to the coordinated output of various neurons involved in the snail feeding motor program.

4.4 Methods

4.4.1 Neuronal culture

Identified B5 neurons were removed from the buccal ganglion of the freshwater pond snail *Helisoma trivolvis* and plated into Falcon Petri dishes as previously described (Rehder & Kater, 1992). Briefly, neurons were plated onto poly-L-Lysine (hydrobromide, MW, 70-150 kDa, 0.25 mg/ml; Sigma, St. Louis, MO, USA)-coated glass coverslips attached to the bottom of 35-mm cell culture dishes (Falcon 1008). B5 neurons were kept in conditioned medium at room temperature. Conditioned medium was prepared by incubating two *Helisoma trivolvis* brains per 1 mL of Leibovitz L-15 medium (Invitrogen, Carlsbad, CA, USA) for 3 - 4 days (Wong et al.,

1981). Neurons were used for experiments 24 - 48 hour after plating. The composition of L-15 medium was as follows (mM): 44.6 NaCl, 1.7 KCl, 1.5 $MgCl_2$, 0.3 $MgSO_4$, 0.14 KH_2PO_4, 0.4 Na_2HPO_4, 1.6 Na pyruvate, 4.1 $CaCl_2$, 5 HEPES, 50 μg/ml gentamicin, and 0.15 mg/ml glutamate in distilled water, pH 7.4.

4.4.2 Electrophysiology

Recordings from the *Helisoma* B5 neuron in whole-cell current-clamp mode were obtained as described previously (Artinian et al., 2010). The patch electrodes were pulled from borosilicate glass tube (OD 1.5mm; ID 0.86mm; Sutter instruments) on a Sutter instruments micropipette puller (P-87) and heat polished (Micro Forge MF-830; Narishige) with a resistance of about 3 - 8 MΩ. Neurons were recorded using Axopatch 2B and 700B amplifiers (Molecular Devices, Union City, CA) and an analog-to-digital converter (Digidata 1440). Data acquisition and analysis were performed using pClamp software version 10 (Molecular Devices). Current-clamp configuration was used to record membrane potential, firing properties, and input resistance. Leibowitz L-15 medium was normally used as extracellular recording solution. In some experiments, L-15 medium was replaced with normal saline containing in (mM): 51.3 NaCl, 1.7 $CaCl_2$, 1.5 $MgCl_2$, and 5 HEPES, pH 7.3 - 7.4 (127 mOsm). Intracellular recording solution contained (mM): 54.4 K-aspartate, 2 $MgCl_2$, 5 HEPES, 5 Dextrose, 5 ATP 0.1 EGTA (127 mOsm). TEA solution was made by replacing 20 mM NaCl with 20 mM TEACl. Low Cl solution was prepared by replacing 51.3 mM NaCl with 51.3 mM Na gluconate in the extracellular solution. Solution replacement was achieved through a gravity-based perfusion system (Warner Instruments). Membrane potentials were corrected for liquid junction potential caused by switching between solutions of different ionic composition. Resting membrane potential of spontaneous firing neuron was determined by measuring the value at the plateau of

the depolarization phase before the membrane potential reached threshold. Analysis of action potential properties was achieved by using the 'template search' function of Clampfit (pClamp 10, Molecular Devices). Initial broadening of action potentials induced by 4AP was measured as the action potential width at one quarter of action potential amplitude from the positive peak, where the effect of 4AP was most obvious. Measurement of input resistance was made by a series of hyperpolarizing current injections from - 50 to - 200 pA in steps of - 50 pA for 3 s, and determined from the slope of a linear fit of the relationship between the peak change in membrane potential and the magnitude of the injected current (Robinson and Cameron, 2000).

For intracellular recordings from B5 neurons located within buccal ganglia, ganglia were pinned down in a dissection chamber containing normal saline. The ganglionic sheath in the vicinity of B5 neuron was cut open using a fine microknife. Neurons were impaled with sharp glass microelectrodes filled with 3 M KCl having resistances of about 20 – 50 MΩ (Sakurai et al., 2006). Neurons were recorded using Axoclamp 2B amplifiers (Molecular Devices, Union City, CA), and data acquisition and analysis were achieved with Spike2 software (Cambridge Electronic Design). Negative current (ranging from - 0.2 nA to - 1 nA, 1 s) was occasionally delivered to measure input resistance during recordings.

4.4.3 Pharmacological agents

All agents were purchased from Sigma. Dopamine (DA) was dissolved in water to make a 100 mM stock solution. R(+)-SCH-23390 hydrochloride (D1 receptor inhibitor), (S)-(-)-Sulpiride (D2 receptor inhibitor), U-73122 hydrate (PLC inhibitor), U-73343 (inactive PLC inhibitor) were dissolved in dimethylsulfoxide (DMSO) to make 100 mM, 100 mM, 5 mM, 5 mM stock solutions, respectively. For patch clamp experiments performed in cell culture, stock solutions were mixed with 50 μl of extracellular solution removed from the recording dish and

directly and gently added back around the periphery of the dish for drugs to equilibrate to their final concentrations. For intracellular recordings from buccal ganglia, stock solutions were mixed in 500 µl of saline solution that was initially removed from the recording dish and then added back. The final concentration of DMSO in the extracellular recording solution was less than 0.1% and that concentration by itself had no measurable effect on neurons. Other solutions used included Na gluconate and the K channel blockers tetraethylammonium chloride (TEA) and 4-aminopyridine (4AP), which were prepared directly in the extracellular solution.

4.4.4 Statistical analysis

All data were expressed as mean ± SEM. Comparisons between two individual groups were made with the Mann-Whitney U-test, and comparisons between two paired groups were achieved by the Wilcoxon signed-rank test using Origin 6 software (OriginLab Corporation, Northampton, MA). Significant differences are indicated as *P < 0.05, **P < 0.01, and ***P < 0.001.

4.5 Results

4.5.1 DA causes a strong hyperpolarization of neuron B5

B5 neurons, isolated from the buccal ganglion of *Helisoma trivolvis*, were cultured for 24 - 48 hour before experiments, at which time all neurons had well-developed neurites with growth cones at their tips. In a previous study, we had shown that B5 neurons at this developmental stage had resting membrane potentials (RMP) of - 43 ± 7 mV and fired action potentials spontaneously with an average frequency ranging from 0.5 Hz to 2 Hz (Artinian *et al.*, 2010). We first asked how bath application of DA might affect the electrical activity of B5 neurons. All neurons treated with DA (1, 5, 20 or 100 µM) showed a strong hyperpolarizing response, and

switched from a state of spontaneous firing to being silent [Fig. 4.1(A)]. The maximal hyperpolarizing response induced by 1 μM DA was - 16.8 ± 4.0 mV (n = 5, Fig. 4.1(B)). This was significantly different from the solvent control, which had no effect (- 1.0 ± 0.7 mV; n = 5, $P < 0.05$, Fig. 4.1(B)). Increasing the DA concentration resulted in a dose-dependent increase in hyperpolarization (5 μM: - 19.2 ± 2.6 mV, n = 4; 20 μM: - 24.9 ± 1.7 mV, n = 7; and 100 μM DA: - 29.1 ± 1.0 mV, n=5; Fig. 4.1(B)). An analysis of the delay between the time of DA addition and the time when the hyperpolarizing response reached its maximum also showed a concentration-dependent effect, with 1 μM DA resulting in a peak at 1014.7 ± 110.6 s (n = 4, Fig. 4.1(C)) after the drug application, while the 20 μM DA group peaked significantly earlier (409.0 ± 45.9 s; n = 7, $P < 0.01$, Fig. 4.1(C)). We used 20 μM DA from here on, because this concentration resulted in a robust hyperpolarization of the membrane potential with a relatively short delay.

While neurons in cell culture and *in situ* often exhibit very similar receptor properties and ionic conductances, there are also reports in which responses *in vitro* differ from those recorded *in situ* (Turrigiano and Marder, 1993; Turrigiano et al., 1994; Haedo and Golowasch, 2006). To test if responses of B5 neurons in culture were representative of their behavior in the ganglion, we next performed intracellular recordings from B5 neurons located within the buccal ganglion. B5 neurons *in situ* fired action potentials, and treatment with 20 μM DA elicited a strong hyperpolarization of RMP, switching neurons from spiking to being silent [Fig. 4.2(A)], just as had been observed in B5 neurons in cell culture [Fig. 4.1(A)]. The maximal hyperpolarizing response was - 18.0 ± 2.0 mV (n = 5, Fig. 4.2(B)), which was significantly different from the vehicle control (+ 0.9 ± 0.5 mV; n = 6, $P < 0.01$, Fig. 4.2(B)). Increasing the concentration to 100

μM DA did not elicit an additional significant effect on membrane potential (- 21.2 ± 2.3 mV; n = 5, Fig. 4.2(B)) when compared to the 20 μM DA group (P = 0.4, Fig. 4.2(B)).

Taken together, DA caused a strong hyperpolarizing effect on *Helisoma* B5 neurons both *in vitro* and *in situ*, converting them from spiking tonically to being silent. Given the similarity of responses to DA in B5 neurons *in vitro* and *in situ*, we performed all experiments from here on in culture, because no DA release from other cellular sources could potentially complicate the interpretation of results.

4.5.2 A D2-like receptor mediates DA's effect on electrical activity

To investigate the signaling pathway that mediated the DA-induced hyperpolarizing effect, we next asked which receptors were activated by DA. There are two major subtypes of DA receptors: D1-like receptors and D2-like receptors. We first focused on the D2-like receptor, because they have been implicated in causing a hyperpolarization of RMP in different neuronal cell types, including several *Lymnaea* neurons (de Vlieger et al., 1986; Audesirk, 1989; Magoski and Bulloch, 1999; Dobson et al., 2006). 100 μM sulpiride, a D2-like receptor antagonist that had been used in *Helisoma* previously (Quinlan et al., 1997), did not change the RMP of B5 neurons (- 0.2 ± 1.2 mV; n = 4, Fig. 4.3(C)), but when 20 μM DA was added in the presence of sulpiride (10 min preincubation), neurons maintained their firing activity (+ 0.7 ± 1.1 mV; n = 4, Fig. 4.3(A) and 3(C)), demonstrating that the hyperpolarizing effect of DA on RMP had been completely abolished (P < 0.05, Fig. 4.3(C)). These data indicated that DA likely acted on a D2-like receptor to hyperpolarize the RMP of B5 neurons.

A D1-like receptor has been suggested to mediate the DA-induced growth cone collapse in the neuron PeA in *Lymnaea stagnalis* (Dobson *et al.*, 2006), a species of fresh water snail that is closely related to *Helisoma trivolvis*. To rule out a potential role of D1-like receptors in

mediating the effect of DA on RMP, we used a D1 receptor antagonist, SCH23390, to investigate whether the DA-induced hyperpolarization could be blocked when the D1-like receptor was inhibited (Magoski et al., 1995; Mukai et al., 2004). Whereas the pretreatment with 100 μM SCH23390, a concentration that has been demonstrated to be effective in *Lymnaea,* did not affect the RMP of B5 neurons (+ 0.4 ± 1.3 mV; n = 4, Fig. 4.3(C)), bath application of 20 μM DA in the presence of SCH23390 still elicited a strong hyperpolarization (- 27.4 ± 1.5 mV; n = 4, Fig. 4.3(B) and 4-3(C)). This hyperpolarization was not significantly different from that induced by DA treatment alone (P = 0.51, Fig. 4.3(C)), suggesting that the effect of DA on the RMP was not mediated via a D1-like receptor.

4.5.3 PLC plays a critical role in DA signaling

To determine the signaling pathway downstream of the D2-like receptor, we first investigated phospholipase C (PLC), a prominent target of the D2 receptor-activated G-protein $G_{q/11}$. Activation of PLC signaling by $G_{q/11}$ has been shown to mediate the DA-induced hyperpolarization in *Lymnaea* PeA neurons (Dobson *et al.*, 2006). The PLC inhibitor, U73122 (0.5 μM), alone slightly hyperpolarized the RMP and silenced the spontaneous firing activity of B5 neurons (- 4.2 ± 0.6 mV; n = 5, Fig. 4.4(A) and 4-4(C)) (Dobson et al., 2006), suggesting that PLC activity was required for the generation of spontaneous firing activity. Interestingly, the hyperpolarizing effect of 20 μM DA on the RMP was blocked in the presence of 0.5 μM U73122 (- 4.6 ± 1.4 mV; n = 5, P < 0.01, Fig. 4.4(A) and 4-4(C)). We next used U73343, the inactive analog of U73122, as a negative control. 0.5 μM U73343 on its own had no effect on RMP (- 0.5 ± 0.9 mV; n = 4, Fig. 4.4(C)), and the addition of 20 μM DA in the presence of U73343 still caused a strong hyperpolarization (- 25.5 ± 0.5 mV; n = 3), which was not significantly different

from the level of the hyperpolarization elicited by DA itself (P = 0.82, Fig. 4.4(C)). These results suggested that DA acted via activation of PLC to hyperpolarize RMP.

4.5.4 K channels mediate the DA-induced hyperpolarizing effect

We next addressed which ion channels might be affected by DA to elicit its hyperpolarizing effect. Using a current-clamp protocol, hyperpolarizing current injections before DA exposure and at the peak of the hyperpolarizing response to the DA treatment indicated that DA caused a decrease in input resistance (R_n) [Fig. 4.5(A)]. R_n was quantified by the slope of the linear fit of the relationship between the peak change in membrane potential and the magnitude of the injected current [Fig. 4.5(B)] (Robinson and Cameron, 2000). 20 μM DA significantly reduced R_n from 542 MΩ to 194 MΩ calculated from the example in Fig. 4.4B, and similar decreases in R_n were observed in other B5 neurons tested (pre: 447.8 ± 34.0 MΩ vs. post DA: 169.8 ± 22.0 MΩ; n = 4, P < 0.01, Fig. 4.5(C)).

The decrease in R_n indicated that the hyperpolarization caused by DA was likely due to the opening of a K and/or a Cl conductance. We first investigated the potential effects of DA on K channels, because DA has been suggested to modulate the activity of K channels by various downstream signaling pathways (Missale *et al.*, 1998). Studies in *Lymnaea* indicated the presence of two types of pharmacologically distinct K channels: one sensitive to tetraethylammonium chloride (TEA) and the other to 4-aminopyridine (4AP). They have been shown to contribute to different phases of action potential repolarization (Sakakibara *et al.*, 2005). The perfusion of a cocktail of 20 mM TEA and 5 mM 4AP, concentrations that have been suggested to be effective to block both K channels in *Helisoma* and *Lymnaea* (Berdan and Easaw, 1992; Staras et al., 2002), caused a decrease in firing frequency by 34.5 ± 2.7% (n = 7, P < 0.05) combined with an increase in action potential amplitude by 21.5 ± 0.3% (n = 7, P < 0.05) [Fig.

4.5(D)]. A comparison of single action potentials showed a significant broadening by 95.5 ± 3.9% ($n = 7$, $P < 0.05$) after treatment with the solution containing a mixture of TEA and 4AP. Bath application of 20 μM DA in the presence of pharmacological inhibition of K channels with TEA and 4AP resulted in a significant reduction of the DA-induced hyperpolarizing response (- 2.5 ± 1.4 mV; $n = 5$, $P < 0.01$, Fig. 4.5(E) and 5(F)). Therefore, K channels were the downstream targets of DA resulting in the hyperpolarization of the RMP of B5 neurons.

We next investigated the potential involvement of Cl channels. With the reduction of the Cl concentration in the extracellular recording solution from 64.2 mM to 12.9 mM, any Cl current would be largely reduced (Woodward and Willows, 2006). Cells were first perfused with low Cl extracellular solution, and then DA was bath applied. The perfusion of low Cl solution did not alter RMP (+ 0.6 ± 0.5 mV; $n = 4$, Fig. 4.5(E)). Interestingly, DA still caused a strong hyperpolarization of RMP [Fig. 4.5(G)], and the magnitude of the hyperpolarization induced by DA in low Cl solution (- 19.8 ± 1.7 mV; $n = 4$, $P = 0.16$, Fig. 4.5(E)) was not significantly different from DA treatment in the control solution. These experiments suggested that Cl channels did not appear to contribute significantly to the hyperpolarization induced by DA.

4.5.5 DA enhances both TEA-sensitive and 4AP-sensitive K currents, with the main target being a 4AP-sensitive K current

We next wanted to differentiate which subtype of K channels was responsible for the hyperpolarizing response induced by DA. The delayed rectifying K current is TEA-sensitive, whereas the 4AP-sensitive, fast activating and rapidly inactivating K current contributes to the initial repolarization of the AP (Staras *et al.*, 2002). Perfusion with 20 mM TEA solution led to a significant broadening of the AP repolarization shoulder by 129.5 ± 8.6% ($n = 8$, $P < 0.01$), which was consistent with the blockage of the delayed rectifying K channels, but TEA had no

effect on RMP (- 1.5 ± 0.7 mV; n = 4, Fig. 4.6(A) and 4-6(E)). Subsequent application of 20 μM DA in the presence of 20 mM TEA caused a strong hyperpolarization (- 18.2 ± 1.5 mV; n = 4, Fig. 4.6(C)), although the hyperpolarization was significantly smaller than the one seen with DA by itself ($P < 0.05$, Fig. 4.6(E)). Hence, a TEA-sensitive K channel partially contributed to the effect of DA on RMP.

We next investigated the contribution of 4AP-sensitive K channels to the DA-induced hyperpolarization. Perfusion of 5 mM 4AP resulted in the initial broadening of the repolarization phase of the action potential (an increase by 41.0 ± 5.8%; n = 8, $P < 0.01$, Fig. 4.6(B)), suggesting that a transient K channel was inhibited by 4AP application in B5 neurons. Whereas 5 mM 4AP caused a small hyperpolarization of RMP (- 4.7 ± 1.5 mV; n = 4, Fig. 4.6(E)), the treatment with 20 μM DA in the presence of 5 mM 4AP did not result in an additional hyperpolarization of RMP (- 4.9 ± 1.8 mV; n = 4, $P < 0.05$, Fig. 4.6(D) and 6(E)) compared to DA by itself. Taken together, DA acted on both TEA-sensitive and 4AP-sensitive K channels to hyperpolarize RMP of B5 neurons, with its main effect on 4AP-sensitive K channels.

4.6 Discussion

DA modulates electrical activities in different cell types, both *in vivo* and *in vitro* (Harris-Warrick et al., 1998; Beaulieu and Gainetdinov, 2011). We report here that DA caused a strong hyperpolarizing and silencing response in B5 neurons of the buccal ganglion of *Helisoma trivolvis* both *in vitro* and in the ganglion. The mechanism by which DA alters cell excitability is schematically shown in Fig. 4.7. DA acted on a D2-like receptor, which in turn activated PLC signaling. The downstream ion channels identified in mediating the DA-induced hyperpolarization were 4AP-sensitive K channels and TEA-sensitive K channels. All

pharmacological blockers used in current research were chosen based on their successful usages either directly in *Helisoma*, or in closely related species, such as *Lymnaea*.

4.6.1 DA signal transduction cascade

A total of five distinct but closely related G-protein coupled DA receptor genes are cloned in vertebrates (Beaulieu and Gainetdinov, 2011). Based on their ability to modulate adenylate cyclase activity and differences in pharmacological properties, DA receptors are separated into two subtypes, D1 (D1 or D5) and D2 (D2, D3 and D5). In invertebrates, the identity of DA receptors is much less understood. DA is reported to activate D1-like receptors and D2-like receptors, which correspond to the vertebrate classification (Magoski et al., 1995; Dobson et al., 2006). In gastropods, only one Aplysia D1-like receptor is cloned and characterized (Barbas et al., 2006). We showed that the D2R inhibitor sulpiride blocked hyperpolarizing responses of DA in *Helisoma* B5 neurons, suggesting that a D2-like receptor is likely to be the target of DA in this neuron. D2-like receptors seem to play critical roles in gastropod nervous systems. Sulpiride blocked the effects of DA in multiple buccal central pattern generator neurons in *Helisoma* (Quinlan *et al.*, 1997). Pharmacological studies of the DA-containing RPeD1 neuron in *Lymnaea* suggest that D2-like receptors located on its *in vivo* target neurons mediate chemoattractive growth cone behavior (Spencer *et al.*, 2000). Moreover, blocking the D2-like receptor eliminates hyperpolarizing responses caused by DA in RPeD1 follower cells VD4, VJ, VI, and RPA (Magoski et al., 1995; Magoski and Bulloch, 1999) and its non-target neuron PeA in *Lymnaea stagnalis* (Dobson *et al.*, 2006). These findings are consistent with the present study of B5 neurons in which the DA-induced hyperpolarization was mediated by a D2-like receptor.

In vertebrates, sulpiride acts as a general D2-like antagonist, but also has affinity for D3 receptors (Freedman et al., 1994; Seabrook et al., 1994). Considering that much less information on DA receptors is available in molluscan systems, the identity of specific subtypes of DA receptors on B5 neurons is presently unclear. Therefore, we chose to characterize DA receptor types by their response to commonly used inhibitors and describe the receptors as D1-like or D2-like receptors to acknowledge this uncertainty.

Upon the activation of D2-like receptors, various downstream signaling pathways can be activated through G proteins, such as $G_{i/o}$ and $G_{q/11}$ (Beaulieu and Gainetdinov, 2011). We found that inhibiting PLC using U73122 abolished the hyperpolarizing responses caused by DA treatment, indicating that the D2-like receptor likely coupled to $G_{q/11}$. This finding is consistent with the results reported in the *Lymnaea* PeA neuron (Dobson *et al.*, 2006), where injection of the non-hydrolyzable GTP analog GDP-β-S or pretreatment with U73122 blocks the DA-induced hyperpolarization. Interestingly, another D2-like receptor-mediated pathway has been reported in the *Lymnaea* RPA neuron, in which DA causes the hyperpolarization of RMP via the $G_{i/o}$ pathway (Dobson *et al.*, 2006).

4.6.2 Ion channels modulated by DA

DA signaling pathways regulate cell excitability via the modulation of various ionic conductances (Turrigiano and Marder, 1993; Harris-Warrick et al., 1998). A wide range of cell types in the cerebral ganglion of *Lymnaea* respond to DA either by depolarization or hyperpolarization. Here, we report that the R_n of B5 neurons was reduced after DA treatment, suggesting the opening of membrane channels. Interestingly, although a K conductance has been suggested to mediate the DA-induced hyperpolarizing responses in different studies (de Vlieger et al., 1986; Magoski and Bulloch, 1999), a further characterization of the types of membrane

channels and the signaling pathway mediating the effect of DA on membrane potential is lacking. In the present study, we report that two types of K channels, a 4AP-sensitive K channel and a TEA-sensitive K channel, were activated by DA, and the 4AP-sensitive K channel had a larger contribution to the hyperpolarization than the TEA-sensitive K channel did. K channels play a critical role in determining action potential shape and firing frequency, so dopaminergic modulation of K channels could potentially alter postsynaptic neural circuitry via changing neuronal firing properties in target neurons (Shieh *et al.*, 2000). The DA-induced changes of K conductances are extensively studied in the 14-neuron pyloric network of the crustacean stomatogastric ganglion. DA modulates a 4AP-sensitive A-type K current (I_A) in almost every pyloric neuron (Harris-Warrick et al., 1995; Harris-Warrick et al., 1998). DA enhances I_A in PD and VD, but reduces it in LP, PY and AB neurons. The opposite effects induced by DA in different cell types are due to the differences at the levels of the DA receptors and intracellular signaling pathways. cAMP/PKA signaling has been found to be important for DA to modulate I_A in LP neurons (Zhang *et al.*, 2010). Additionally, this K current has been shown to be enhanced by tonic stimulation with nanomolar DA concentration through a translation-dependent mechanism involving the target of rapamycin pathway in crustacean LP neurons (Rodgers *et al.*, 2011), a process thought to dampen extrinsic excitatory inputs.

4.6.3 DA as a neurotransmitter in regulating neuronal functions in Helisoma

The current study revealed an important role for DA in modulating the electrical activity of *Helisoma* B5 neurons. While the purpose of this dopaminergic modulation is presently unknown, the strong and prolonged hyperpolarization induced by DA would likely alter the efficacy of presynaptic inputs and the output onto postsynaptic targets. It has been suggested in the crustacean pyloric network that neuromodulatory inputs of DA can tune an anatomically

defined circuit to produce a variety of circuit outputs (Marder and Calabrese, 1996; Harris-Warrick et al., 1998). Moreover, a tonic background concentration of DA was shown to convert NMDA receptor-independent long-term potentiation to long-term depression in rat PFC neurons (Matsuda *et al.*, 2006). Similar modulatory effects on neuronal activity have been reported in related gastropods. For instance, nitric oxide transforms the inhibitory effect of glutamate into an excitatory response in the *Lymnaea* buccal neuron B4, and this effect is thought to modify feeding behaviors (D'Yakonova T and D'Yakonova V, 2008). In an early study of neurite regeneration performed on the *Helisoma* B19 neuron, the inhibition of neurite elongation normally observed after the serotonin application is eliminated when acetylcholine is co-applied (McCobb et al., 1988), arguing that the membrane potential serves as an integrator of the effects elicited by excitatory and inhibitory neurotransmitters/ neuromodulators.

The DA-induced changes in electrophysiological properties may also exert morphological effects on developing or regenerating neurons via changes of internal Ca dynamics. Electrically silencing a neuron may reduce the intracellular free Ca concentration compared to a spontaneously spiking B5 neuron. This reduction in Ca could, in turn, alter neurite growth rates and axonal pathfinding (Rehder and Kater, 1992). In fact, studies in *Lymnaea* revealed that the DA-containing neuron RPeD1 can cause collapse or repel a nontarget growth cone (Spencer *et al.*, 2000), a process that is thought to prevent inappropriate contacts between developing neurons. Additionally, the membrane potential has long been understood to be critical for controlling growth cone motility, and neuromodulators have been shown to regulate the membrane potential through their effects on ionic conductances (McCobb and Kater, 1988).

DA is a critical neurotransmitter involved in *Helisoma* feeding behaviors (Murphy, 2001). A food stimulus excites dopaminergic buccal interneuron N1a, inducing fictive feeding motor

patterns (Quinlan *et al.*, 1997). A brief inhibition of the N1a activity by hyperpolarizing current injection resets the phase of the fictive feeding pattern. Studies on the *Helisoma* B5 neuron (Murphy and Kater, 1980), as well as in its homologues in *Lymnaea* (Perry *et al.*, 1998) and *Clione* (Malyshev and Balaban, 2009), indicate that these neurons extend axons via the ipsilateral esophageal trunk nerve (*Helisoma*) and dorsobuccal nerves (*Lymnaea*) and project to the surface of the proesophagus. Experiments using an isolated foregut preparation reveal that manipulations of the neuronal activity of *Lymnaea* B2 neurons changed the tension of esophageal muscles (Perry *et al.*, 1998). An increase in firing activity in B2 neurons induces gut contraction, whereas silencing of B2 activity suppresses spontaneous esophageal muscle contractions. Switching the electrical activity from a spontaneously firing state to being silent by DA in B5 neurons may reduce gut contractile activity and thereby affect feeding. A combined study of the effect of DA on B5 neurons and feeding at the electrophysiological and behavioral levels will provide additional insights in our understanding of the role of DA in feeding in *Helisoma*.

4.7 Figures

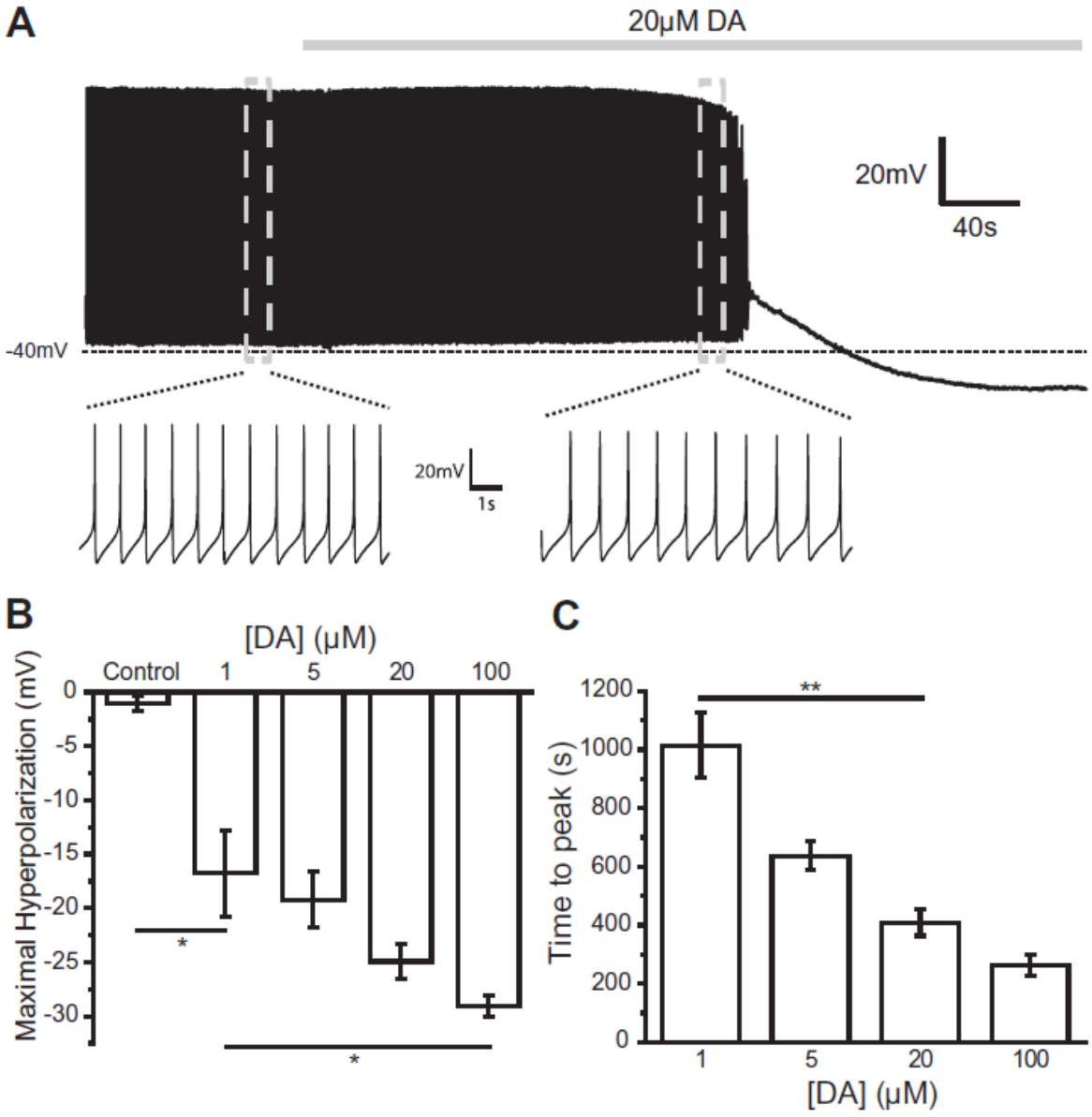

Figure 4.1 DA induces membrane hyperpolarization and subsequent silencing of spontaneously firing B5 neurons *in vitro*.

A: A spontaneously firing B5 neuron was hyperpolarized and stopped firing after the treatment with DA (20 µM, bath application; gray bar). Note that in order to capture the entire time course from the addition of DA to the maximum of the hyperpolarization, the time line had to be

compressed, resulting in a loss of resolution of individual APs. To allow an analysis of individual APs, representative firing activities before and after the addition of DA (marked by gray dashed boxed) are shown at higher time resolution below the main recording trace. Since the changes of membrane potential were the main interest in this study, representative data showing long-term recordings, which best reflected the strong hyperpolarizing responses induced by DA, are presented in the rest of the paper. B: Quantification of the changes of RMP showing that DA concentration ranging from 1 μM to 100 μM significantly hyperpolarized the membrane potential of B5 neurons. Furthermore, the hyperpolarizing level induced by 100 μM DA was statistically different from that of the 1 μM DA group. C: Quantification of time delay between DA addition and the peak of the hyperpolarizing response. Note that maximal hyperpolarization was reached faster with increased concentrations of DA.

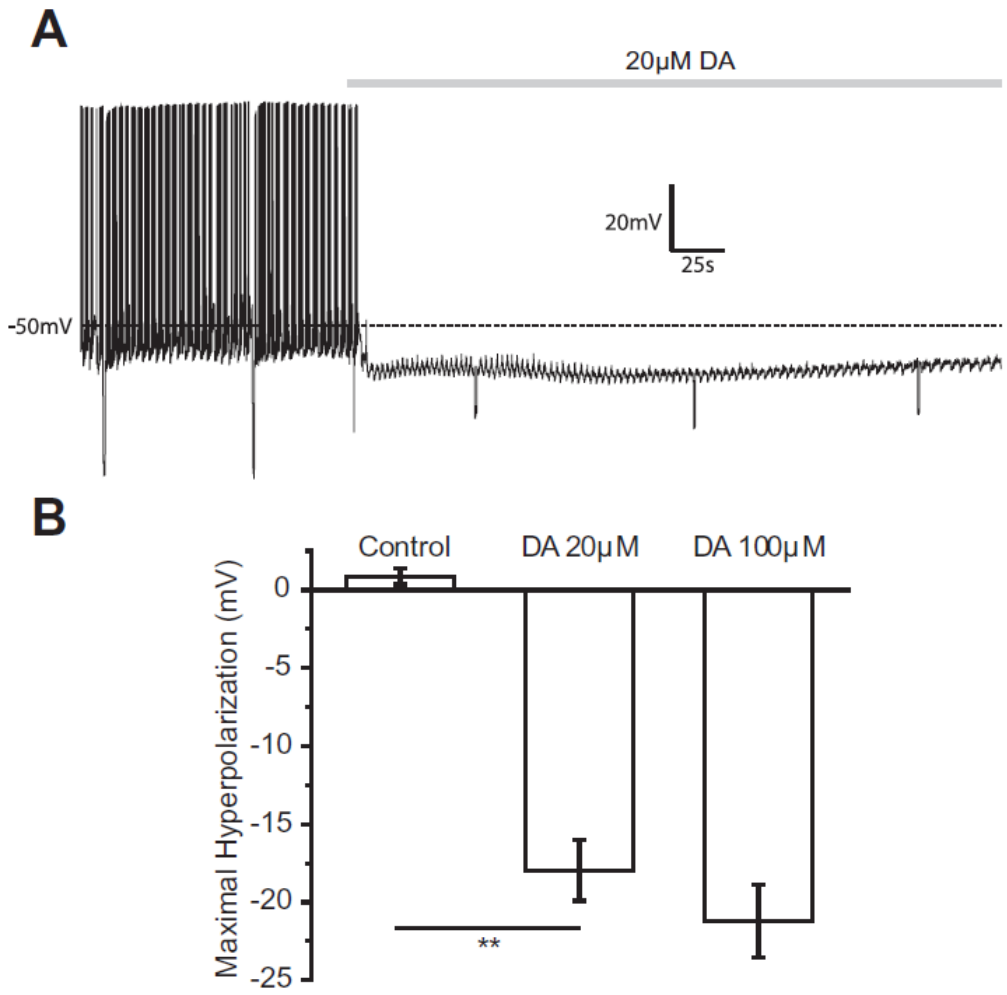

Figure 4.2 DA elicits a strong hyperpolarization in B5 neurons *in situ*.

A: A representative recording of a B5 neuron located within the buccal ganglion. The neuron was spiking before treatment and was silenced by a strong hyperpolarization in response to 20 μM DA. Brief negative current injections (- 0.4 nA, 1s) were applied to measure the effect of DA on neuronal input resistance. B: Quantification of the maximal changes of membrane potential by DA. 20 μM DA and 100 μM DA significantly hyperpolarized the membrane potential of B5 neurons compared to the vehicle control group.

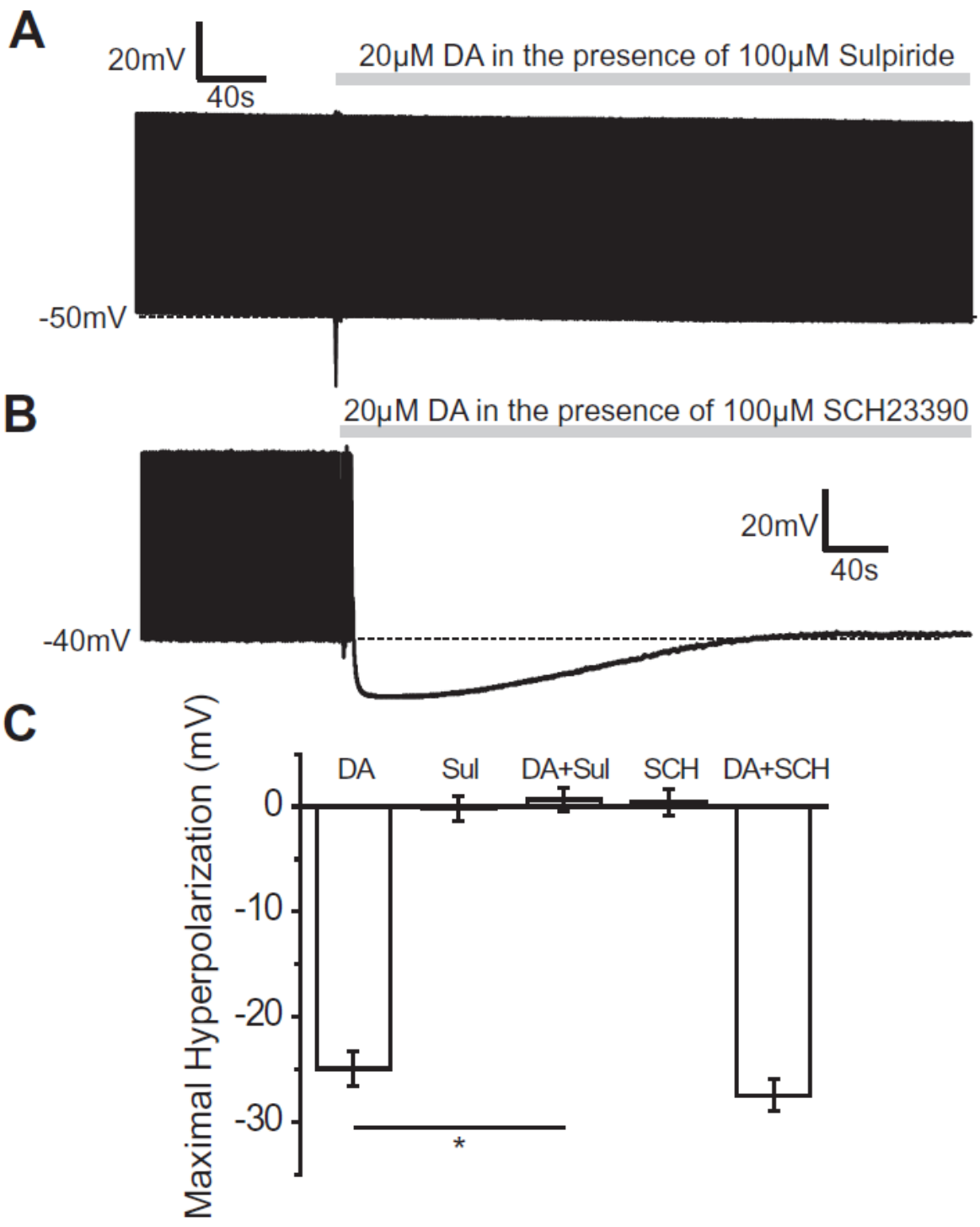

Figure 4.3 D2-like receptors mediate the DA-induced hyperpolarizing response.

A: A representative recording of a B5 neuron pretreated with 100 μM D2 receptor antagonist sulpiride before and after the treatment with 20 μM DA. D2-like receptor inhibition fully blocked the hyperpolarizing effect of DA, indicated by the continued spiking activity. B: Example of a spontaneously firing B5 neuron pretreated with 100 μM D1 receptor inhibitor, SCH23390, and subsequently treated with DA (20 μM). Note that DA still strongly hyperpolarized the membrane potential in the presence of the inhibitor, suggesting that DA did not act via a D1-like receptor. C: Quantification of experiments shown in A and B. The hyperpolarizing response induced by DA plus SCH23390 was not significantly different from DA on its own, whereas the DA effect was fully inhibited when B5 neurons were pretreated with sulpiride.

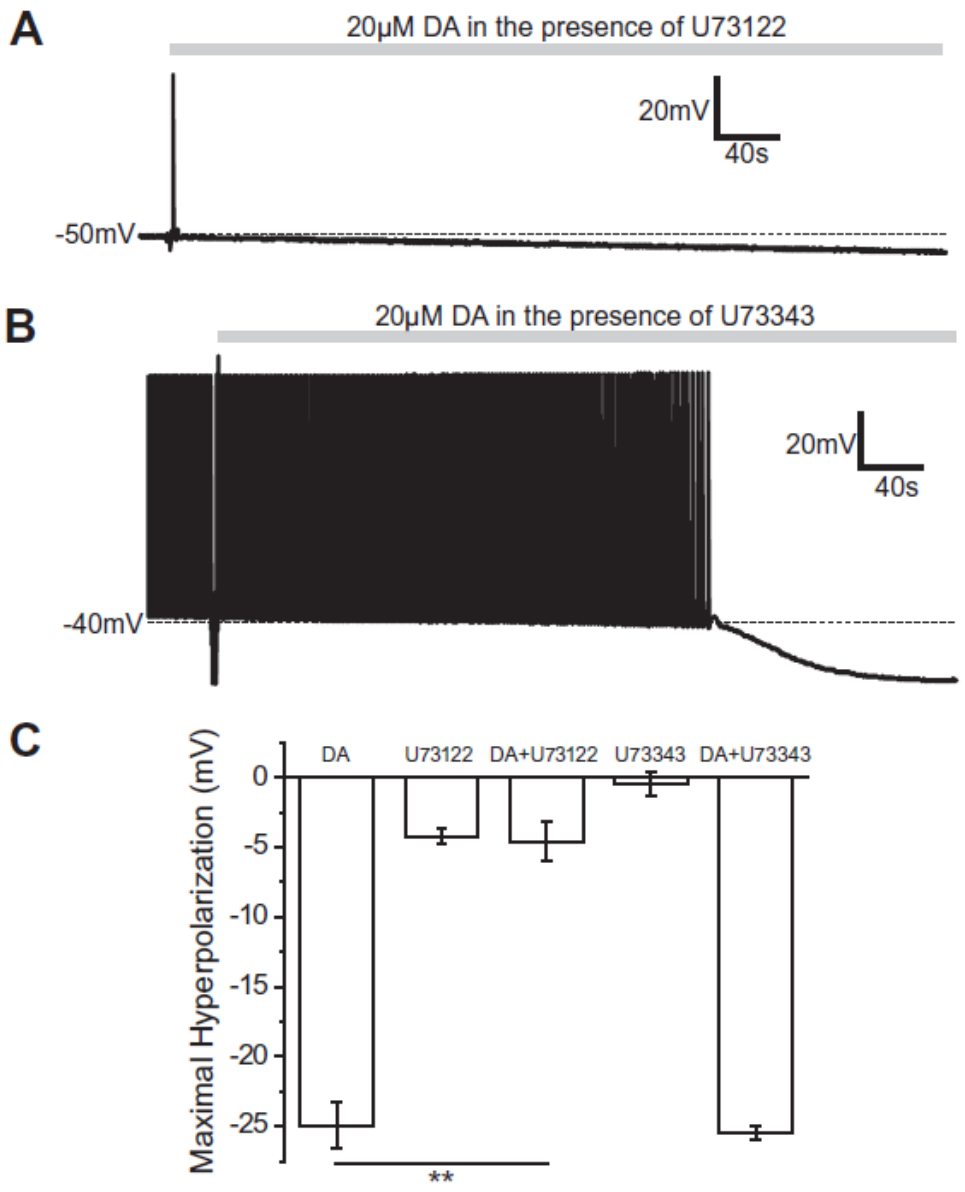

Figure 4.4 Inhibition of PLC activity blocks the DA-induced hyperpolarization of membrane potential.

A: Representative recording of a neuron pretreated with 0.5 μM PLC inhibitor U73122 before and after the treatment with 20 μM DA. Whereas the PLC inhibitor by itself caused a small hyperpolarization and resulted in silencing, the subsequence application of DA did not have an additional effect on membrane potential. B: Pre-incubation with 0.5 μM U73343, the negative

control for U73122, did not inhibit the DA-induced hyperpolarization. C: Quantification of experiments such as shown in A and B. U73122 pretreatment significantly inhibited DA's effect on the membrane potential, whereas DA still elicited a hyperpolarizing response in the presence of the inactive analog U73343. Interestingly, U73122 but not its inactive control U73343 induced a slight membrane hyperpolarization and prevented B5 neurons from firing, suggesting the importance of PLC activity for maintaining the spontaneous firing activity in B5 neurons.

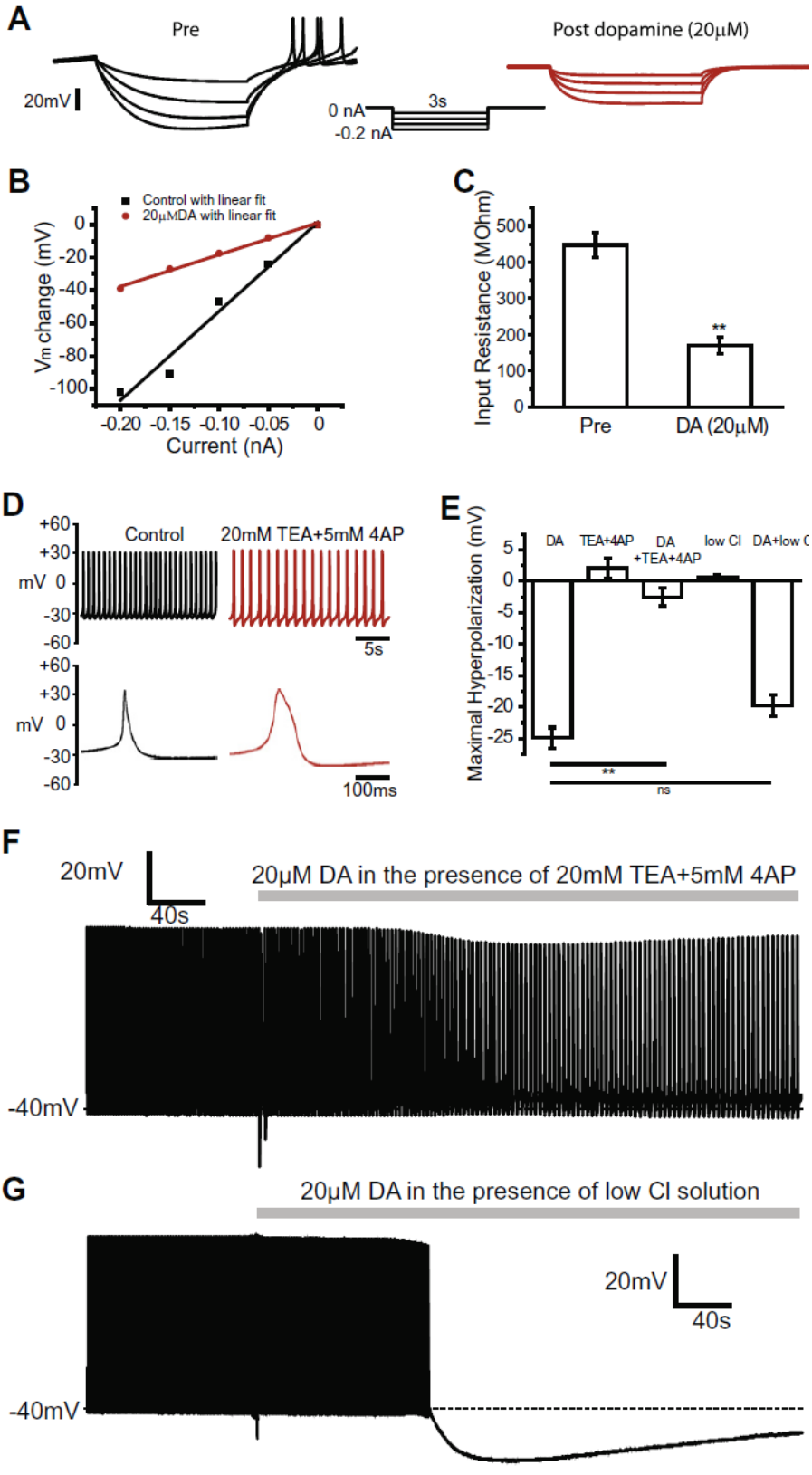

Figure 4.5 DA reduces input resistance by opening K conductances.

A: Representative recordings of the changes of membrane voltage in response to hyperpolarizing current steps (from – 50 pA to – 200 pA, 3 s) before (left) and after (right) 20 μM DA treatment. Note a decrease in input resistance (R_n) after DA exposure. B: Graph of the peak changes in membrane potential as a function of injected current for determination of R_n from the slope of the graphs. C: Quantification of experiments such as in B suggesting that R_n was significantly decreased after DA exposure. D: A representative recording from a B5 neuron suggesting that the inhibition of K conductances with TEA and 4AP slowed the spontaneous firing activity (top) and caused action potential broadening (bottom). E: Quantification of the changes of membrane potential showing that the DA effect was fully blocked in the presence of TEA (20mM) and 4AP (5mM), but that a low Cl solution had no significant effect on the DA-induced hyperpolarizing response. F: 20 μM DA caused only a small decrease in action potential frequency but did not induce a significant hyperpolarization in the presence of K channels blockers TEA (20 mM) and 4AP (5 mM). G: Response of a representative B5 neuron in a solution of low extracellular Cl and after treatment with DA. Neurons still responded to 20 μM DA with a strong hyperpolarization, suggesting that the hyperpolarization was likely not mediated by a Cl conductance.

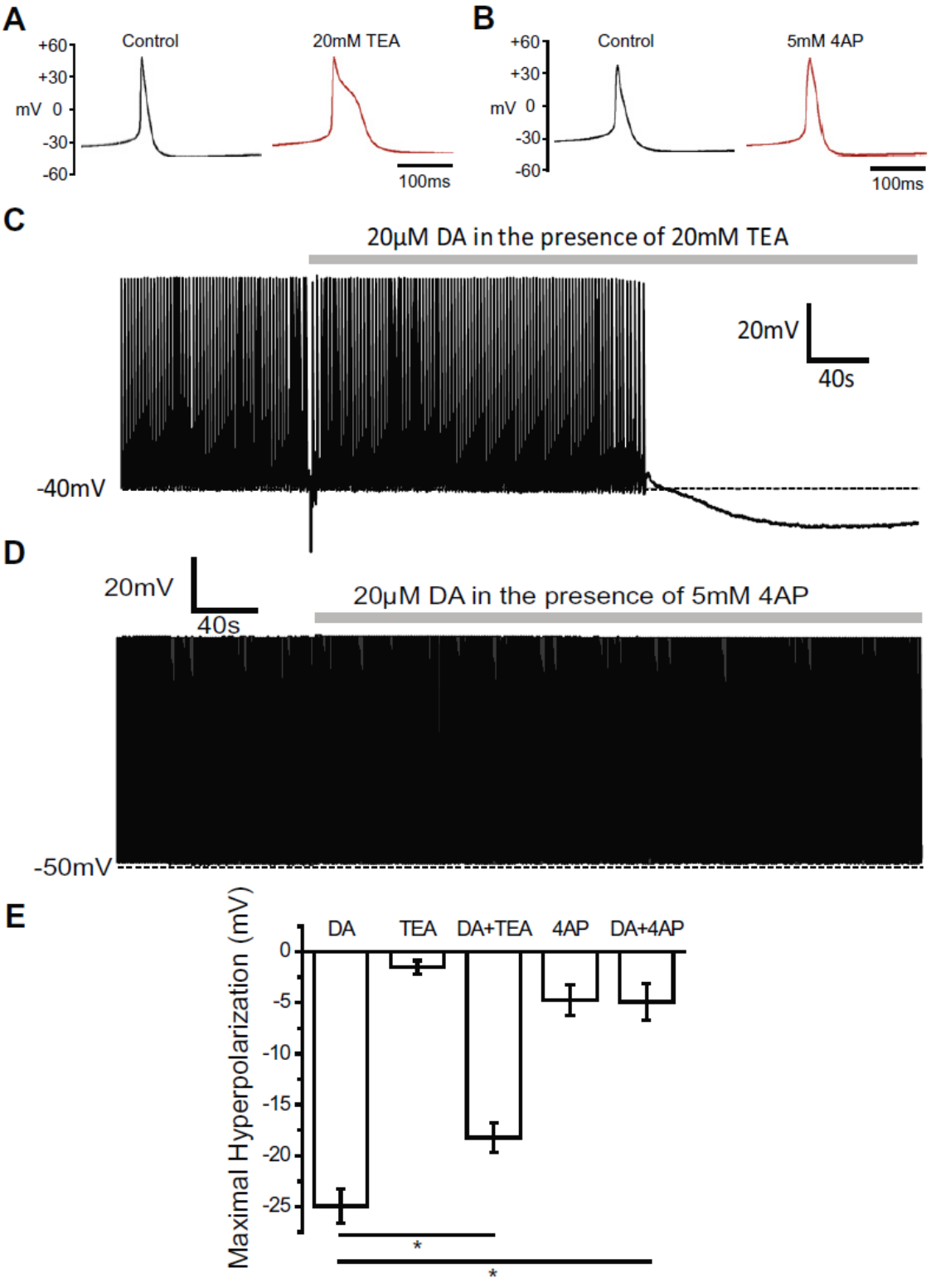

Figure 4.6 Both TEA-sensitive and 4AP-sensitive K channels contribute to the DA-induced hyperpolarizing response, but 4AP-sensitive K channels are the major target.

A: Comparison of single action potentials showing the broadening of the repolarization shoulder after treatment with 20 mM TEA compared to the control condition. B: Comparison of single action potentials showing the widening of the initial repolarization after the treatment with 5 mM 4AP. C: A representative trace of a B5 neuron treated with DA (20 μM) in the presence of TEA (20 mM). Note that the DA plus TEA treatment resulted in the typical hyperpolarization, albeit of a smaller amplitude than DA treatment by itself. D: A representative recording of a B5 neuron pretreated with 5 mM 4AP and after addition of 20 μM DA. In the presence of 4AP, DA did not elicit an obvious hyperpolarizing response, as evidenced by the continuous spiking activity of the neuron. E: Quantification of the changes in membrane potential in response to treatment above. TEA pretreatment partially inhibited the effect of DA on RMP, whereas 4AP treatment inhibited the remaining hyperpolarizing response induced by DA.

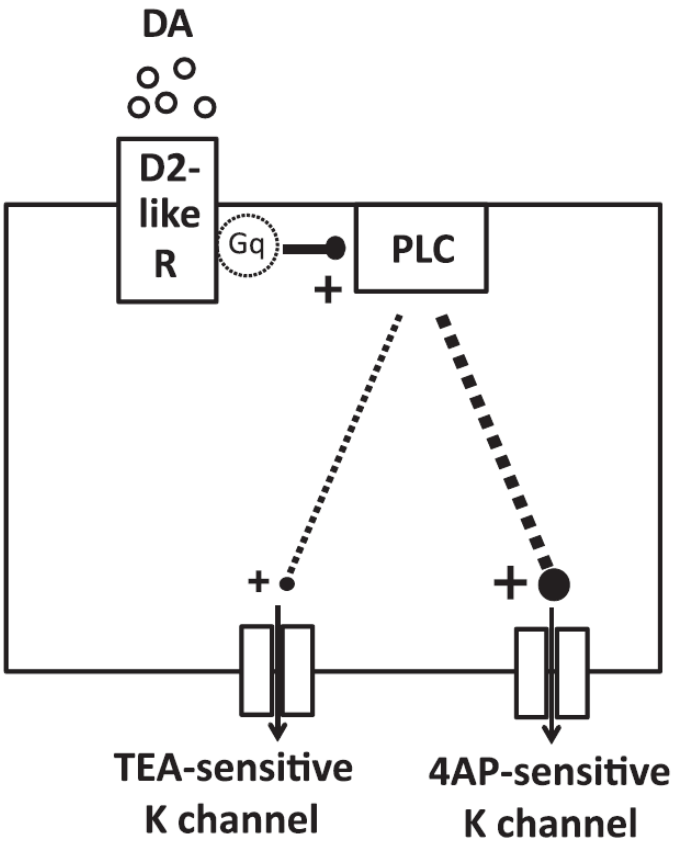

Figure 4.7 Proposed model of the pathway by which DA causes a strong hyperpolarization in *Helisoma* B5 neurons.

DA binds to D2-like receptors, which in turn activate PLC (likely through the G-protein $G_{q/11}$; activation is indicated by '+'). PLC activation results in the subsequent opening of two types of K channels, a TEA-sensitive and a 4AP-sensitive K channel. Our results suggest that the main effect of DA stimulation is mediated via a 4AP-sensitive K channel. The mechanism(s) by which the PLC activation in B5 neurons results in the modulation of K channel activity is presently unknown (indicated by dotted lines).

CHAPTER 5 GENERAL DISCUSSION

During neuronal development, the growing state of a neuron is partially determined by environmental cues. These cues act on the membrane receptors of growing neurons and, in turn, trigger intracellular signaling cascades. These signals can, for example, result in changes in the growth cone motility affecting axon pathfinding, in the modulation of electrical activity influencing neuronal circuitry, or a combination of both. Several well-known neurotransmitters and neuromodulators have been implicated to act as environmental cues (Lauder and Schambra, 1999; Farrar and Spencer, 2008). The aim of this dissertation is to further our understanding of the mechanisms by which neurotransmitters and/or neuromodulators elicit their effects on growth cone properties and electrical activity. I approached this question in three studies: 1) To investigate how ACh regulates growth cone motility via its modulation of electrical property and intracellular Ca; 2) To examine how NO affects the electrical activity of B19 neurons, with a focus on comparing the regulation of ion channels between B5 and B19 neurons; 3) To study how DA acts as a regulator of electrical activity and to understand its signaling cascade. A schematic summary of the findings is illustrated in Fig. 5.1.

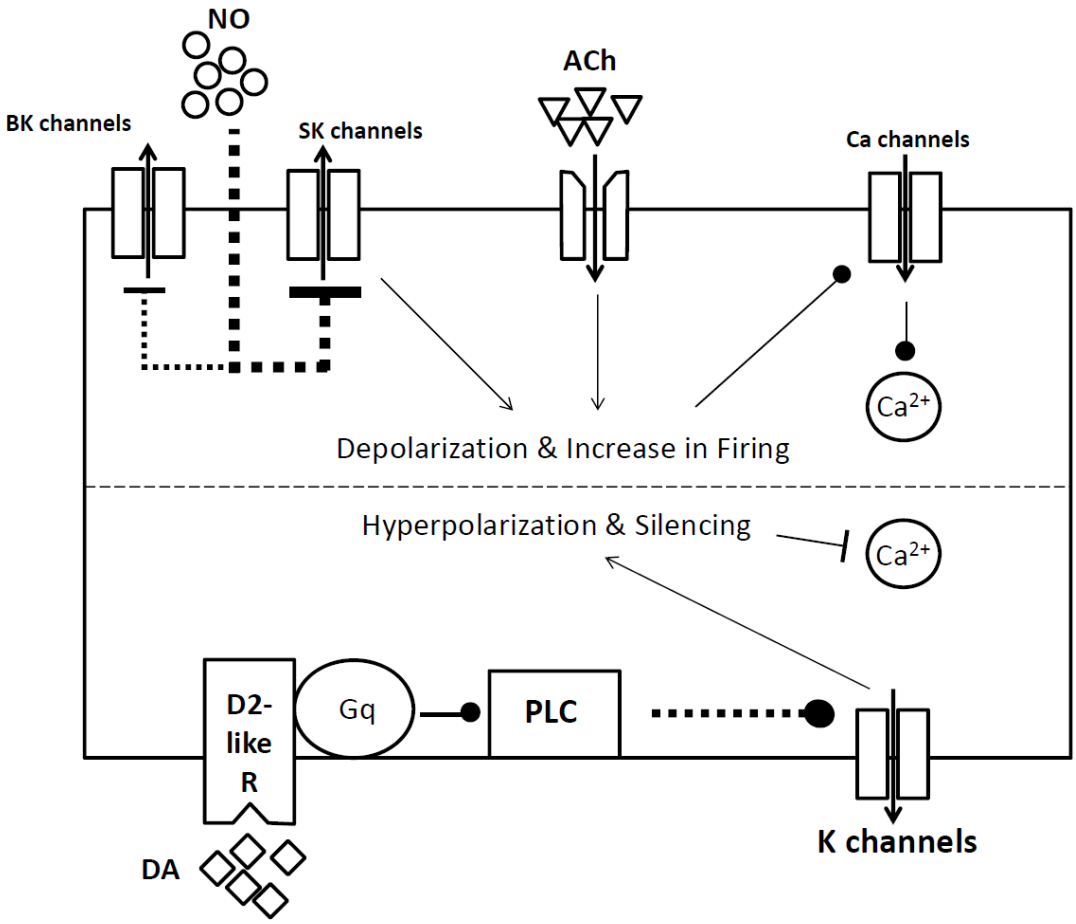

Figure 5.1 Proposed signaling pathway by which ACh, NO, and DA regulate electrical activity and intracellular Ca.

ACh binds to nAChRs, which causes membrane depolarization and an increase in firing activity in *Helisoma* B5 neurons. This cholinergic effect on electrical property elevates $[Ca]_i$ in growth cones potentially via the opening of VGCCs, which results in filopodial elongation. NO application inhibits two types of Ca-activated K channels, BK and SK channels, which depolarize the membrane potential of B19 neurons (similar channel targets of NO as found in B5 neurons). SK channels serve as the main target of NO. On the other hand, DA binds to D2-like receptors, which activate PLC signaling (potentially through the G protein G_q) in B5 neurons.

PLC in turn activates K channels to hyperpolarize the membrane potential and silence the spontaneous firing activity in B5 neurons. This hyperpolarization is likely to reduce the $[Ca]_i$ in growth cones. Please note that results from neurons B5 and B19 are shown together in this schematic drawing of a neuron. Activation is indicated by '●', whereas inhibition is shown by '|'.

5.1 The actions of neurotransmitters are mediated by their membrane receptors

Specific ligands activate either ionotropic and/or metabotropic receptors, through which they initiate a variety of cellular functions. For example, ACh is shown to activate nAChRs to cause the chemoattractive behavior of growth cone turning in *Xenopus* spinal neurons (Zheng et al., 1994), whereas DA can bind to a variety of G-protein coupled receptors to activate distinct signaling mechanisms (Beaulieu and Gainetdinov, 2011).

Although much is known about ACh being a critical neurotransmitter in the nervous system (Phillis, 2005), its role during neuronal development and its associated signaling mechanisms are less understood. There are mainly two types of acetylcholine receptors: nAChRs, which are ionotropic receptors known to directly pass cations (Dani and Bertrand, 2007), and muscarinic ACh receptors (mAChRs), which are coupled to G proteins (Abrams et al., 2006). In Chapter 2, evidence is provided to show that nAChRs mediate the effects of ACh in *Helisoma* B5 neurons at the electrophysiological, intracellular Ca, and growth cone morphological level. Inhibition of nAChRs with TC eliminates all neuronal responses to the stimulation of ACh, whereas the nAChR agonist DMPP mimics the effects of ACh. Activation of the ionotropic nAChRs immediately introduces the influx of cations, which results in membrane depolarization and an elevation in $[Ca]_i$ to cause filopodial elongation in growth cones. mAChR can also be involved in ACh effects, because both nAChRs and mAChRs have been shown to contribute to the decrease in the extension rate of developing mouse thalamic axons (Rudiger and Bolz, 2008).

These two types of ACh receptors are found to mediate different components of elevation in $[Ca]_i$ and membrane currents evoked by ACh in rat intracardiac ganglion neurons (Beker et al., 2003). Because the effect of ACh on filopodial length, membrane potential, and $[Ca]_i$ in this dissertation could be fully explained by activation of nAChRs, I did not investigate any potential involvement of mAChRs.

Neurons can be affected by NO through different mechanisms, ranging from activation of its canonical target, soluble guanylyl cyclase (sGC), to protein nitrosylation and lipid peroxidation (for reviews see (Stamler et al., 1992; Davis et al., 2001; Ahern et al., 2002; Brown and Borutaite, 2002; Foster et al., 2003)). In Chapter 3, the receptor of NO was not characterized, but sGC is likely to function as a key mediator of the effects of NO. sGC is known to be the intracellular receptor for the unconventional neuromodulator NO (Davis et al., 2001; Ahern et al., 2002; Garthwaite, 2008). NO activates sGC signaling to modulate neuronal excitability and synaptic strength, through which NO controls learning and memory, as well as animal feeding (Bon and Garthwaite, 2003; Susswein and Chiel, 2012). Moreover, sGC signaling is known to be a mediator for the effects of NO on membrane channels, such as various types of Ca channels in neurons of the medial nucleus of the trapezoid body (Tozer et al., 2012), and hyperpolarization-activated cyclic nucleotide-modulated cation channels in cerebellar nuclei neurons (Wilson and Garthwaite, 2010). In the related gastropod *Lymnaea stagnalis*, sGC has been found to mediate the NO-induced prolonged depolarization of the cerebral giant cell (Ribeiro et al., 2008). Studies on *Helisoma* neurons suggest that NO elongates growth cone filopodia and slows down neurite outgrowth via sGC (Van Wagenen and Rehder, 1999; Trimm and Rehder, 2004). Additionally, sGC is important in mediating the effects of intrinsic NO on VGCCs (Artinian et al., 2012). These examples strongly suggest a role for sGC in mediating the effect of NO in B19 neurons. In

addition to sGC signaling, NO might directly modulate ion channels by protein nitrosylation (Foster et al., 2003). Such modification of NO has been shown to inhibit human K channels (Nunez et al., 2006). Future studies of the signaling mechanisms mediating the effects of NO on intracellular proteins and membrane channels will be of interest.

DA can activate various receptors, including D1-like and D2-like receptors, to initiate distinct G-protein coupled receptor-mediating signaling pathways (Missale et al., 1998). In Chapter 4, I describe that the D2-like receptor, a metabotropic receptor, plays a critical role in mediating DA-induced membrane hyperpolarization in buccal neuron B5. Inhibition of D2-like receptors with sulpiride completely blocks the hyperpolarization induced by DA addition. The DA/D2-like receptor pathway seems to be involved in the modulation of electrical activity of multiple central pattern generator neurons in *Helisoma* (Quinlan et al., 1997) and cerebral neurons in *Lymnaea*, a closely related species (Dobson et al., 2006). In addition, this DA signaling has also been shown to be important in target cell selection (Spencer et al., 1996; Spencer et al., 1998). Physiological DA release from growth cones of *Lymnaea* neuron, right pedal dorsal 1, attracts growth cones from its *in vivo* target cell for building synaptic connections, a process that requires the involvement of D2-like receptors (Spencer et al., 2000).

Taken together, the identification of the physiological role of a particular neurotransmitter/neuromodulator and its receptor is an important step towards understanding its functions in the nervous system. Depending on the distinct receptor, a variety of signaling pathways are activated to evoke different neuronal behaviors.

5.2 Intracellular Ca is the converging target of various neurotransmitters

Neurotransmitters and/or neuromodulators bind to receptors, which initiate distinct intracellular signaling events. As a critical intracellular second messenger, Ca plays a central role

during neuronal development, influencing processes such as neurite outgrowth and growth cone pathfinding (Gomez and Zheng, 2006; Zheng and Poo, 2007). How activation of different ionotropic and metabotropic receptors will affect the intracellular Ca dynamics is an important question to help understand the action of neurotransmitters.

Some ionotropic receptors, such as AMPA receptors and nAChRs, have been shown to be permeable to Ca ions (Seguela et al., 1993; Liu and Zukin, 2007). Different subtypes of nAChRs vary in their ability to pass Ca ions and can be quantified experimentally by determining the permeability ratio for Ca over Na (P_{Ca}/P_{Na} values) (Fucile, 2004). The homopentameric nAChRs, containing α7 to α9 subunits, possess a higher permeability to Ca ions than heteropentameric receptors (Fucile, 2004). In the mouse cochlear cell line UB/OC-2, the homomeric α9 receptor has an estimated P_{Ca}/P_{Na} value of 80 (Jagger et al., 2000), whereas most heteromeric nAChRs show minimal Ca permeability with P_{Ca}/P_{Na} values less than 1, such as the human α4β4 nAChRs (Lax et al., 2002). Compared to mammalian systems, much less is known about molluscan nAChRs at the molecular level. Dr. Smit's group in the Netherlands cloned 12 nAChR subunits in *Lymnaea* (van Nierop et al., 2006), of which they functionally expressed the homomeric receptor containing A-subunits, highly similar to mammalian α subunit, in *Xenopus* oocytes. They also reported their presence in most nervous tissues, including a high level of expression in the buccal ganglion (van Nierop et al., 2005). Although they did not further characterize the Ca permeability of the receptors, the sequence comparison suggests that the *Lymnaea* A subunit is most closely related to the human α7 subunit, a unit with high Ca permeability (Seguela et al., 1993; Uteshev, 2010).

In this dissertation, I show that nAChRs mediate an ACh-induced increase in $[Ca]_i$ in growth cones. Removal of the extracellular Ca completely blocks the effects of ACh on growth

cone $[Ca]_i$ and filopodial dynamics, suggesting the importance of Ca influx in this process. One important next step towards understanding ACh signaling is to determine whether Ca flows directly through nAChRs or indirectly through VGCCs that open in response to membrane depolarization. To differentiate between these two possibilities would require the separate measurement of current through the nAChRs and the VGCCs. Ongoing studies of cloning nAChRs from *Helisoma* in the Rehder lab showed that the A subunit is expressed in B5 neurons based on single-cell PCR data (unpublished data). Considering the high similarity between *Lymnaea* and *Helisoma* A subunits and the Human α7 subunit, B5 neurons expressing the nAChR A subunit are expected to be highly permeable to Ca ions. This would predict that nAChRs in B5 neurons may contribute a significant amount of the increase in $[Ca]_i$ seen in response to ACh. Future investigations of the Ca permeability of *Helisoma* nAChR subunits in heterologous expression systems will provide answers to this question.

In addition to Ca influx via Ca permeable membrane channels and receptors, Ca release from intracellular stores is another main source contributing to the elevation of Ca in the cytosol (Berridge et al., 2003). In *Helisoma* B5 neurons, NO has been shown to activate sGC to cause Ca release from intracellular stores via RyRs, and this increase in $[Ca]_i$ was further amplified by Ca influx via VGCCs (Welshhans and Rehder, 2005; Welshhans and Rehder, 2007). Although the current dissertation did not directly measure the changes in $[Ca]_i$ in B19 neurons, the membrane depolarization induced by two NO donors, NOC7 and DEA/NO, is likely to cause Ca release from stores via an intracellular second messenger mechanism as well as Ca influx via VGCCs. For those neurons responding to NO with an increase in firing frequency, the Ca influx component might contribute more to the overall Ca increase than release from Ca stores, but future experiments will have to clarify the relative contributions of the two sources of Ca.

Additionally, the inhibition of Ca-activated K channels induced by NO may provide for the opportunity of Ca influx via AP broadening. In fact, Ca-activated K channels are a common target of NO in both B5 and B19 neurons. APs are broadened after treatment with NOC7 in a BK channel-dependent manner in B5 neurons (Artinian et al., 2010), as evidenced by the finding that the specific inhibitor of BK channels, IbTX, mimics the effect of NO on AP waveform. With the prolonged AP duration, Ca channels can open for longer periods of time and introduce more Ca with each AP. The notion that AP waveform determines the $[Ca]_i$ is further strengthened by the result that broadening of APs by the inhibition of K channels with TEA induced a significant increase in $[Ca]_i$ in growth cones of B5 neurons (unpublished data).

5.3 Electrical responses connect neurotransmitters to growth cone motility

Electrical activity of a neuron is tightly linked to the $[Ca]_i$ dynamics, which plays critical roles during neuronal development (Spitzer, 2006). Electrical stimulation of developing neurons cease growth cone advance and neurite outgrowth (Cohan and Kater, 1986; Fields et al., 1990; Cohan, 1992). In addition, manipulations of electrical activity lead to changes in growth cone turning in response to guidance cues (Ming et al., 2001). These lines of evidence raise the possibility that electrical activity serves as the mediator for neurotransmitters to function at the growth cone level. Ca signals act downstream of membrane depolarization, which in turn may alter the growth cone cytoskeleton through changes in F-actin dynamics to elongate filopodia (Mattila and Lappalainen, 2008).

ACh treatment activates nAChRs, resulting in a significant depolarization of the membrane potential as well as an increase in firing activity. Both changes in electrical properties are important for Ca influx via Ca-permeable nAChRs or VGCCs, which accounts for the

increase in $[Ca]_i$ in growth cones necessary for ACh-induced filopodial elongation. Therefore, the electrical response mediates the action of ACh to change growth cone filopodial dynamics.

In Chapter 3, I reported that NO depolarizes the membrane potential of B19 neurons. 74.6% of recorded neurons are silent, whereas the rest of B19 neurons fire AP spontaneously before the drug treatment. Nevertheless, all B19 neurons respond to NO by membrane depolarization. Although the main focus here is to understand how NO modulates the electrical activity of B19 neurons, I am also interested to know whether NO elevates the $[Ca]_i$ and has effects on growth cone motility in B19 neurons as it does in B5 neurons (Van Wagenen and Rehder, 1999). To answer this question requires linking the modulatory effect of NO at the electrophysiological level to the study at the growth cone level. Depending on the initial state and the resting membrane potential of B19 neurons, the depolarization by NO is expected to result in different $[Ca]_i$. For example, silent neurons with a membrane potential of about – 40 mV that become depolarized by about 4 mV in response to NO remain silent, and this depolarization may also not be enough to open VGCCs. Therefore, these neurons will maintain their $[Ca]_i$ at basal levels and are not expected to show a filopodial response in growth cones. The other two types of NO responses, silent neurons that become spiking and spiking neurons that increase their firing frequency due to membrane depolarization induced by NO, are expected to respond with a Ca elevation, similar to that seen in B5 neurons in response to NO. Under these conditions, neuronal firing activity can immediately translate a change in membrane potential into functional Ca signals due to Ca influx via VGCCs. Therefore, growth cones of B19 neurons may respond to NO application by filopodial elongation as those of B5 neurons do (Artinian et al., 2010). However, we previously reported that B19 neurons do not respond to NO with a significant increase in filopodial length (Van Wagenen and Rehder, 2001), suggesting that these

neurons might be depolarized only to a degree that did not result in a significant increase in $[Ca]_i$. We have recently started experiments in which the electrical activity, the $[Ca]_i$, and growth cone motility are measured simultaneously, and this novel approach will help us in future experiments to address how these parameters are connected.

An increase in the firing frequency or a release of Ca from intracellular stores results in an elevation of $[Ca]_i$ (Berridge, 1998). How will $[Ca]_i$ be affected when a firing neuron is being silenced? As shown in Chapter 4, application of DA was found to hyperpolarize and silence spontaneously firing B5 neurons both *in vitro* and *in vivo*. Whereas continuous spontaneous firing activity is expected to maintain a certain elevated basal $[Ca]_i$, the strong hyperpolarization in response of DA, resulting in cell silencing, should decrease Ca influx and lead to a reduction in the basal Ca concentration. It will be interesting to investigate how a reduction in $[Ca]_i$ via membrane hyperpolarization might affect filopodial dynamics. In a growth cone turning assay using growth cones of *Xenopus* spinal neurons, Sema3A application was shown to induce a hyperpolarization of the membrane potential and act as a repulsive cue (Nishiyama et al., 2008).

The state of electrical activity of a neuron set by one neurotransmitter and/or neuromodulator might influence the neuronal response to another stimulation. The sustained depolarization in B19 neurons induced by NO may change the response of this neuron to presynaptic inputs. Indeed, the synaptic strength of serotonergic neurotransmission between the cerebral giant cell and the buccal neuron B4 in *Lymnaea* is enhanced by NO-induced background membrane depolarization (Straub et al., 2007). In addition, 5HT has been shown to suppress neurite outgrowth by exciting developing B19 neurons in *Helisoma*. The excitatory effect of 5HT is abolished when these neurons are treated with ACh, which acts as an inhibitory neurotransmitter in B19 neurons (McCobb et al., 1988).

The notion that the electrical activity of a neuron may serve as an integrator to determine the responses of growth cones or neuronal excitability to external stimulation is further supported by evidence provided in cultured *Xenopus* spinal neurons. Manipulation of the membrane potential of growth cones by clamping them at a more depolarized potential converts the Sema3A-induced repulsion to attraction (Nishiyama et al., 2008). Moreover, electrical stimulation of neurons switches the myelin-associated glycoprotein-induced repulsion to attraction (Ming et al., 2001).

5.4 Growth cone filopodial dynamics

Filopodia are known as sensory extensions of the growth cone that constantly explore the environment for guidance cues by elongation and retraction (Kater et al., 1994; Mattila and Lappalainen, 2008). Elongation of growth cone filopodia has been found to precede a reduction in neurite extension rate, a phenomenon termed 'slow down and search' behavior (Trimm and Rehder, 2004). The advantage of elongated filopodia and a slower rate of growth cone advance would be the ability to sample a larger area of the terrain ahead of the growth cone for a longer duration, which is thought to aid in the accurate decision-making of the navigating growth cone. The 'slow down and search' behavior has been reported in B5 neurons under the condition of either exogenous treatment with NO or direct inhibition of intracellular phosphatidylinositol-3-kinase activity (Trimm and Rehder, 2004; Tornieri et al., 2006). Moreover, the concept that one signaling molecule affects both growth cone motility and neurite outgrowth is further supported by findings in chick embryo sensory neurons and cultured mouse hippocampal neurons (Oberstar et al., 1997; Kim et al., 2011).

ACh, in this dissertation, has been found to act as a local signal to elongate filopodia, since physically isolated growth cones respond to treatment with ACh in a similar fashion as

intact growth cones do. By an increase in the exploratory radius of the growth cone, ACh would likely facilitate a decision-making process in the growing neurite, which may have an impact on neurite advance.

Homogeneous filopodial elongation across the entire growth cone was observed when ACh was added to the culture dish. Filopodia are expected to elongate to a different extent, when ACh is applied asymmetrically. An asymmetrical response of growth cones to guidance cues has been well-demonstrated in cultured *Xenopus* spinal neurons (Zheng et al., 1994; Hong et al., 2000; Henley and Poo, 2004). Repetitive pulse application of chemicals through a micropipette can create a relatively stable gradient. In their case, the growing axons turn towards the higher gradient of ACh (Zheng et al., 1994). The ACh-induced chemoattractive behavior can be explained considering the localized filopodial responses. Filopodia on the side facing the higher concentration of ACh would elongate further, due to stronger Ca signals induced by ACh, compared to the other side facing the lower concentration. Therefore, the navigating growth cone is expected to gradually turn towards the higher gradient of ACh. In another example, an asymmetry in filopodia distribution induced by glutamate gradients has been shown to determine the chemoattraction of growing axons (Zheng et al., 1996).

NO has been known to regulate growth cone filopodial dynamics in *Helisoma* B5 neurons in the Rehder lab. Physiological release of NO from nNOS-expressing neuron or treatment with NO donors causes filopodial elongation through a Ca-dependent mechanism (Van Wagenen and Rehder, 1999; Tornieri and Rehder, 2007). A previous study in the lab suggested that the growth cones of B19 neurons respond to the NO donor, NOC7, to a much lesser degree than that of B5 neurons (Van Wagenen and Rehder, 2001). However, NOC7 inhibits Ca-activated K channels and depolarizes the membrane potential of B19 neurons in a similar fashion

than it does in B5 neurons. The question whether growth cones of B19 neurons respond to NO is worthwhile to revisit in light of new tools allowing us to record growth cone Ca and electrical activity simultaneously. The current working hypothesis to explain the difference in response between the two neuron types is that the magnitude of the response to NO and the properties of the APs differ between B5 and B19 neurons. Additionally, the modulation of growth cone filopodia by NO may also affect axon pathfinding of growing axons. Indeed, NO gradients caused asymmetric Ca signals to lead to growth cone repulsion in developing dorsal root ganglion neurons (Tojima et al., 2009).

Taken together, growth cone filopodia are critical structures that influence neurite extension and axon pathfinding. Neurotransmitters and/or neuromodulators are able to regulate filopodial dynamics via the modulation of neuronal electrical activity and $[Ca]_i$ in growth cones.

5.5 Neurotransmitters modulate activity of ion channels

Neurotransmitters can either activate ionotropic receptors to directly alter cell excitability or bind to metabotropic receptors to trigger intracellular signaling cascades, which, in turn, modulate ion channels indirectly. Although the effect of DA in the modulation of CNG channels (Rodgers et al., 2011), K channels (Podda et al., 2010), and Ca channels (Wang et al., 2011) has been extensively studied in other systems, the understanding of how DA modulates ionic conductances to change cell excitability in gastropods is incomplete. DA is known to be a critical neurotransmitter in gastropod feeding (Murphy, 2001), and DA application activates the feeding motor pattern and triggers feeding movements in *Helisoma* (Quinlan et al., 1997). Previous studies suggested the involvement of a K conductance in dopaminergic synaptic transmission (Magoski and Bulloch, 1999). Here, I report that DA causes a strong hyperpolarization and silencing in firing B5 neurons both *in vitro* and *in situ*, and this hyperpolarizing effect is

mediated by both TEA-sensitive K channels and 4AP-sensitive K channels via a D2-like receptor/PLC pathway. This study has advanced our understanding of the action of DA on B5 neurons and will provide insights in the role of DA in feeding in *Helisoma*.

K channels largely contribute to shaping the waveform of the AP and maintaining the membrane potential, which make them ideal targets for neurotransmitters and neuromodulators to regulate cell excitability. Inhibition of TEA-sensitive K channels, which contribute to the delayed rectifying K current, leads to significant broadening of the repolarization shoulder of the AP, whereas the blockade of 4AP-sensitive K channels, that mediate a fast-activating and rapidly inactivating K current, causes a widening of the early repolarization phase of the AP. The hyperpolarizing effect of DA is completely blocked in the presence of a solution containing both TEA and 4AP, and the inhibition of each channel subtype significantly reduces the effect of DA on membrane potential. Therefore, I conclude that DA acts as a positive regulator of K channels, activating both TEA-sensitive and 4AP-sensitive K channels. Studies using neurons of the stomatogastric ganglion of the spiny lobster show that the signaling pathways of DA can be quite diverse and result in a positive or negative modulation of K channels (Harris-Warrick, 2011). DA has been found to reduce the 4AP-sensitive transient K current via the D1 receptor/G_s/PKA pathway in the lateral pyloric neuron (Zhang et al., 2010). D2 receptors, expressed in the pyloric dilator neuron, mediate the DA-induced enhancement of the transient K current (Harris-Warrick et al., 1998).

Within the list of K channels, Ca-activated K channels, BK channels and SK channels, have been found to be the main target of NO in the *Helisoma* nervous system. BK channels are important in determining the width of the AP and the magnitude of fast AHP (Shao et al., 1999; Faber and Sah, 2003), whereas SK channels are critical in setting the resting membrane potential,

spike frequency, and slow AHP (Adelman et al., 2012; Vandael et al., 2012). Unlike the DA-induced activation of K channels and hyperpolarizing responses, NO elevation caused a strong inhibition of BK and SK channels, resulting in membrane depolarization in both B5 and B19 neurons (Artinian et al., 2010). Moreover, Ca-activated K channels have been reported to be modulated by NO signaling in other snail neurons, avian ciliary ganglia neurons, and mammalian vascular smooth muscle (Cetiner and Bennett, 1993; Bolotina et al., 1994; Schrofner et al., 2004), suggesting the existence of a conserved signaling mechanism of NO on Ca-activated K channels.

5.6 Modulation of neuronal activity influences synaptic transmission

Neurotransmitters are known to act in synapses where they lead to excitation or inhibition of post-synaptic neurons. In addition to this important function, evidence of modulatory roles of neurotransmitters on both sides of synaptic terminals, with the goal of fine tuning synaptic efficacy, is emerging (Kupfermann, 1979). The release of neurotransmitters from pre-synaptic terminals can act on the neuron itself to auto-regulate neuronal activity. Excitatory nAChRs located at the presynaptic terminal play a critical physiological role in enhancing the release of various neurotransmitters through a positive feedback mechanism (Dani and Bertrand, 2007). For example, ACh release is enhanced by presynaptic nicotinic autoreceptors at the developing neuromuscular synapse (Fu and Liu, 1997). Similar enhancement of neurotransmitter release mediated by presynaptic nAChRs has been reported in dopaminergic (Wonnacott et al., 2000), glutamatergic (McGehee et al., 1995) and GABAergic transmission (Zappettini et al., 2011). On the other hand, inhibitory receptors on the presynaptic terminal, such as D2-like receptors found in the current dissertation can directly silence the active presynaptic neuron and dampen synaptic transmission through a negative feedback mechanism (Benoit-Marand et al., 2001; Mizuno et al., 2007). Such auto-inhibition is commonly found in many neurotransmitter systems, including

dopaminergic (Moquin and Michael, 2009), histaminergic (Arrang et al., 1987), and adrenergic synapses (Miyamoto et al., 2008), and will attenuate the total amount of neurotransmitter released during neuronal activity by limiting the presynaptic depolarization.

Receptors located at the post-synaptic terminal can either directly participate in the regulation of post-synaptic neuronal activity or modulate the response of target neurons to other presynaptic inputs. A modulatory effect of NO on post-synaptic neurons has been demonstrated in the *Lymnaea* nervous system (Straub et al., 2007). The synapse between the cerebral giant cell and the B4 neuron in the *Lymnaea* feeding circuitry is not only serotonergic but also nitrergic (Walcourt-Ambakederemo and Winlow, 1995; Patel et al., 2006). Blockade of the endogenous NO production strongly reduces the serotonergic response of the B4 neuron to cerebral giant cell activity (Straub et al., 2007). Here I report that NO causes a significant membrane depolarization and an increase in cell excitability in a target neuron B19, which may potentially explain the enhanced serotonergic effect of the cerebral giant cell on B4 neuron. Endogenous produced NO functions to depolarize the membrane potential of postsynaptic neuron B4 and increases its neuronal excitability, resulting in an increase in response to 5HT release from the presynaptic neuron, the cerebral giant cell. In the mouse auditory pathway, NO is found to modulate the glutamatergic synaptic efficacy through inhibiting post-synaptic Kv3 potassium currents. Furthermore, DA/D2 receptor signaling is shown to modulate both excitatory and inhibitory neurotransmission in the rat oval bed nucleus of the stria terminalis (Krawczyk et al., 2011).

In summary, in addition to serving as classic neurotransmitters between synapses, neurotransmitter/neuromodulator can also act on autoreceptor at the pre-synaptic terminal to alter synaptic efficacy, and/or modulate the neuronal activity of post-synaptic neurons in response to other stimuli.

5.7 Implications for gastropod feeding

The buccal ganglion of *Helisoma* contains the circuitry of the central pattern generator for feeding. Due to the relative simplicity of their nervous systems and robustness of their behaviors, gastropods provide good model systems for the study of the organization and modulation of neuronal activity and the coordination of behaviors, such as feeding (Murphy, 2001). To understand the signaling mechanisms by which neurotransmitter/neuromodulator affects neurons within the feeding circuitry will provide insight into how the neuronal activity is linked to the ultimate behavioral output.

Both identifiable B5 and B19 neurons are located in the buccal ganglion and have been implicated to be involved in the feeding behavior in *Helisoma* (Murphy, 2001). The B5 neuron is an effector motor neuron innervating the esophagus (Scannell et al., 2008). The way B5 neurons control the activity of the esophagus has been studied in its homologue, the B2 neuron in *Lymnaea* (Perry et al., 1998). Electrical excitation of B2 neurons initiates contractile activity of the esophagus, whereas suppression of spiking reduces the contraction of the esophagus. Moreover, treatment with ACh mimicked the effects of a depolarizing current injection on both neuronal activity and esophagus contractile activity in *Lymnaea* B2 neurons (Perry et al., 1998), suggesting the presence of an excitatory cholinergic response. This study extends our perspective of the functional role of cholinergic modulation beyond the regulation of growth cone motility as studied in Chapter 2, and implicates that the release of ACh onto B5 neurons *in vivo* may promote the movement of esophagus. In addition, B5 neurons *in situ* respond to DA with a strong hyperpolarization and silencing of neuronal activity, which is similar to the neuronal response induced by hyperpolarizing current injection (Perry et al., 1998). Therefore, DA may

act as a negative regulator for esophagus contraction, and the release of DA is expected to lead to the relaxation of esophagus muscle groups.

The B19 neuron is immediately downstream of the feeding central pattern generator, which innervates muscle groups in the radula (Turner et al., 2011). It displays bursting activity during the hyper-retraction phase of the feeding cycle in *Helisoma*, which helps to bring food particles into the esophagus (Murphy, 2001). Physiological release of NO is expected to depolarize B19 neurons and increase their cell excitability *in vivo*. This effect of NO may shorten the inter-burst interval of B19 neurons, which would accelerate the rate of hyper-retraction of the odontophore during feeding motor activity. Indeed, NO has been found to act as a general regulator of feeding in gastropods (Susswein and Chiel, 2012). In studies using *Aplysia* and *Lymnaea*, NO is shown to contribute to all stages of feeding behavior, including the maintenance of food arousal (Katzoff et al., 2006), resistance of swallowing (Miller et al., 2011; Miller et al., 2011), and formation of the memory of food inedibility (Kemenes et al., 2002; Katzoff et al., 2010). These functional effects of NO are elicited by the spatial and temporal regulation of NO signaling within the nervous system. Additionally, the fact that NO controls the resting membrane potential of both B5 and B19 neurons via a similar set of ion channel targets suggests that NO signaling might be conserved across different neuronal cell types. NO can freely pass the cell membrane and act on target neurons in the vicinity of NO-releasing neurons (Kiss and Vizi, 2001; Artinian et al., 2010), which makes NO an ideal modulator to coordinate the electrical activity of various neurons within neuronal circuits including, but not limited to, feeding.

5.8 Conclusion

This dissertation focuses on three specific aims that address questions about the signaling mechanisms of neurotransmitters/neuromodulators in the regulation of neuronal electrical properties and growth cone motility in developing neurons. As shown in aim 1, ACh activates nAChRs and leads to membrane depolarization and an elevation of $[Ca]_i$ in growth cones, which cause filopodial elongation in B5 neurons. The results demonstrate that electrophysiological changes elicited by ACh in B5 neurons can affect growth cone motility and elucidate the underlying signaling pathway. In aim 2, NO is shown to specifically inhibit Ca-activated K channels, BK and SK channels, thereby modulating the neuronal excitability of B19 neurons. These channels were shown previously to be the target of NO in another neuron, B5, suggesting that Ca-activated K channels might be conserved targets of NO signaling. Aim 3 reveals that DA causes a strong hyperpolarization and silencing effect on B5 neurons via a D2-like receptor/PLC/K channel mechanism. Therefore, DA may serve as a prominent inhibitory neurotransmitter in the feeding circuitry of *Helisoma*. Taken together, the classical neurotransmitters ACh and DA, and unconventional neurotransmitter/neuromodulator NO have strong effects on neuronal electrical properties by directly or indirectly regulating the activity of ion channels and receptors. Additionally, these studies clearly link the electrical activity in identified neurons to growth cone motility. This might further explain why neurotransmitters like ACh are capable of controlling growth cone behaviors in developing neurons and might have implications for processes such as axon pathfinding and growth cone guidance during development *in vivo*. The accurate formation of neuronal connectivity is crucial for the normal function of the nervous system and proper behaviors to be produced. Therefore, this dissertation not only provides novel information about the role of neurotransmitter/neuromodulator in

developing neurons, but may also help our understanding of the causes of clinic conditions, in which the miswiring of the nervous system results in psychiatric disorders. Furthermore, this dissertation provides insight into the signaling pathways underlying the actions of neurotransmitter/neuromodulator in developing neurons, thereby strengthening the foundation for a better understanding of complex motor programs and behaviors *in vivo*.

REFERENCES

Abrams P, Andersson KE, Buccafusco JJ, Chapple C, de Groat WC, Fryer AD, Kay G, Laties A, Nathanson NM, Pasricha PJ, Wein AJ. 2006. Muscarinic receptors: their distribution and function in body systems, and the implications for treating overactive bladder. Br J Pharmacol 148:565-578.

Adelman JP, Maylie J, Sah P. 2012. Small-conductance Ca2+-activated K+ channels: form and function. Annu Rev Physiol 74:245-269.

Adelman JP, Shen KZ, Kavanaugh MP, Warren RA, Wu YN, Lagrutta A, Bond CT, North RA. 1992. Calcium-activated potassium channels expressed from cloned complementary DNAs. Neuron 9:209-216.

Ahern GP, Klyachko VA, Jackson MB. 2002. cGMP and S-nitrosylation: two routes for modulation of neuronal excitability by NO. Trends Neurosci 25:510-517.

Allen TG, Brown DA. 1996. Detection and modulation of acetylcholine release from neurites of rat basal forebrain cells in culture. J Physiol 492 (Pt 2):453-466.

Armstrong CM, Hille B. 1998. Voltage-gated ion channels and electrical excitability. Neuron 20:371-380.

Arrang JM, Garbarg M, Schwartz JC. 1987. Autoinhibition of histamine synthesis mediated by presynaptic H3-receptors. Neuroscience 23:149-157.

Artinian L, Tornieri K, Zhong L, Baro D, Rehder V. 2010. Nitric oxide acts as a volume transmitter to modulate electrical properties of spontaneously firing neurons via apamin-sensitive potassium channels. J Neurosci 30:1699-1711.

Artinian L, Zhong L, Yang H, Rehder V. 2012. Nitric oxide as intracellular modulator: internal production of NO increases neuronal excitability via modulation of several ionic conductances. Eur J Neurosci 36:3333-3343.

Audesirk TE. 1989. Characterization of pre- and postsynaptic dopamine receptors in Lymnaea. Comp Biochem Physiol C 93:115-119.

Bahls F. 1987. Acetylcholine-induced responses in the salivary gland cells of Helisoma trivolvis. Cell Mol Neurobiol 7:35-47.

Barbas D, Zappulla JP, Angers S, Bouvier M, Mohamed HA, Byrne JH, Castellucci VF, DesGroseillers L. 2006. An aplysia dopamine1-like receptor: molecular and functional characterization. J Neurochem 96:414-427.

Bean BP. 2007. The action potential in mammalian central neurons. Nat Rev Neurosci 8:451-465.

Bear JE, Svitkina TM, Krause M, Schafer DA, Loureiro JJ, Strasser GA, Maly IV, Chaga OY, Cooper JA, Borisy GG, Gertler FB. 2002. Antagonism between Ena/VASP proteins and actin filament capping regulates fibroblast motility. Cell 109:509-521.

Beaulieu JM, Gainetdinov RR. 2011. The physiology, signaling, and pharmacology of dopamine receptors. Pharmacol Rev 63:182-217.

Beker F, Weber M, Fink RH, Adams DJ. 2003. Muscarinic and nicotinic ACh receptor activation differentially mobilize Ca2+ in rat intracardiac ganglion neurons. J Neurophysiol 90:1956-1964.

Benoit-Marand M, Borrelli E, Gonon F. 2001. Inhibition of dopamine release via presynaptic D2 receptors: time course and functional characteristics in vivo. J Neurosci 21:9134-9141.

Berdan RC, Easaw JC. 1992. Modulation of sprouting in organ culture after axotomy of an identified molluscan neuron. J Neurobiol 23:433-450.

Berridge MJ. 1998. Neuronal calcium signaling. Neuron 21:13-26.

Berridge MJ, Bootman MD, Roderick HL. 2003. Calcium signalling: dynamics, homeostasis and remodelling. Nat Rev Mol Cell Biol 4:517-529.

Bevan MD, Atherton JF, Baufreton J. 2006. Cellular principles underlying normal and pathological activity in the subthalamic nucleus. Curr Opin Neurobiol 16:621-628.

Bicker G. 2007. Pharmacological approaches to nitric oxide signalling during neural development of locusts and other model insects. Arch Insect Biochem Physiol 64:43-58.

Blaine JT, Ribera AB. 2001. Kv2 channels form delayed-rectifier potassium channels in situ. J Neurosci 21:1473-1480.

Bolotina VM, Najibi S, Palacino JJ, Pagano PJ, Cohen RA. 1994. Nitric oxide directly activates calcium-dependent potassium channels in vascular smooth muscle. Nature 368:850-853.

Bon CL, Garthwaite J. 2003. On the role of nitric oxide in hippocampal long-term potentiation. J Neurosci 23:1941-1948.

Brosenitsch TA, Katz DM. 2001. Physiological patterns of electrical stimulation can induce neuronal gene expression by activating N-type calcium channels. J Neurosci 21:2571-2579.

Brosenitsch TA, Katz DM. 2002. Expression of Phox2 transcription factors and induction of the dopaminergic phenotype in primary sensory neurons. Mol Cell Neurosci 20:447-457.

Brown GC, Borutaite V. 2002. Nitric oxide inhibition of mitochondrial respiration and its role in cell death. Free Radic Biol Med 33:1440-1450.

Candia S, Garcia ML, Latorre R. 1992. Mode of action of iberiotoxin, a potent blocker of the large conductance Ca(2+)-activated K+ channel. Biophys J 63:583-590.

Carlier MF, Ducruix A, Pantaloni D. 1999. Signalling to actin: the Cdc42-N-WASP-Arp2/3 connection. Chem Biol 6:R235-240.

Catterall WA. 2000. Structure and regulation of voltage-gated Ca2+ channels. Annu Rev Cell Dev Biol 16:521-555.

Catterall WA. 2011. Voltage-gated calcium channels. Cold Spring Harb Perspect Biol 3:a003947.

Cetiner M, Bennett MR. 1993. Nitric oxide modulation of calcium-activated potassium channels in postganglionic neurones of avian cultured ciliary ganglia. Br J Pharmacol 110:995-1002.

Chen Y, Zhou Y, Lin X, Wong HC, Xu Q, Jiang J, Wang S, Lurtz MM, Louis CF, Veenstra RD, Yang JJ. 2011. Molecular interaction and functional regulation of connexin50 gap junctions by calmodulin. Biochem J 435:711-722.

Cheng HJ, Bagri A, Yaron A, Stein E, Pleasure SJ, Tessier-Lavigne M. 2001. Plexin-A3 mediates semaphorin signaling and regulates the development of hippocampal axonal projections. Neuron 32:249-263.

Cheng S, Geddis MS, Rehder V. 2002. Local calcium changes regulate the length of growth cone filopodia. J Neurobiol 50:263-275.

Chien CB, Rosenthal DE, Harris WA, Holt CE. 1993. Navigational errors made by growth cones without filopodia in the embryonic Xenopus brain. Neuron 11:237-251.

Clapham DE. 2003. TRP channels as cellular sensors. Nature 426:517-524.

Clementi F, Fornasari D, Gotti C. 2000. Neuronal nicotinic receptors, important new players in brain function. Eur J Pharmacol 393:3-10.

Cobb SR, Davies CH. 2005. Cholinergic modulation of hippocampal cells and circuits. J Physiol 562:81-88.

Coetzee WA, Amarillo Y, Chiu J, Chow A, Lau D, McCormack T, Moreno H, Nadal MS, Ozaita A, Pountney D, Saganich M, Vega-Saenz de Miera E, Rudy B. 1999. Molecular diversity of K+ channels. Ann N Y Acad Sci 868:233-285.

Cohan CS. 1992. Depolarization-induced changes in neurite elongation and intracellular Ca2+ in isolated Helisoma neurons. J Neurobiol 23:983-996.

Cohan CS, Kater SB. 1986. Suppression of neurite elongation and growth cone motility by electrical activity. Science 232:1638-1640.

Colon-Ramos DA. 2009. Synapse formation in developing neural circuits. Curr Top Dev Biol 87:53-79.

Cowan WM. 2001. Viktor Hamburger and Rita Levi-Montalcini: the path to the discovery of nerve growth factor. Annu Rev Neurosci 24:551-600.

D'Yakonova T L, D'Yakonova V E. 2008. Modification of the effects of glutamate by nitric oxide (NO) in a pattern-generating network. Neurosci Behav Physiol 38:407-413.

Dani JA, Bertrand D. 2007. Nicotinic acetylcholine receptors and nicotinic cholinergic mechanisms of the central nervous system. Annu Rev Pharmacol Toxicol 47:699-729.

Davis KL, Martin E, Turko IV, Murad F. 2001. Novel effects of nitric oxide. Annu Rev Pharmacol Toxicol 41:203-236.

de Vlieger TA, Lodder JC, Stoof JC, Werkman TR. 1986. Dopamine receptor stimulation induces a potassium dependent hyperpolarizing response in growth hormone producing neuroendocrine cells of the gastropod mollusc Lymnaea stagnalis. Comp Biochem Physiol C 83:429-433.

Dent EW, Gupton SL, Gertler FB. 2011. The growth cone cytoskeleton in axon outgrowth and guidance. Cold Spring Harb Perspect Biol 3.

Dobson KS, Dmetrichuk JM, Spencer GE. 2006. Different receptors mediate the electrophysiological and growth cone responses of an identified neuron to applied dopamine. Neuroscience 141:1801-1810.

Durkaya G, Zhong L, Rehder V, Dietz N. 2009. Nano-scale Topographical Studies on the Growth Cones of Nerve Cells using AFM. Bulletin of the American Physical Society 54.

Durkaya G, Zhong L, Rehder V, Dietz N. 2009. Surface Morphological Studies on Nerve Cells by AFM. Bulletin of the American Physical Society 54.

Elliott CJ, Vehovszky A. 2000. Comparative pharmacology of feeding in molluscs. Acta Biol Hung 51:153-163.

Evans AR, Euteneuer S, Chavez E, Mullen LM, Hui EE, Bhatia SN, Ryan AF. 2007. Laminin and fibronectin modulate inner ear spiral ganglion neurite outgrowth in an in vitro alternate choice assay. Dev Neurobiol 67:1721-1730.

Faber ES, Sah P. 2003. Calcium-activated potassium channels: multiple contributions to neuronal function. Neuroscientist 9:181-194.

Farrar NR, Spencer GE. 2008. Pursuing a 'turning point' in growth cone research. Dev Biol 318:102-111.

Fields RD, Neale EA, Nelson PG. 1990. Effects of patterned electrical activity on neurite outgrowth from mouse sensory neurons. J Neurosci 10:2950-2964.

Foster MW, McMahon TJ, Stamler JS. 2003. S-nitrosylation in health and disease. Trends Mol Med 9:160-168.

Freedman SB, Patel S, Marwood R, Emms F, Seabrook GR, Knowles MR, McAllister G. 1994. Expression and pharmacological characterization of the human D3 dopamine receptor. J Pharmacol Exp Ther 268:417-426.

Fu WM, Liou HC, Chen YH. 1998. Nerve terminal currents induced by autoreception of acetylcholine release. J Neurosci 18:9954-9961.

Fu WM, Liu JJ. 1997. Regulation of acetylcholine release by presynaptic nicotinic receptors at developing neuromuscular synapses. Mol Pharmacol 51:390-398.

Fucile S. 2004. Ca2+ permeability of nicotinic acetylcholine receptors. Cell Calcium 35:1-8.

Fucile S, Sucapane A, Eusebi F. 2005. Ca2+ permeability of nicotinic acetylcholine receptors from rat dorsal root ganglion neurones. J Physiol 565:219-228.

Gallo G, Lefcort FB, Letourneau PC. 1997. The trkA receptor mediates growth cone turning toward a localized source of nerve growth factor. J Neurosci 17:5445-5454.

Garthwaite J. 2008. Concepts of neural nitric oxide-mediated transmission. Eur J Neurosci 27:2783-2802.

Glebova NO, Ginty DD. 2004. Heterogeneous requirement of NGF for sympathetic target innervation in vivo. J Neurosci 24:743-751.

Gomez T. 2005. Neurobiology: channels for pathfinding. Nature 434:835-838.

Gomez TM, Robles E, Poo M, Spitzer NC. 2001. Filopodial calcium transients promote substrate-dependent growth cone turning. Science 291:1983-1987.

Gomez TM, Spitzer NC. 2000. Regulation of growth cone behavior by calcium: new dynamics to earlier perspectives. J Neurobiol 44:174-183.

Gomez TM, Zheng JQ. 2006. The molecular basis for calcium-dependent axon pathfinding. Nat Rev Neurosci 7:115-125.

Haedo RJ, Golowasch J. 2006. Ionic mechanism underlying recovery of rhythmic activity in adult isolated neurons. J Neurophysiol 96:1860-1876.

Harris-Warrick RM. 2011. Neuromodulation and flexibility in Central Pattern Generator networks. Curr Opin Neurobiol 21:685-692.

Harris-Warrick RM, Coniglio LM, Barazangi N, Guckenheimer J, Gueron S. 1995. Dopamine modulation of transient potassium current evokes phase shifts in a central pattern generator network. J Neurosci 15:342-358.

Harris-Warrick RM, Johnson BR, Peck JH, Kloppenburg P, Ayali A, Skarbinski J. 1998. Distributed effects of dopamine modulation in the crustacean pyloric network. Ann N Y Acad Sci 860:155-167.

Haydon PG. 1988. The formation of chemical synapses between cell-cultured neuronal somata. J Neurosci 8:1032-1038.

Haydon PG, Cohan CS, McCobb DP, Miller HR, Kater SB. 1985. Neuron-specific growth cone properties as seen in identified neurons of Helisoma. J Neurosci Res 13:135-147.

Haydon PG, Man-Son-Hing H. 1988. Low- and high-voltage-activated calcium currents: their relationship to the site of neurotransmitter release in an identified neuron of Helisoma. Neuron 1:919-927.

Haydon PG, Zoran MJ. 1989. Formation and modulation of chemical connections: evoked acetylcholine release from growth cones and neurites of specific identified neurons. Neuron 2:1483-1490.

Henley J, Poo MM. 2004. Guiding neuronal growth cones using Ca2+ signals. Trends Cell Biol 14:320-330.

Henley JR, Huang KH, Wang D, Poo MM. 2004. Calcium mediates bidirectional growth cone turning induced by myelin-associated glycoprotein. Neuron 44:909-916.

Herrera GM, Nelson MT. 2002. Differential regulation of SK and BK channels by Ca(2+) signals from Ca(2+) channels and ryanodine receptors in guinea-pig urinary bladder myocytes. J Physiol 541:483-492.

Hirst GD, Johnson SM, van Helden DF. 1985. The slow calcium-dependent potassium current in a myenteric neurone of the guinea-pig ileum. J Physiol 361:315-337.

Hong K, Nishiyama M, Henley J, Tessier-Lavigne M, Poo M. 2000. Calcium signalling in the guidance of nerve growth by netrin-1. Nature 403:93-98.

Hopper RA, Garthwaite J. 2006. Tonic and phasic nitric oxide signals in hippocampal long-term potentiation. J Neurosci 26:11513-11521.

Hui K, Feng ZP. 2008. NCS-1 differentially regulates growth cone and somata calcium channels in Lymnaea neurons. Eur J Neurosci 27:631-643.

Hume RI, Role LW, Fischbach GD. 1983. Acetylcholine release from growth cones detected with patches of acetylcholine receptor-rich membranes. Nature 305:632-634.

Itier V, Bertrand D. 2001. Neuronal nicotinic receptors: from protein structure to function. FEBS Lett 504:118-125.

Jaffe DB, Wang B, Brenner R. 2011. Shaping of action potentials by type I and type II large-conductance Ca(2)+-activated K+ channels. Neuroscience 192:205-218.

Jagger DJ, Griesinger CB, Rivolta MN, Holley MC, Ashmore JF. 2000. Calcium signalling mediated by the 9 acetylcholine receptor in a cochlear cell line from the immortomouse. J Physiol 527 Pt 1:49-54.

Jarjour AA, Manitt C, Moore SW, Thompson KM, Yuh SJ, Kennedy TE. 2003. Netrin-1 is a chemorepellent for oligodendrocyte precursor cells in the embryonic spinal cord. J Neurosci 23:3735-3744.

Jensen ML, Schousboe A, Ahring PK. 2005. Charge selectivity of the Cys-loop family of ligand-gated ion channels. J Neurochem 92:217-225.

Jiang J, Zhou Y, Zou J, Chen Y, Patel P, Yang JJ, Balog EM. 2010. Site-specific modification of calmodulin Ca(2)(+) affinity tunes the skeletal muscle ryanodine receptor activation profile. Biochem J 432:89-99.

Jonsson M, Gurley D, Dabrowski M, Larsson O, Johnson EC, Eriksson LI. 2006. Distinct pharmacologic properties of neuromuscular blocking agents on human neuronal nicotinic acetylcholine receptors: a possible explanation for the train-of-four fade. Anesthesiology 105:521-533.

Kabotyanski EA, Baxter DA, Cushman SJ, Byrne JH. 2000. Modulation of fictive feeding by dopamine and serotonin in aplysia. J Neurophysiol 83:374-392.

Kang J, Huguenard JR, Prince DA. 2000. Voltage-gated potassium channels activated during action potentials in layer V neocortical pyramidal neurons. J Neurophysiol 83:70-80.

Kater SB, Davenport RW, Guthrie PB. 1994. Filopodia as detectors of environmental cues: signal integration through changes in growth cone calcium levels. Prog Brain Res 102:49-60.

Kater SB, Mattson MP, Cohan C, Connor J. 1988. Calcium regulation of the neuronal growth cone. Trends Neurosci 11:315-321.

Kater SB, Rehder V. 1995. The sensory-motor role of growth cone filopodia. Curr Opin Neurobiol 5:68-74.

Katzoff A, Ben-Gedalya T, Hurwitz I, Miller N, Susswein YZ, Susswein AJ. 2006. Nitric oxide signals that aplysia have attempted to eat, a necessary component of memory formation after learning that food is inedible. J Neurophysiol 96:1247-1257.

Katzoff A, Miller N, Susswein AJ. 2010. Nitric oxide and histamine signal attempts to swallow: A component of learning that food is inedible in Aplysia. Learn Mem 17:50-62.

Kemenes I, Kemenes G, Andrew RJ, Benjamin PR, O'Shea M. 2002. Critical time-window for NO-cGMP-dependent long-term memory formation after one-trial appetitive conditioning. J Neurosci 22:1414-1425.

Kemenes I, Straub VA, Nikitin ES, Staras K, O'Shea M, Kemenes G, Benjamin PR. 2006. Role of delayed nonsynaptic neuronal plasticity in long-term associative memory. Curr Biol 16:1269-1279.

Keramidas A, Moorhouse AJ, Schofield PR, Barry PH. 2004. Ligand-gated ion channels: mechanisms underlying ion selectivity. Prog Biophys Mol Biol 86:161-204.

Kim SM, Bae J, Cho IH, Choi KY, Park YJ, Ryu JH, Chun JS, Song WK. 2011. Control of growth cone motility and neurite outgrowth by SPIN90. Exp Cell Res 317:2276-2287.

Kiss JP, Vizi ES. 2001. Nitric oxide: a novel link between synaptic and nonsynaptic transmission. Trends Neurosci 24:211-215.

Kobayashi S, Ogawa H, Fujito Y, Ito E. 2000. Nitric oxide suppresses fictive feeding response in Lymnaea stagnalis. Neurosci Lett 285:209-212.

Kobilka BK. 2007. G protein coupled receptor structure and activation. Biochim Biophys Acta 1768:794-807.

Komuro H, Rakic P. 1996. Intracellular Ca2+ fluctuations modulate the rate of neuronal migration. Neuron 17:275-285.

Krawczyk M, Sharma R, Mason X, Debacker J, Jones AA, Dumont EC. 2011. A switch in the neuromodulatory effects of dopamine in the oval bed nucleus of the stria terminalis associated with cocaine self-administration in rats. J Neurosci 31:8928-8935.

Kupfermann I. 1979. Modulatory actions of neurotransmitters. Annu Rev Neurosci 2:447-465.

Kuzhikandathil EV, Yu W, Oxford GS. 1998. Human dopamine D3 and D2L receptors couple to inward rectifier potassium channels in mammalian cell lines. Mol Cell Neurosci 12:390-402.

Lauder JM, Schambra UB. 1999. Morphogenetic roles of acetylcholine. Environ Health Perspect 107 Suppl 1:65-69.

Lax P, Fucile S, Eusebi F. 2002. Ca(2+) permeability of human heteromeric nAChRs expressed by transfection in human cells. Cell Calcium 32:53-58.

Le Novere N, Changeux JP. 1995. Molecular evolution of the nicotinic acetylcholine receptor: an example of multigene family in excitable cells. J Mol Evol 40:155-172.

Lee SP, So CH, Rashid AJ, Varghese G, Cheng R, Lanca AJ, O'Dowd BF, George SR. 2004. Dopamine D1 and D2 receptor Co-activation generates a novel phospholipase C-mediated calcium signal. J Biol Chem 279:35671-35678.

Lee US, Cui J. 2010. BK channel activation: structural and functional insights. Trends Neurosci 33:415-423.

Letourneau PC. 1978. Chemotactic response of nerve fiber elongation to nerve growth factor. Dev Biol 66:183-196.

Li X, Gao X, Liu G, Xiong W, Wu J, Rao Y. 2008. Netrin signal transduction and the guanine nucleotide exchange factor DOCK180 in attractive signaling. Nat Neurosci 11:28-35.

Li Y, Grenklo S, Higgins T, Karlsson R. 2008. The profilin:actin complex localizes to sites of dynamic actin polymerization at the leading edge of migrating cells and pathogen-induced actin tails. Eur J Cell Biol 87:893-904.

Li Y, Jia YC, Cui K, Li N, Zheng ZY, Wang YZ, Yuan XB. 2005. Essential role of TRPC channels in the guidance of nerve growth cones by brain-derived neurotrophic factor. Nature 434:894-898.

Liss B, Roeper J. 2008. Individual dopamine midbrain neurons: functional diversity and flexibility in health and disease. Brain Res Rev 58:314-321.

Liu SJ, Zukin RS. 2007. Ca2+-permeable AMPA receptors in synaptic plasticity and neuronal death. Trends Neurosci 30:126-134.

LoTurco JJ, Owens DF, Heath MJ, Davis MB, Kriegstein AR. 1995. GABA and glutamate depolarize cortical progenitor cells and inhibit DNA synthesis. Neuron 15:1287-1298.

Lowery LA, Van Vactor D. 2009. The trip of the tip: understanding the growth cone machinery. Nat Rev Mol Cell Biol 10:332-343.

Lukowiak K, Martens K, Orr M, Parvez K, Rosenegger D, Sangha S. 2006. Modulation of aerial respiratory behaviour in a pond snail. Respir Physiol Neurobiol 154:61-72.

Luo Y, Raible D, Raper JA. 1993. Collapsin: a protein in brain that induces the collapse and paralysis of neuronal growth cones. Cell 75:217-227.

Magoski NS, Bauce LG, Syed NI, Bulloch AG. 1995. Dopaminergic transmission between identified neurons from the mollusk, Lymnaea stagnalis. J Neurophysiol 74:1287-1300.

Magoski NS, Bulloch AG. 1999. Dopamine activates two different receptors to produce variability in sign at an identified synapse. J Neurophysiol 81:1330-1340.

Malyshev AY, Balaban PM. 2009. Buccal neurons activate ciliary beating in the foregut of the pteropod mollusk Clione limacina. J Exp Biol 212:2969-2976.

Maness PF, Schachner M. 2007. Neural recognition molecules of the immunoglobulin superfamily: signaling transducers of axon guidance and neuronal migration. Nat Neurosci 10:19-26.

Marder E, Calabrese RL. 1996. Principles of rhythmic motor pattern generation. Physiol Rev 76:687-717.

Marinissen MJ, Gutkind JS. 2001. G-protein-coupled receptors and signaling networks: emerging paradigms. Trends Pharmacol Sci 22:368-376.

Matsuda Y, Marzo A, Otani S. 2006. The presence of background dopamine signal converts long-term synaptic depression to potentiation in rat prefrontal cortex. J Neurosci 26:4803-4810.

Mattila PK, Lappalainen P. 2008. Filopodia: molecular architecture and cellular functions. Nat Rev Mol Cell Biol 9:446-454.

Mattson MP, Kater SB. 1987. Calcium regulation of neurite elongation and growth cone motility. J Neurosci 7:4034-4043.

Mattson MP, Taylor-Hunter A, Kater SB. 1988. Neurite outgrowth in individual neurons of a neuronal population is differentially regulated by calcium and cyclic AMP. J Neurosci 8:1704-1711.

McCobb DP, Cohan CS, Connor JA, Kater SB. 1988. Interactive effects of serotonin and acetylcholine on neurite elongation. Neuron 1:377-385.

McCobb DP, Haydon PG, Kater SB. 1988. Dopamine and serotonin inhibition of neurite elongation of different identified neurons. J Neurosci Res 19:19-26.

McCobb DP, Kater SB. 1988. Membrane voltage and neurotransmitter regulation of neuronal growth cone motility. Dev Biol 130:599-609.

McGehee DS, Heath MJ, Gelber S, Devay P, Role LW. 1995. Nicotine enhancement of fast excitatory synaptic transmission in CNS by presynaptic receptors. Science 269:1692-1696.

Miller N, Saada R, Fishman S, Hurwitz I, Susswein AJ. 2011. Neurons controlling Aplysia feeding inhibit themselves by continuous NO production. PLoS ONE 6:e17779.

Miller N, Saada R, Markovich S, Hurwitz I, Susswein AJ. 2011. L-arginine via nitric oxide is an inhibitory feedback modulator of Aplysia feeding. J Neurophysiol 105:1642-1650.

Ming G, Henley J, Tessier-Lavigne M, Song H, Poo M. 2001. Electrical activity modulates growth cone guidance by diffusible factors. Neuron 29:441-452.

Ming GL, Song HJ, Berninger B, Holt CE, Tessier-Lavigne M, Poo MM. 1997. cAMP-dependent growth cone guidance by netrin-1. Neuron 19:1225-1235.

Missale C, Nash SR, Robinson SW, Jaber M, Caron MG. 1998. Dopamine receptors: from structure to function. Physiol Rev 78:189-225.

Mitchell KJ. 2011. The genetics of neurodevelopmental disease. Curr Opin Neurobiol 21:197-203.

Mitchell KJ. 2011. The miswired brain: making connections from neurodevelopment to psychopathology. BMC Biol 9:23.

Miyamoto T, Kawada T, Yanagiya Y, Akiyama T, Kamiya A, Mizuno M, Takaki H, Sunagawa K, Sugimachi M. 2008. Contrasting effects of presynaptic alpha2-adrenergic autoinhibition and pharmacologic augmentation of presynaptic inhibition on sympathetic heart rate control. Am J Physiol Heart Circ Physiol 295:H1855-1866.

Mizuno T, Schmauss C, Rayport S. 2007. Distinct roles of presynaptic dopamine receptors in the differential modulation of the intrinsic synapses of medium-spiny neurons in the nucleus accumbens. BMC Neurosci 8:8.

Moody WJ. 1998. Control of spontaneous activity during development. J Neurobiol 37:97-109.

Moore SW, Tessier-Lavigne M, Kennedy TE. 2007. Netrins and their receptors. Adv Exp Med Biol 621:17-31.

Moquin KF, Michael AC. 2009. Tonic autoinhibition contributes to the heterogeneity of evoked dopamine release in the rat striatum. J Neurochem 110:1491-1501.

Moroz LL, Kohn AB. 2011. Parallel evolution of nitric oxide signaling: diversity of synthesis and memory pathways. Front Biosci 16:2008-2051.

Moroz LL, Park JH, Winlow W. 1993. Nitric oxide activates buccal motor patterns in Lymnaea stagnalis. Neuroreport 4:643-646.

Mukai ST, Kiehn L, Saleuddin AS. 2004. Dopamine stimulates snail albumen gland glycoprotein secretion through the activation of a D1-like receptor. J Exp Biol 207:2507-2518.

Murphy AD. 2001. The neuronal basis of feeding in the snail, Helisoma, with comparisons to selected gastropods. Prog Neurobiol 63:383-408.

Murphy AD, Kater SB. 1980. Differential discrimination of appropriate pathways by regenerating identified neurons in Helisoma. J Comp Neurol 190:395-403.

Neely MD, Nicholls JG. 1995. Electrical activity, growth cone motility and the cytoskeleton. J Exp Biol 198:1433-1446.

Nikonenko I, Boda B, Steen S, Knott G, Welker E, Muller D. 2008. PSD-95 promotes synaptogenesis and multiinnervated spine formation through nitric oxide signaling. J Cell Biol 183:1115-1127.

Nishiyama M, Hoshino A, Tsai L, Henley JR, Goshima Y, Tessier-Lavigne M, Poo MM, Hong K. 2003. Cyclic AMP/GMP-dependent modulation of Ca2+ channels sets the polarity of nerve growth-cone turning. Nature 423:990-995.

Nishiyama M, Togashi K, von Schimmelmann MJ, Lim CS, Maeda S, Yamashita N, Goshima Y, Ishii S, Hong K. 2011. Semaphorin 3A induces CaV2.3 channel-dependent conversion of axons to dendrites. Nat Cell Biol 13:676-685.

Nishiyama M, von Schimmelmann MJ, Togashi K, Findley WM, Hong K. 2008. Membrane potential shifts caused by diffusible guidance signals direct growth-cone turning. Nat Neurosci 11:762-771.

Nordman JC, Kabbani N. 2012. An interaction between alpha7 nicotinic receptors and a G-protein pathway complex regulates neurite growth in neural cells. J Cell Sci 125:5502-5513.

Nunez L, Vaquero M, Gomez R, Caballero R, Mateos-Caceres P, Macaya C, Iriepa I, Galvez E, Lopez-Farre A, Tamargo J, Delpon E. 2006. Nitric oxide blocks hKv1.5 channels by S-nitrosylation and by a cyclic GMP-dependent mechanism. Cardiovasc Res 72:80-89.

Oberstar JV, Challacombe JF, Roche FK, Letourneau PC. 1997. Concentration-dependent stimulation and inhibition of growth cone behavior and neurite elongation by protein kinase inhibitors KT5926 and K-252a. J Neurobiol 33:161-171.

Owen A, Bird M. 1995. Acetylcholine as a regulator of neurite outgrowth and motility in cultured embryonic mouse spinal cord. Neuroreport 6:2269-2272.

Patel BA, Arundell M, Parker KH, Yeoman MS, O'Hare D. 2006. Detection of nitric oxide release from single neurons in the pond snail, Lymnaea stagnalis. Anal Chem 78:7643-7648.

Patil N, Cox DR, Bhat D, Faham M, Myers RM, Peterson AS. 1995. A potassium channel mutation in weaver mice implicates membrane excitability in granule cell differentiation. Nat Genet 11:126-129.

Perry SJ, Straub VA, Kemenes G, Santama N, Worster BM, Burke JF, Benjamin PR. 1998. Neural modulation of gut motility by myomodulin peptides and acetylcholine in the snail Lymnaea. J Neurophysiol 79:2460-2474.

Phillis JW. 2005. Acetylcholine release from the central nervous system: a 50-year retrospective. Crit Rev Neurobiol 17:161-217.

Podda MV, Riccardi E, D'Ascenzo M, Azzena GB, Grassi C. 2010. Dopamine D1-like receptor activation depolarizes medium spiny neurons of the mouse nucleus accumbens by inhibiting inwardly rectifying K+ currents through a cAMP-dependent protein kinase A-independent mechanism. Neuroscience 167:678-690.

Prast H, Philippu A. 2001. Nitric oxide as modulator of neuronal function. Prog Neurobiol 64:51-68.

Quinlan EM, Arnett BC, Murphy AD. 1997. Feeding stimulants activate an identified dopaminergic interneuron that induces the feeding motor program in Helisoma. J Neurophysiol 78:812-824.

Rashid AJ, So CH, Kong MM, Furtak T, El-Ghundi M, Cheng R, O'Dowd BF, George SR. 2007. D1-D2 dopamine receptor heterooligomers with unique pharmacology are coupled to rapid activation of Gq/11 in the striatum. Proc Natl Acad Sci U S A 104:654-659.

Rehder V, Jensen JR, Dou P, Kater SB. 1991. A comparison of calcium homeostasis in isolated and attached growth cones of the snail Helisoma. J Neurobiol 22:499-511.

Rehder V, Kater SB. 1992. Regulation of neuronal growth cone filopodia by intracellular calcium. J Neurosci 12:3175-3186.

Rehder V, Williams CV, Kater SB. 1996. Functional compartmentalization of the neuronal growth cone: determining calcium's place in signaling cascades. Perspect Dev Neurobiol 4:215-226.

Ribeiro M, Straub VA, Schofield M, Picot J, Benjamin PR, O'Shea M, Korneev SA. 2008. Characterization of NO-sensitive guanylyl cyclase: expression in an identified interneuron involved in NO-cGMP-dependent memory formation. Eur J Neurosci 28:1157-1165.

Ridley AJ. 2006. Rho GTPases and actin dynamics in membrane protrusions and vesicle trafficking. Trends Cell Biol 16:522-529.

Robinson DW, Cameron WE. 2000. Time-dependent changes in input resistance of rat hypoglossal motoneurons associated with whole-cell recording. J Neurophysiol 83:3160-3164.

Rodgers EW, Fu JJ, Krenz WD, Baro DJ. 2011. Tonic nanomolar dopamine enables an activity-dependent phase recovery mechanism that persistently alters the maximal conductance of the hyperpolarization-activated current in a rhythmically active neuron. J Neurosci 31:16387-16397.

Rodgers EW, Krenz WD, Baro DJ. 2011. Tonic dopamine induces persistent changes in the transient potassium current through translational regulation. J Neurosci 31:13046-13056.

Romey G, Hugues M, Schmid-Antomarchi H, Lazdunski M. 1984. Apamin: a specific toxin to study a class of Ca2+-dependent K+ channels. J Physiol (Paris) 79:259-264.

Rudiger T, Bolz J. 2008. Acetylcholine influences growth cone motility and morphology of developing thalamic axons. Cell Adh Migr 2:30-37.

Sadamoto H, Hatakeyama D, Kojima S, Fujito Y, Ito E. 1998. Histochemical study on the relation between NO-generative neurons and central circuitry for feeding in the pond snail, Lymnaea stagnalis. Neurosci Res 32:57-63.

Sakakibara M, Okuda F, Nomura K, Watanabe K, Meng H, Horikoshi T, Lukowiak K. 2005. Potassium currents in isolated statocyst neurons and RPeD1 in the pond snail, Lymnaea stagnalis. J Neurophysiol 94:3884-3892.

Sakurai A, Darghouth NR, Butera RJ, Katz PS. 2006. Serotonergic enhancement of a 4-AP-sensitive current mediates the synaptic depression phase of spike timing-dependent neuromodulation. J Neurosci 26:2010-2021.

Salie R, Niederkofler V, Arber S. 2005. Patterning molecules; multitasking in the nervous system. Neuron 45:189-192.

Sandhiya S, Dkhar SA. 2009. Potassium channels in health, disease & development of channel modulators. Indian J Med Res 129:223-232.

Scannell E, Dell'Ova CA, Quinlan EM, Murphy AD, Kleckner NW. 2008. Pharmacology of ionotropic and metabotropic glutamate receptors on neurons involved in feeding behavior in the pond snail, Helisoma trivolvis. J Exp Biol 211:824-833.

Schrofner S, Zsombok A, Hermann A, Kerschbaum HH. 2004. Nitric oxide decreases a calcium-activated potassium current via activation of phosphodiesterase 2 in Helix U-cells. Brain Res 999:98-105.

Scott RS, Bustillo D, Olivos-Ore LA, Cuchillo-Ibanez I, Barahona MV, Carbone E, Artalejo AR. 2011. Contribution of BK channels to action potential repolarisation at minimal cytosolic Ca2+ concentration in chromaffin cells. Pflugers Arch 462:545-557.

Seabrook GR, Kemp JA, Freedman SB, Patel S, Sinclair HA, McAllister G. 1994. Functional expression of human D3 dopamine receptors in differentiated neuroblastoma x glioma NG108-15 cells. Br J Pharmacol 111:391-393.

Seguela P, Wadiche J, Dineley-Miller K, Dani JA, Patrick JW. 1993. Molecular cloning, functional properties, and distribution of rat brain alpha 7: a nicotinic cation channel highly permeable to calcium. J Neurosci 13:596-604.

Shao LR, Halvorsrud R, Borg-Graham L, Storm JF. 1999. The role of BK-type Ca2+-dependent K+ channels in spike broadening during repetitive firing in rat hippocampal pyramidal cells. J Physiol 521 Pt 1:135-146.

Shen K, Cowan CW. 2010. Guidance molecules in synapse formation and plasticity. Cold Spring Harb Perspect Biol 2:a001842.

Shibata R, Nakahira K, Shibasaki K, Wakazono Y, Imoto K, Ikenaka K. 2000. A-type K+ current mediated by the Kv4 channel regulates the generation of action potential in developing cerebellar granule cells. J Neurosci 20:4145-4155.

Shieh CC, Coghlan M, Sullivan JP, Gopalakrishnan M. 2000. Potassium channels: molecular defects, diseases, and therapeutic opportunities. Pharmacol Rev 52:557-594.

Shim S, Goh EL, Ge S, Sailor K, Yuan JP, Roderick HL, Bootman MD, Worley PF, Song H, Ming GL. 2005. XTRPC1-dependent chemotropic guidance of neuronal growth cones. Nat Neurosci 8:730-735.

Sit ST, Manser E. 2011. Rho GTPases and their role in organizing the actin cytoskeleton. J Cell Sci 124:679-683.

Small DH, Reed G, Whitefield B, Nurcombe V. 1995. Cholinergic regulation of neurite outgrowth from isolated chick sympathetic neurons in culture. J Neurosci 15:144-151.

Snider WD. 1994. Functions of the neurotrophins during nervous system development: what the knockouts are teaching us. Cell 77:627-638.

Spafford JD, Dunn T, Smit AB, Syed NI, Zamponi GW. 2006. In vitro characterization of L-type calcium channels and their contribution to firing behavior in invertebrate respiratory neurons. J Neurophysiol 95:42-52.

Spafford JD, Munno DW, Van Nierop P, Feng ZP, Jarvis SE, Gallin WJ, Smit AB, Zamponi GW, Syed NI. 2003. Calcium channel structural determinants of synaptic transmission between identified invertebrate neurons. J Biol Chem 278:4258-4267.

Spencer GE, Klumperman J, Syed NI. 1998. Neurotransmitters and neurodevelopment. Role of dopamine in neurite outgrowth, target selection and specific synapse formation. Perspect Dev Neurobiol 5:451-467.

Spencer GE, Lukowiak K, Syed NI. 1996. Dopamine regulation of neurite outgrowth from identified Lymnaea neurons in culture. Cell Mol Neurobiol 16:577-589.

Spencer GE, Lukowiak K, Syed NI. 2000. Transmitter-receptor interactions between growth cones of identified Lymnaea neurons determine target cell selection in vitro. J Neurosci 20:8077-8086.

Spitzer NC. 2006. Electrical activity in early neuronal development. Nature 444:707-712.

Spitzer NC, Root CM, Borodinsky LN. 2004. Orchestrating neuronal differentiation: patterns of Ca2+ spikes specify transmitter choice. Trends Neurosci 27:415-421.

Stamler JS, Singel DJ, Loscalzo J. 1992. Biochemistry of nitric oxide and its redox-activated forms. Science 258:1898-1902.

Staras K, Gyori J, Kemenes G. 2002. Voltage-gated ionic currents in an identified modulatory cell type controlling molluscan feeding. Eur J Neurosci 15:109-119.

Steinert JR, Kopp-Scheinpflug C, Baker C, Challiss RA, Mistry R, Haustein MD, Griffin SJ, Tong H, Graham BP, Forsythe ID. 2008. Nitric oxide is a volume transmitter regulating postsynaptic excitability at a glutamatergic synapse. Neuron 60:642-656.

Steinert JR, Robinson SW, Tong H, Haustein MD, Kopp-Scheinpflug C, Forsythe ID. 2011. Nitric oxide is an activity-dependent regulator of target neuron intrinsic excitability. Neuron 71:291-305.

Stocker M. 2004. Ca(2+)-activated K+ channels: molecular determinants and function of the SK family. Nat Rev Neurosci 5:758-770.

Straub VA, Grant J, O'Shea M, Benjamin PR. 2007. Modulation of serotonergic neurotransmission by nitric oxide. J Neurophysiol 97:1088-1099.

Sunahara RK, Seeman P, Van Tol HH, Niznik HB. 1993. Dopamine receptors and antipsychotic drug response. Br J Psychiatry Suppl:31-38.

Susswein AJ, Chiel HJ. 2012. Nitric oxide as a regulator of behavior: new ideas from Aplysia feeding. Prog Neurobiol 97:304-317.

Talavera K, Nilius B, Voets T. 2008. Neuronal TRP channels: thermometers, pathfinders and life-savers. Trends Neurosci 31:287-295.

Tessier-Lavigne M, Goodman CS. 1996. The molecular biology of axon guidance. Science 274:1123-1133.

Togashi K, von Schimmelmann MJ, Nishiyama M, Lim CS, Yoshida N, Yun B, Molday RS, Goshima Y, Hong K. 2008. Cyclic GMP-gated CNG channels function in Sema3A-induced growth cone repulsion. Neuron 58:694-707.

Tojima T, Itofusa R, Kamiguchi H. 2009. The nitric oxide-cGMP pathway controls the directional polarity of growth cone guidance via modulating cytosolic Ca2+ signals. J Neurosci 29:7886-7897.

Tornieri K, Rehder V. 2007. Nitric oxide release from a single cell affects filopodial motility on growth cones of neighboring neurons. Dev Neurobiol 67:1932-1943.

Tornieri K, Welshhans K, Geddis MS, Rehder V. 2006. Control of neurite outgrowth and growth cone motility by phosphatidylinositol-3-kinase. Cell Motil Cytoskeleton 63:173-192.

Torreano PJ, Cohan CS. 1997. Electrically induced changes in Ca2+ in Helisoma neurons: regional and neuron-specific differences and implications for neurite outgrowth. J Neurobiol 32:150-162.

Torreano PJ, Waterman-Storer CM, Cohan CS. 2005. The effects of collapsing factors on F-actin content and microtubule distribution of Helisoma growth cones. Cell Motil Cytoskeleton 60:166-179.

Torres GE, Arfken CL, Andrade R. 1996. 5-Hydroxytryptamine4 receptors reduce afterhyperpolarization in hippocampus by inhibiting calcium-induced calcium release. Mol Pharmacol 50:1316-1322.

Tozer AJ, Forsythe ID, Steinert JR. 2012. Nitric oxide signalling augments neuronal voltage-gated L-type (Ca(v)1) and P/q-type (Ca(v)2.1) channels in the mouse medial nucleus of the trapezoid body. PLoS ONE 7:e32256.

Tricoire L, Vitalis T. 2012. Neuronal nitric oxide synthase expressing neurons: a journey from birth to neuronal circuits. Front Neural Circuits 6:82.

Trimm KR, Rehder V. 2004. Nitric oxide acts as a slow-down and search signal in developing neurites. Eur J Neurosci 19:809-818.

Turner MB, Szabo-Maas TM, Poyer JC, Zoran MJ. 2011. Regulation and restoration of motoneuronal synaptic transmission during neuromuscular regeneration in the pulmonate snail Helisoma trivolvis. Biol Bull 221:110-125.

Turrigiano G, Abbott LF, Marder E. 1994. Activity-dependent changes in the intrinsic properties of cultured neurons. Science 264:974-977.

Turrigiano GG, Marder E. 1993. Modulation of identified stomatogastric ganglion neurons in primary cell culture. J Neurophysiol 69:1993-2002.

Uteshev VV. 2010. Evaluation of Ca2+ permeability of nicotinic acetylcholine receptors in hypothalamic histaminergic neurons. Acta Biochim Biophys Sin (Shanghai) 42:8-20.

van Nierop P, Bertrand S, Munno DW, Gouwenberg Y, van Minnen J, Spafford JD, Syed NI, Bertrand D, Smit AB. 2006. Identification and functional expression of a family of nicotinic acetylcholine receptor subunits in the central nervous system of the mollusc Lymnaea stagnalis. J Biol Chem 281:1680-1691.

van Nierop P, Keramidas A, Bertrand S, van Minnen J, Gouwenberg Y, Bertrand D, Smit AB. 2005. Identification of molluscan nicotinic acetylcholine receptor (nAChR) subunits involved in formation of cation- and anion-selective nAChRs. J Neurosci 25:10617-10626.

Van Wagenen S, Rehder V. 1999. Regulation of neuronal growth cone filopodia by nitric oxide. J Neurobiol 39:168-185.

Van Wagenen S, Rehder V. 2001. Regulation of neuronal growth cone filopodia by nitric oxide depends on soluble guanylyl cyclase. J Neurobiol 46:206-219.

Vandael DH, Zuccotti A, Striessnig J, Carbone E. 2012. Ca(V)1.3-driven SK channel activation regulates pacemaking and spike frequency adaptation in mouse chromaffin cells. J Neurosci 32:16345-16359.

Waites CL, Craig AM, Garner CC. 2005. Mechanisms of vertebrate synaptogenesis. Annu Rev Neurosci 28:251-274.

Walcourt-Ambakederemo A, Winlow W. 1995. 5-HT receptors on identified Lymnaea neurones in culture: pharmacological characterization of 5-HT3 receptors. Gen Pharmacol 26:553-561.

Wallner M, Meera P, Toro L. 1999. Molecular basis of fast inactivation in voltage and Ca2+-activated K+ channels: a transmembrane beta-subunit homolog. Proc Natl Acad Sci U S A 96:4137-4142.

Wang D, Grillner S, Wallen P. 2011. 5-HT and dopamine modulates CaV1.3 calcium channels involved in postinhibitory rebound in the spinal network for locomotion in lamprey. J Neurophysiol 105:1212-1224.

Wang GX, Poo MM. 2005. Requirement of TRPC channels in netrin-1-induced chemotropic turning of nerve growth cones. Nature 434:898-904.

Wanner IB, Wood PM. 2002. N-cadherin mediates axon-aligned process growth and cell-cell interaction in rat Schwann cells. J Neurosci 22:4066-4079.

Welnhofer EA, Zhao L, Cohan CS. 1997. Actin dynamics and organization during growth cone morphogenesis in Helisoma neurons. Cell Motil Cytoskeleton 37:54-71.

Welshhans K, Rehder V. 2005. Local activation of the nitric oxide/cyclic guanosine monophosphate pathway in growth cones regulates filopodial length via protein kinase G, cyclic ADP ribose and intracellular Ca2+ release. Eur J Neurosci 22:3006-3016.

Welshhans K, Rehder V. 2007. Nitric oxide regulates growth cone filopodial dynamics via ryanodine receptor-mediated calcium release. Eur J Neurosci 26:1537-1547.

White SH, Magoski NS. 2012. Acetylcholine-evoked afterdischarge in Aplysia bag cell neurons. J Neurophysiol 107:2672-2685.

Wilson GW, Garthwaite J. 2010. Hyperpolarization-activated ion channels as targets for nitric oxide signalling in deep cerebellar nuclei. Eur J Neurosci 31:1935-1945.

Wong RG, Hadley RD, Kater SB, Hauser GC. 1981. Neurite outgrowth in molluscan organ and cell cultures: the role of conditioning factor(s). J Neurosci 1:1008-1021.

Wonnacott S, Kaiser S, Mogg A, Soliakov L, Jones IW. 2000. Presynaptic nicotinic receptors modulating dopamine release in the rat striatum. Eur J Pharmacol 393:51-58.

Woodin MA, Munno DW, Syed NI. 2002. Trophic factor-induced excitatory synaptogenesis involves postsynaptic modulation of nicotinic acetylcholine receptors. J Neurosci 22:505-514.

Woodward OM, Willows AO. 2006. Dopamine modulation of Ca(2+) dependent Cl(-) current regulates ciliary beat frequency controlling locomotion in Tritonia diomedea. J Exp Biol 209:2749-2764.

Xue S, Qiao J, Pu F, Cameron M, Yang JJ. 2013. Design of a novel class of protein-based magnetic resonance imaging contrast agents for the molecular imaging of cancer biomarkers. Wiley Interdiscip Rev Nanomed Nanobiotechnol 5:163-179.

Yang N, Higuchi O, Ohashi K, Nagata K, Wada A, Kangawa K, Nishida E, Mizuno K. 1998. Cofilin phosphorylation by LIM-kinase 1 and its role in Rac-mediated actin reorganization. Nature 393:809-812.

Yanyi C, Shenghui X, Yubin Z, Jie YJ. 2010. Calciomics: prediction and analysis of EF-hand calcium binding proteins by protein engineering. Sci China Chem 53:52-60.

Yao WD, Rusch J, Poo M, Wu CF. 2000. Spontaneous acetylcholine secretion from developing growth cones of Drosophila central neurons in culture: effects of cAMP-pathway mutations. J Neurosci 20:2626-2637.

Yen JC, Chan JY, Chan SH. 1999. Involvement of apamin-sensitive SK channels in spike frequency adaptation of neurons in nucleus tractus solitarii of the rat. J Biomed Sci 6:418-424.

Zakharenko S, Chang S, O'Donoghue M, Popov SV. 1999. Neurotransmitter secretion along growing nerve processes: comparison with synaptic vesicle exocytosis. J Cell Biol 144:507-518.

Zappettini S, Grilli M, Lagomarsino F, Cavallero A, Fedele E, Marchi M. 2011. Presynaptic nicotinic alpha7 and non-alpha7 receptors stimulate endogenous GABA release from rat hippocampal synaptosomes through two mechanisms of action. PLoS ONE 6:e16911.

Zhang H, Rodgers EW, Krenz WD, Clark MC, Baro DJ. 2010. Cell specific dopamine modulation of the transient potassium current in the pyloric network by the canonical D1 receptor signal transduction cascade. J Neurophysiol 104:873-884.

Zheng JQ, Felder M, Connor JA, Poo MM. 1994. Turning of nerve growth cones induced by neurotransmitters. Nature 368:140-144.

Zheng JQ, Poo MM. 2007. Calcium signaling in neuronal motility. Annu Rev Cell Dev Biol 23:375-404.

Zheng JQ, Wan JJ, Poo MM. 1996. Essential role of filopodia in chemotropic turning of nerve growth cone induced by a glutamate gradient. J Neurosci 16:1140-1149.

Zhong LR, Artinian L, Rehder V. 2013. Dopamine suppresses neuronal activity of Helisoma B5 neurons via a D2-like receptor, activating PLC and K channels. Neuroscience 228:109-119.

Zhong LR, Estes S, Artinian L, Rehder V. 2013. Acetylcholine elongates neuronal growth cone filopodia via activation of nicotinic acetylcholine receptors. Dev Neurobiol.

Zhou Y, Xue S, Yang JJ. 2013. Calciomics: integrative studies of Ca2+-binding proteins and their interactomes in biological systems. Metallomics 5:29-42.